Fenton-like oxidation of organic pollutants in the presence of iron (II, III) oxides

Xiaofei Xue

JOINT PhD

WUHAN UNIVERSITY AND

UNIVERSITY HENRI POINCARE

Oxydation par la réaction de Fenton modifiée des polluants organiques en présence des oxydes de fer (II, III)

Fenton-like oxidation of organic pollutants in the presence of iron (II, III) oxides

by

Xiaofei Xue

Speciality: Environmental Science

Ecole Doctorale Lorraine de Chimie et Physique Moléculaires

Date of defence: May 29th, 2009
Place of defence: Wuhan University, Wuhan city, PR CHINA.

Composition of PhD defence

M. MAILHOT G.	Directeur de recherche CNRS (Université Blaise Pascal)	Referee
M. CHOVELON J-M.	Professeur (Université Lyon 1)	Examiner
M. BAO Z.	Professor (China University of Geosciences)	Referee
M. WU F.	A. Professor (Wuhan University)	Examiner
M. DENG N.	Professeur (Wuhan University)	Supervisor
M. HUMBERT B.	Professeur (Nancy Université)	Supervisor
M. HANNA K.	A. Professeur (Nancy Université)	Co-Supervisor

Laboratoire de Chimie Physique et Microbiologie pour l'Environnement, LCPME UMR7564, CNRS, FRANCE and Department of Environmental science, Wuhan University, CHINA.

Résumé

Cette thèse avait pour but d'étudier les phénomènes physico-chimiques se produisant à l'interface solide minéral/solution en présence d'un oxydant et d'un polluant organique. L'apport du fer comme catalyseur pour l'oxydation du polluant était évalué en sélectionnant deux types d'oxydes mixtes (Fe^{II}, Fe^{III}) de fer. Il s'agit d'interactions solide/polluant, oxydant/solide et oxydant/polluant dont les mécanismes réactionnels sont loin d'être compris. Les mécanismes d'oxydoréduction des composés organiques dans la phase aqueuse en contact avec ces minéraux sont fortement influencés par leurs propriétés de surface, leur réactivité vis-à-vis des polluants et la nature des oxydants utilisés. En effet, les phénomènes se produisant à l'interface minéral/solution pourraient avoir un impact significatif d'une part sur l'efficacité de l'oxydation et d'autre part sur la stabilité du système solide. Des caractérisations spectroscopiques couplées à des analyses chimiques ont permis à la fois de décrire les mécanismes d'oxydoréduction à l'interface solide/liquide et de suivre l'efficacité de l'oxydation ainsi que l'évolution structurale du solide. L'influence de l'oxydation sur la nature minéralogique du solide a été abordée. De même, l'effet de la présence des agents chélatants agissant comme pièges des radicaux hydroxyles libres ($^{\bullet}OH$) sur la performance de l'oxydation a été également étudié.

Les résultats présentés dans ce manuscrit contribuent à la bonne compréhension des mécanismes se produisant à l'interface oxyde/solution lors de l'oxydation par Fenton modifiée. Ce travail a permis de mettre en évidence les paramètres optimums durant la dégradation d'un polluant organique comme le pentachlorophénol (PCP) dans le système magnétite/H_2O_2. De plus, les facteurs influençant le contact oxydant-polluant en comparant deux polluants (RhodamineB et Pentachlorophénol) et deux types d'oxydes mixtes de fer ont été déterminés. Parmi ces facteurs, on peut citer l'hydrophobicité, l'équilibre acido-basique et l'adsorptivité de la molécule, et le contenu en Fe^{II}, surface spécifique, minéralogie et propriétés de surface du solide. Il s'agit alors d'une étape significative dans l'évaluation et le suivi de la réaction d'oxydation des polluants organiques dans les sols et les eaux contaminés. L'utilisation de ces données expérimentales a permis une bonne description de la réactivité intrinsèque des oxydes de fer et aussi une optimisation de la réaction d'oxydation.

L'utilisation d'un agent complexant fort du fer comme l'EDTA conduit à de meilleurs résultats en phase homogène à pH7. Cependant, l'utilisation de l'oxalate comme les cyclodextrines devient plus intéressante en phase hétérogène. Ces résultats mettent en évidence le rôle important des interactions physico-chimiques à l'interface catalyseur solide/solution dans la détermination de la performance de la réaction d'oxydation du Fenton hétérogène.

Abstract

As an advanced oxidation processe, Fenton reaction (Fenton reagent: (Fe^{2+}/H_2O_2)) is one of the most powerful oxidation used world around, which has been proved to be a promising and attractive treatment method for the degradation of a large number of hazardous and organic pollutant. Fenton process can generate free hydroxyl radical ($HO^{\bullet}$), a strong oxidant capable of reacting with practically all types of organic and inorganic compounds. However, the classic Fenton reaction has some disadvantages such as the Fe(III)-iron sludge was produced during the reaction and the solution needed acidification before carrying out the reaction. To overcome these drawbacks, many researchers focused on using modified Fenton system, the so called Fenton-like system. In this research, iron solid mineral was used instead of soluble iron and it offers significant advantages in separation. Since in this case, the catalyst can be easily recovered by sedimentation or filtration and be further used.

Iron is the most abundant transition metal in natural environment. It widely exists in soil, fresh waters, ocean and atmosphere as a kind of mineral on surface of the Earth. Different kinds of iron oxides, such as goethite, hematite, magnetite, and ferrihydrite, are among the most ubiquitous forms of iron species under environmental relative conditions (pH 4-9). In this thesis, two kinds of mixed iron (II, III) oxides were chosen, which have different Fe^{II}/Fe^{III} ratio, special surface area (SSA), mean particle diameter, site density and so on. Two kinds of model pollutant (pentachlorophenol (PCP) and Rhodamine B (RhB)) which are widely used chemicals all over the world were selecetd. They are toxic, persistant, very resistant to biodegradation and considered as priority organic pollutant by USEPA.

Firstly, PCP was chosen as a model pollutant, to investigate the oxidation of PCP on the surface of magnetite used as heterogeneous catalyst. Oxidation experiments were carried out under various experimental conditions at neutral pH and correlated with the adsorption behavior. The surface reactivity of magnetite was evaluated by

conducting the kinetic study of both H_2O_2 decomposition and PCP oxidation experiments. The occurrence of the optimum values of H_2O_2 and magnetite concentrations for the effective degradation of PCP could be explained by the scavenging reactions with H_2O_2 or iron oxide surface. All batch experiments indicate that Fenton-like oxidation of PCP was controlled by surface mechanism reaction and the species compete with each other for adsorption on a fixed number of surface active sites. The apparent degradation rate was dominated by the rate of intrinsic chemical reactions on the oxide surface rather than the rate of mass transfer. Raman analysis suggested that the sorbed PCP was removed from magnetite surface at the first stage of oxidation reaction. All X-ray powder diffraction (XRD), X-ray photoelectron spectroscopy (XPS), Mössbauer spectroscopy and chemical analyses showed that the magnetite catalyst exhibited low iron leaching, good structural stability and no loss of performance in second reaction cycle.

Secondly, Rhodamine B (RhB) was chosen as a model compound pollutant. Two types of iron (II, III) oxides were used as heterogeneous catalysts and characterized by XRD, Mössbauer spectroscopy, BET surface area, particle size and chemical analyses. The catalytic efficiency of iron (II, III) oxide to promote Fenton-like reaction was examined at neutral pH. The adsorption to the catalyst changed significantly with the pH value and the sorption isotherm was fitted using the Langmuir model for both solids. Both sorption and FTIR results indicated that surface complexation reaction may take place in the system. The variation of oxidation efficiency against H_2O_2 dosage and amount of exposed surface area per unit volume was evaluated and correlated with the adsorption behavior in the absence of oxidant. There is also an optimum amount of H_2O_2 value for the degradation of RhB. The phenomena could also be explained by the scavenging effect of hydroxyl radical by H_2O_2 or by iron oxide surface (like the oxidation of PCP). Sorption and decolourization rate of RhB as well as H_2O_2 decomposition rate were found to be depended on the surface characteristics of iron oxide. The kinetic oxidation experiments showed that structural Fe^{II} content strongly affect the reactivity towards H_2O_2 decomposition and therefore RhB

decolourization. The site density and sorption ability of RhB on surface may also influence the oxidation performance in iron oxide/H_2O_2 system. The iron (II, III) oxides catalysts exhibited low iron leaching, good structural stability and no loss of performance in second reaction cycle. The sorption on the surface of iron oxide with catalytic oxidation using hydrogen peroxide would be an effective oxidation process for the contaminants.

Finally, the effect of chelating agent on the heterogeneous Fenton reaction rate of pentachlorophenol in the presence of magnetite was investigated. Six kinds of chelating agents including oxalate, EDTA, CMCD, tartarate, citrate and succinate were chosen. The PCP oxidation rate in this system was significantly improved by using chelating agents at neutral pH. The kinetic rate constant was increased by 5.7, 4, 3.2, 2.4, 2.5 and 1.7 times with oxalate, EDTA, CMCD, tartarate, citrate and succinate, respectively. The enhancement factor of heterogeneous oxidation rate was found to be not correlated with that of dissolved iron dissolution amount. In homogeneous Fenton system (dissolved Fe^{2+} or Fe^{3+}), EDTA-driven reaction showed the highest oxidation rate, while oxalate seems to be more efficiency in heterogeneous Fenton system (Fe_3O_4). This observation could be explained by the inactivation of iron surface sites which become unavailable for the interactions with H_2O_2 to initiate Fenton-like reactions. Indeed, EDTA can bind more strongly than oxalate to magnetite surface and compete more actively with H_2O_2 or PCP for the sorption on the surface active sites. These results demonstrated that the chelating agent-promoted dissolution of magnetite did not play the key role in determining the efficiency of heterogeneous Fenton oxidation. The surface interactions of oxidant with the catalyst surface appear to be the rate-determining step in heterogeneous Fenton system, rather than the iron oxide dissolution rate.

Acknowledgements

I would like to thank very much to my supervisor Dr. khalil Hanna. During the year in France, he not only helped me with my work, but also gave many helps for my living. It is my pleasure and I'm very lucky to work with him, I learned many things from him. He helped me about the experiment, he helped me about the papers, and also he helped me with my thesis. Without his help I can't finish all my works in two years. Without his support I can't made the interuniversity program between Nancy University and Wuhan University.

I would like to thanks my supervisor Pro.Deng Nansheng. Thanks for his guidance during the four years study in Wuhan university, thanks for his support of the interuniversity program between Nancy university and Wuhan university.

I would like to thanks Mr. Feng Wu, for his kindly help and guide about my experiments during my study in Wuhan University, and also thanks for his help about making the interuniversity program.

Special thanks for Pr. Bernard Humbert for the help of the interuniversity agreement between Nancy University and Wuhan University.

Thanks for my friend Benoit Rusch, during the year I study in Nancy University. He had given many help to me about my experiments. And he also gave many help to my living in France. I'm always very happy to work together with him. And also thanks for the kindly help from my colleague Dr. Kone Tiangoua.

Thanks for Mustapha Abdelmoula for Mössbouer analysis and for many helpful discussions with regards to the magnetite structure, Thanks for Christelle Despas for the help of using the HPLC. Thanks for Cedric for the help of FTIR and RAMAN.

Thanks for the help of Ms. Mei Xiao and Ms.Ling Zhang for the experimental equipment and also the other help when I was in Wuhan University.

Thanks for Mr. Guanghui Wang, he gave a lots of help to me when I was in Wuhan university. I'm very happy to work with Dr Xu Zhang, Dr Beibei Wang, Dr Lin Deng, Dr Yuanxiang Liu, Dr. Li Guo, Dr Lei Wang, Ms. Liu Yang and also thanks for their help. I'm happy to be colleague with Dr. Wenyu Hang, Ms. Liwei Hou, Mr. Xuwei Wu, Mr. Zhiping Wang, Mr. Liwei Bai.

Thanks for the fund support of China Scholarship Council (CSC) affiliated with the Ministry of Education of the P.R.China. Thanks for choosing me and giving me this chance. Thanks for Mr. Xiaotao Zhang who is working in the Education Service of China Embassy in Paris France.

Finally, I would especially like to thank my family; my parents and my wife's parents for always being there with encouragement; I would like to thank my wife Cui, for her love, understanding and support, I can overcome any difficulties. We have been together since college, we work hard together to pursue the happies of life for many years, I cannot imagine life without her.

Publication list

1. Xiaofei Xue, Khalil Hanna, Nansheng Deng. Fenton-like oxidation of Rhodamine B in the presence of two types of iron (II, III) oxide.
Journal of Hazardous Materials, In Press, Available online 3 December 2008.

2. Xiaofei Xue, Khalil Hanna, Mustapha Abdelmoula, Nansheng Deng. Adsorption and oxidation of PCP on the surface of magnetite: Kinetic experiments and spectroscopic investigations.
Applied Catalysis B: Environmental, In Press, Available online 15 January 2009.

3. Xiaofei Xue, Khalil Hanna, Christelle Despas, Nansheng Deng. Effect of chelating agent on the oxidation rate of PCP in the magnetite /H_2O_2 system at neutral pH.
Journal of Molecular Catalysis A: Chemical, In press, 2009.

CONTENTS

CHAPTER 1

CHAPTER 1. INTRODUCTION

1.1 Background

The widespread presence of persistent organic chemicals in wastewater effluents from industries or even normal households is a serious environmental problem. Contamination of soil and groundwater by these organic chemicals imposes significant threats on water resources and public health. Some types of pollutants in water and soil are complex organic molecules which are often difficult to degrade, such as some phenolic compounds, dyes and so on. As a consequence, there is an increasing social pressure towards a sustainable use of water and a renewed interest in improving existing technologies for water treatment [Centi and Perathoner et al., 2001].

Many physical, chemical, and biophysical processes have been studied for their ability to destroy these organic pollutants. The conventional wastewater treatment technologies for these toxic substances include biological treatment processes, chemical coagulation processes, adsorption by activated carbon, and the chemical processes. However, many kinds of serious toxic pollutants such as chlorophenol (monochlorophenol, trichlorophenol, p-chlorophenol, pentachlorophenol), are resistant to the biological treatment and the degradation ratio was very slow. Adsorption processes just transfer the form of the pollutant from water to solid, and the further treatment is needed.

Chemical oxidation is a powerful method for the remediation of wastewater and contaminated groundwater. The Chemical oxidants most commonly employed to date include peroxide, ozone, and permanganate. These oxidants have been able to cause the rapid and complete chemical destruction of many toxic organic chemicals. In these

decades, in order to treat the resistant, toxic, and poorly biodegradable pollutants efficiently, a so called advanced oxidation processes (AOPs) was investigated and applied [Mijangos et al., 2006]. AOPs have been defined as those oxidation treatment based on the reaction of hydroxyl radical in an aqeous solution, it is a powerful and extremely reactive oxidant agent that can destroy organic pollutants efficiently [Mijangos et al., 2006; Esplugas et al., 2002; Santos et al., 2002; Sedlak, et al., 1991; Potter, et al., 1993; Neyens et al., 2003; Chamarro et al., 2001].

Fenton reaction (Fenton reagent: (Fe^{2+}/H_2O_2) as one of the AOPs [Duarte et al., 2009; Chiron et al., 2000, Neyens and Baeyens, 2002; Perez et al., 2002; Will et al., 2004], is one of the most powerful oxidation used world around, has been proved to be a promising and attractive treatment method for the degradation of a large number of hazardous and organic pollutant [Oliveira et al., 2006; Pera-Titus et al., 2003; Lin et al., 2000; Ormad et al., 2001; Sabhi et al., 2001]. These processes can generate free hydroxyl radical ($HO^{\bullet}$), a strong oxidant capable of reacting with practically all types of organic and inorganic compounds [Oliveira et al., 2006; Pera-Titus et al., 2003; Hurling et al., 2000; Sun et al., 1993]. Fenton's reagent in the destruction of organic compounds is limited by the slurry system because it produces a significant amount of Fe(III)-iron sludge, which requires further separation and disposal [Hsueh et al., 2005], and also is less appropriate since it leads to high metal (iron or other transition metal) concentrations in the final effluent [Duarte et al. 2009]. So during these years, many researchers focused on the using of modified Fenton system the so called Fenton-like system to treat the organic pollutant. In some research, iron solid mineral was used instead of soluble iron and it offers significant advantages in separation since in this case, the catalyst can be easily recovered by sedimentation or filtration and further used. [Mecozzi et al., 2006], and also the reaction could be carried out at neutral pH without acidified the solution before the reaction.

Chlorophenols have been used in numerous applications which produce industrial wastewaters that, like landfill leachates, contaminate the surrounding soil and water courses, affecting public health [Oliveira et al., 2006; Gupta et al., 2002; Aksu and Yener, 2001; Pera-Titus et al., 2003; Henke, 2002; Valenzuela et al, 1997]. Dye is the one of the most common toxic pollutant in the natural environment over the world. Dye and dye intermediate manufacturing industries, textile units, are typical industries that dump toxic organic compounds to the nearer water courses, thus making the water polluted [Ramirez et al., 2007a; Kabita et al., 2001]. Two types of pollutants were chosen as model pollutants in this research. They are one kind of chlorophenol and one kind of dye which named pentachlorophenol (PCP) and Rhodamine B (RhB) respectively. Each of them is widely used chemicals all over the world, toxic, resistant to biodegradation and till now there were not too much research focused on using Fenton-like system to remove this two type of pollutants in the aqueous.

1.2 Research goals and objectives

The objective of this research was to investigate a heterogeneous Fenton-like reaction to oxidize model pollutant under using of different kinds of iron (II,III) oxides which have different Fe^{II}/Fe^{III} ratio, special surface area (SSA), mean particle diameter, Site Density and so on. We determined which is the suitable condition and investigated some important factors in the Fenton-like system, to gain insight into the heterogeneous Fenton reaction, to get more information about the mechanism. And also we chose some types of chelating agents in the system to improve the oxidation, and investigated some parameters to see the best oxidation condition; this can help us to know more deeply about the heterogeneous Fenton reaction. To meet these goals the following specific objectives were defined:

1. Compare different iron oxides in oxidizing the model pollutants to determine the oxidation efficiency.
2. Conduct batch experiments to elucidate the role that adsorption of pollutant on the surface of iron oxides could affect the oxidation efficiency of the heterogeneous Fenton-like reaction, and to investigate the mechanism of the heterogeneous Fenton-like reaction.
3. Choose groups of chelating agents to see the key role that which affect the oxidation efficiency, whether it was the total dissolved iron in the solution or the sorption and surface reaction happened on the surface of iron oxides.

1.3 Organization of thesis

This dissertation is divided into five chapters. Chapter 1 is an introduction which included background, research goals and objectives, and organization of thesis.

Chapter 2 collected the related literatures presents a review of related research work about this study. These literatures included four parts:

2.1. Advanced oxidation progresses (AOPs)

2.2. Fenton Reaction

2.3. Heterogeneous Fenton-like Reaction

2.4. Model pollutant

Chapter 3 is experimental materials and methods, it investigated the material and analytic methods used in this research and some of the experimental methods and procedure were also included.

Chapter 4 is the result and discussion of all the batch of experiments. The first part of the chapter 4 was named Adsorption and oxidation of PCP on the surface of magnetite: Kinetic experiments and spectroscopic investigations. In the study, the oxidation of

PCP on the surface of magnetite used as heterogeneous catalyst has been investigated under various experimental conditions (initial substrate concentration, H_2O_2 dose, solid loading and temperature) at neutral pH and correlated with the adsorption behavior. All batch experiments in this work indicate that Fenton-like oxidation of PCP was controlled by surface mechanism reaction and the species compete with each other for adsorption on a fixed number of surface active sites.

The second part of chapter 4 was named Fenton-like oxidation of Rhodamine B in the presence of two types of iron (II, III) oxide. In this study, the catalytic efficiency of iron (II, III) oxide to promote Fenton-like reaction was examined by employing Rhodamine B (RhB) as a model compound at neutral pH. Two types of iron (II, III) oxides were used as heterogeneous catalysts. H_2O_2 dosage, surface characteristics of iron oxide, structural Fe^{II} content and some other factors could influence the oxidation performance in iron oxide/H_2O_2 system. The sorption on surface of iron oxide with catalytic oxidation using hydrogen peroxide would be an effective oxidation process for the contaminants.

The third part of chapter 4 was named effect of chelating agent on the oxidation rate of PCP in the magnetite/H_2O_2 system. This part mainly worked on the degradation of PCP under using chelating agents in the iron oxide/ H_2O_2 system. Six kinds of chelating agents were chosen which were: oxalic acid, EDTA, CMCD, Tartaric Acid, Citric Acid and Succinic Acid. Batch of experiments proved that the surface reaction of PCP, chelating agents, and some types of Fe-chelating agent complex on the iron oxides surface play a main role in the iron oxides//H_2O_2/chelating agent system.

Chapter 5 provides the general conclusion and recommendations.

CHAPTER 2

CHAPTER 2. LITERATURE REVIEW

Fenton's reagent was discovered about 100 years ago by a French researcher who named Henry J. H. Fenton, he reported that H_20_2 could be activated by Fe(II) salts to oxidize tartaric acid [Fenton, 1894]. In order to remember him and show the respect of this foundation, later researchers named it Fenton reagent which is peroxides (usually H_2O_2) combined with Fe(II) salts. But its application as an oxidizing process for destroying toxic organics was not applied until the late 1960s [Huang et al. 1993]. From the last few decades to present, Fenton and related reactions have become of great interest for their relevance to biological chemistry, synthesis, the chemistry of natural waters. Fenton reaction wastewater treatment processes are known to be very effective in removaling many hazardous organic pollutants from water which the conventional wastewater treatment technologies are hard to deal with. The main advantage is the complete destruction of contaminants to harmless compounds, e.g.CO_2, water and inorganic salts [Neyens and Baeyens, 2003].

Fenton reaction belongs to a so called AOPs (advanced oxidation progresses) technologies, which was first called and named by Glaze et al., (1987), the AOPs technologies based on the generation of hydroxyl radical ($HO^{\bullet}$) and have some main advantages. Firstly, it can generate amount of free $HO^{\bullet}$ the oxidation in a short time. Secondly, $HO^{\bullet}$ can non-selectively react with all types of organic and inorganic compounds, and the recontamination is low compared with conventional chemical progresses. Because normally the intermediate pollutant or the byproduct will continue to be oxidized in the system by $HO^{\bullet}$ and eventually come to the total mineralization. Thirdly, different AOPs are easy to combine with each other or other pollutant treatment processes to improve the removal of the contamination, such as UV/H_2O_2 combined with Fe^2/H_2O_2 used to be called photo-assisted Fenton reaction (or photo Fenton reaction). AOPs are well known to us and universally used all over the world and the $HO^{\bullet}$ is the key role.

In the Fenton reaction, the $HO^{\bullet}$ plays a dominant role in the oxidation of pollutant, that was well investigated and accepted by most of the researchers. Actually in the early studies Wieland, and Franke (1927), Haber and Weiss (1934) proposed that the active oxidant generated by the Fenton reaction is the hydroxyl radical ($HO^{\bullet}$) and after 12 years Waters (1946) also reported about that. Hydroxyl radical is one of the most powerful oxidants known (E^{o} = 2.73 V). After that, many groups of researchers worked on this field and explained many kinds of mechanism. In a series of elegant papers on the decomposition of H_2O_2, Barb et al. (1949, 1951a, 1951b) and Kremer and Stein (1959) expanded upon and revised the original mechanism proposed by Haber and Weiss (1934) to provide what is now referred to as the "classical" or "free radical" Fenton chain reaction, because it involved $HO^{\bullet}$ production as the key step. But some part of the mechanism is now still under discussion. The reaction which Haber and Weiss proposed and named as Haber-Weiss reaction was argued by George (1947), Abel (1948), and Medalia and Kolthoff (1949). They believed the main reaction was not really occurred. In This part of thesis we will follow some main points of the mechanism and give a review of them.

In the last few decades, the importance of $HO^{\bullet}$ reactions in the natural environment, in biological systems, and in useful chemical processes including waste treatment has been recognized, and over 1700 rate constants for $HO^{\bullet}$ reactions with organic and inorganic compounds in aqueous solution have been tabulated [Buxton et al., 1988]. Therefore, high valence iron species and alkoxyl radicals ($RO^{\bullet}$) have also been proposed by many researchers [eg: Sheldon and Kochi, 1980; Rahhal and Richter, 1988; Bossmann et al., 1998; Buda et al., 2001]. All in all, Fenton and related reactions have become of great interest for their relevance to biological chemistry, synthesis, the chemistry of natural waters, and the treatment of hazardous wastes. And also the Fenton and related reactions are viewed as potentially convenient and economical ways to generate oxidizing species for treating chemical wastes. But there are some disadvantages of the Fenton reaction to treat the pollutant. The first is the solution must

be preacitified at a very low level to initial the reaction. The second is during the reaction there will produce sludge which could be thought as a secondary contamination. The third is the use of catalysis could not be recycled and the iron in the solution after reaction is also a contamination to the environment. In this research we mainly worked on one kind of Fenton-like reaction using the iron oxides with H_2O_2 to oxidize the modal pollutant, which called heterogeneous Fenton-like reaction to overcome the disadvantages of the classic Fenton reaction.

2.1 Advanced oxidation processes (AOPs)

Current levels of removing the pollutants from water which can be achieved using the conventional water treatment technologies are usually not more sufficient, especially when waste water streams contain significant amounts of hardly biodegradable chemicals or even compounds having phytotoxic effect on the micro-organisms responsible for biological degradation of the organic waste (such as polyphenolic) [Perathoner and Centi et al., 2005]. Thus in recent years, advanced oxidation processes (AOPs) have been widely used in wastewater treatment [Stafford et al., 1994; Lunar et al., 2000; Kurbus et al., 2003; Brillas et al., 2003; Trojanowicz et al., 2002].

There are several other areas in which advanced oxidation processes (AOPs) was applied, although in principle more costly than conventional water treatment trains (sometimes up to 10 times more costly) [Buitrago et al., 2002], Therefore, there are several incentives to develop novel AOPs. The use of catalysts in several cases improve the performances and lower the costs of these technologies by (i) increasing the reaction rates, (ii) allowing the use of more compact reactors and milder conditions for operations, (iii) allowing a better finishing (better decolourization, elimination of harmful byproducts in traces, etc.) and improved efficiency in pollutants removal, and often also (iv) improving the selective use of the oxidizing agents in converting the target chemicals [Perathoner and Centi, 2005].

Catalytic AOPs find application in various areas. For example, in the treatment of wastewater from (i) dyeing and printing [Gemeay et al., 2003; Lei et al., 1997; Kim et al., 2003], (ii) Kraft-pulp bleaching [Pintar et al., 2004; Pintar et al., 2004; Sonnen et al., 1997], (iii) petrochemical industry [Lin and Ho, 1997], (iv) olive milling [Chakchouk et al., 1994], (v) H-acid manufacturing process [Zhu et al., 2002] and (vi) wood pyrolysis and cooking plant [Armbruster et al., 2002], although the commercial processes are still limited [Luck, 1999].

There are many types of AOPs, however, due to the report of the researchers, AOPs has three main basically types, which depending on the type of oxidant (oxygen, hydrogen peroxide and ozone). In addition, a fourth type is represented by photocatalytic processes, Notwithstanding the significant differences in various AOPs, the common aspect is the fact that the main feature of them is producing ·OH radicals to oxidize various organic contaminants (although not the only one).

2.2 Fenton reaction

2.2.1 Background of Henry John Horstman Fenton

One hundred years ago, Henry John Horstman Fenton published a short paper on the oxidation of tartaric acid by hydrogen peroxide and iron(II) in the Proceedings section of the Journal of the Chemical Society. A full description appeared a year later in the Transactions of that journal. However, in 1893, Fenton did not write for the first time about tartaric acid, hydrogen peroxide, and iron: in 1876 the first note on the oxidation of tartaric acid was published in Chemical News, and a second short note appeared in the same journal in 1881 [Koppenol, 1993]. Fenton's main work was shown in Figure 2.1.

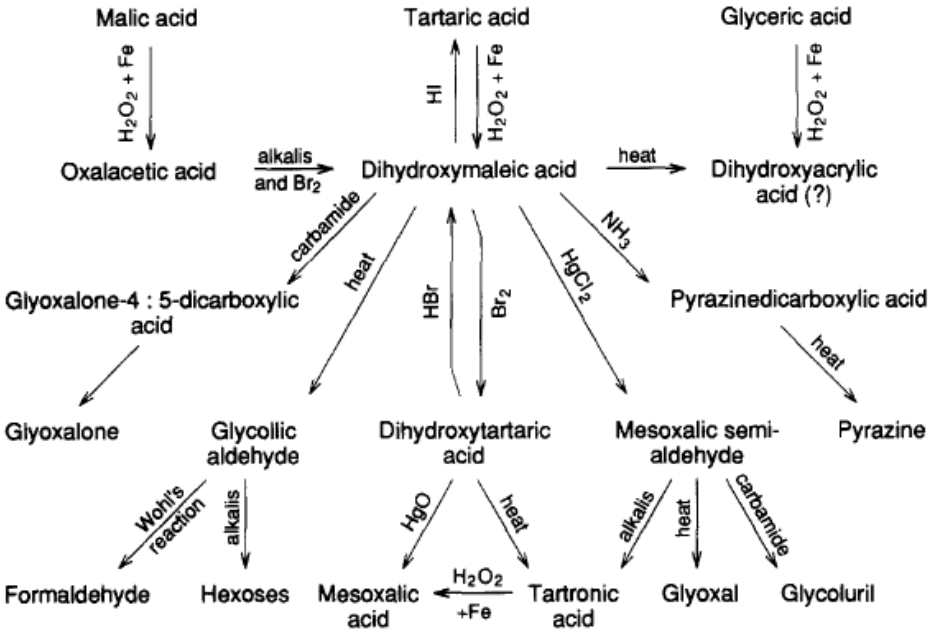

Figure 2.1. Overview of "Fenton" reactions studied by Fenton and his coworkers, [Koppenol, 1993; Bielski, 1978].

2.2.2 Fundamental chemistry of the Fenton reaction

The mechanism of the reaction between iron(II) and hydrogen peroxide has been widely assumed to be the following, based upon a comprehensive paper published by Barb et al. (1957). The mixture of H_2O_2 and ferrous iron, which generates hydroxyl radicals according to the reaction

$$Fe^{2+} + H_2O_2 \rightarrow Fe^{3+} + {}^{\bullet}OH + HO^{-} \qquad (2.1)$$

The ferrous iron (Fe^{2+}) initiates and catalyses the decomposition of H_2O_2, resulting in the generation of hydroxyl radicals. The generation of the radicals involves a complex reaction sequence in an aqueous solution [Dunford. 2002].

$$Fe^{2+} + H_2O_2 \rightarrow Fe^{3+} + {}^{\bullet}OH + HO^{-} \qquad \text{(chain initiation)} \qquad (2.1)$$

$$Fe^{2+} + {}^{\bullet}OH \rightarrow Fe^{3+} + HO^{-} \quad (2.2)$$

$${}^{\bullet}OH + H_2O_2 \rightarrow HO_2^{-} + H_2O \quad (2.3)$$

$$HO_2^{\bullet} + Fe^{2+} \rightarrow Fe^{3+} + HO_2^{-} \quad (2.4)$$

$$HO_2^{\bullet} + Fe^{3+} \rightarrow Fe^{2+} + O_2 + H^{+} \quad (2.5)$$

They noted that reaction (2.5) might be better written as

$$O_2^{\bullet -} + Fe^{3+} \rightarrow Fe^{2+} + O_2 \quad (2.5')$$

The above scheme is a chain mechanism in which iron(II) is regenerated. Rate constants for many of the above elementary reactions have been obtained by radiation chemists and are summarized in Table 2.1. An intensive investigation of reaction (2.4) showed that it is a composite reaction that can be broken down into elementary steps [Jayson et al., 1973] which were shown as:

$$HO_2^{\bullet} + Fe^{2+} \xrightarrow{k_{4A}} Fe^{3} + HO_2^{-} \quad (2.4A)$$

$$Fe^{3} + HO_2^{-} + Fe^{2+} \underset{k_{-4B}}{\overset{k_{4B}}{\rightleftharpoons}} Fe^{3} + HO_2^{-}Fe^{2+} \quad (2.4B)$$

$$Fe^{3} + {}^{\bullet}HO_2^{-} \xrightarrow{k_{4C}} Fe^{3+} + HO_2^{-} \quad (2.4C)$$

The iron-peroxide species are outer-sphere complexes. The authors obtained spectra for $Fe^{3+}HO_2$ and $Fe^{3+}HO_2^{-}Fe^{2+}$. They also showed a different dissociation for the

binuclear iron complex:

$$Fe^{3} + HO_2^{-}Fe^{2+} \xrightarrow{k_{4D}} Fe^{2+}HO_2^{-} + Fe^{3+} \qquad (2.4D)$$

Table 2.1 Elementary rate constants for the reaction of hydrogen peroxide with iron(II) according to the mechanism of Barb et al. 1957. Data from [Dunford. 2002].

Reaction numbers	Rate constant	References
(2.1)	(53. x 0.7) M^{-1} S^{-1}	Barb et al., 1957
(2.2)	(3.3x0.6) × 10^8 M^{-1} S^{-1}	Buxton et al., 1988
(2.3)	2.7 × 10^7 M^{-1} S^{-1}	Christensen et al., 1982
(2.4A)	(1.20x0.05) × 10^6 M^{-1} S^{-1}	Jayson et al., 1973
(2.4B)	(6.8x0.5) × 10^5 M^{-1} S^{-1}	Jayson et al., 1973
(2.4_B)	(2.5x0.1) × 10^4 S^{-1}	Jayson et al., 1973
(2.4C)	(1.8x0.01) × 10^3 S^{-1}	Jayson et al., 1973
(2.5)	Range: < 1.2 × 10^4 to 3.6 × 10^5 M^{-1} S^{-1}	Bielski et al., 1985

Clearly, after the reaction (2.1), the newly formed ferric ions may catalyse hydrogen peroxide, causing it to be decomposed into water and oxygen. Ferrous ions and radicals are also formed in the reactions [Neyens and Baeyens, 2003]. The reactions are shown as below:

$$Fe^{3+} + H_2O_2 \leftrightarrow Fe\text{–}OOH^{2+} + H^{+} \qquad (2.6)$$

$k = 0.001–0.01 M^{-1} s^{-1}$ [Walling and Goosen, 1973].

$$Fe\text{–}OOH^{2+} \rightarrow HO_2^{\bullet} + Fe^{2+} \qquad (2.7)$$

The reaction of hydrogen peroxide with ferric ions is referred to as a Fenton-like reaction [reactions (2.6) and (2.7)] [Walling and Goosen, 1973; De Laat and Gallard,

1985]. And also these two reactions could be combined into one (2.8):

$$Fe^{3+} + H_2O_2 \rightarrow Fe^{2+} + HO_2^{\bullet} + H^+ \qquad (2.8)$$

So the reaction chain from (2.1) to (2.5) could be also written like following [Barb et al. 1949; 1951a; 1951b]:

$$Fe^{2+} + H_2O_2 \rightarrow Fe^{3+} + {}^{\bullet}OH + HO^- \qquad \text{(chain initiation)} \qquad (2.1)$$

$$Fe^{3+} + H_2O_2 \rightarrow Fe^{2+} + HO_2^{\bullet} + H^+ \qquad (2.8)$$

$$Fe^{2+} + {}^{\bullet}OH \rightarrow Fe^{3+} + HO^- \qquad (2.2)$$

$${}^{\bullet}OH + H_2O_2 \rightarrow HO_2^- + H_2O \qquad (2.3)$$

$$HO_2^{\bullet} + Fe^{2+} + H^+ \rightarrow Fe^{3+} + H_2O_2 \qquad (2.9)$$

$$HO_2^{\bullet} + Fe^{3+} \rightarrow Fe^{2+} + O_2 + H^+ \qquad (2.5)$$

And the reaction (2.10) may happen:

$$HO_2^{\bullet} + HO_2^{\bullet} \rightarrow H_2O_2 + O_2 \qquad (2.10)$$

reactions analogous to equations (2.9) (2.5) to (2.10) involving superoxide anion $O_2^{-\bullet}$ the conjugate base of $HO_2^{\bullet}$ [PKa=4.8; Sawyer and Valentine, 1981;Bielski and Cabelli, 1991]. Some papers also mentioned the reaction (2.11) may happen:

$$HO_2^{\bullet} + H_2O_2 \rightarrow {}^{\bullet}OH + H_2O + O_2 \qquad (2.11)$$

However the reaction (2.11) was under argument, it is extremely slow [k_s= 3 $M^{-1}s^{-1}$; Koppenol et al., 1978] compared to others of $HO_2^{\bullet}$ and can be neglected. And also

Bray stated: "the specific rate of the reaction $2\,HO_2^{\bullet} \rightarrow H_2O_2 + O_2$ is much greater than that of $HO_2^{\bullet} + H_2O_2 \rightarrow {}^{\bullet}OH + H_2O + O_2$" [Brey, 1938].

Actually the reaction (2.8) is too slow and is several orders of magnitude slower than reaction (2.1), the desired oxidant for degrading the target pollutant ($^{\bullet}OH$) is produced by reaction (2.1). After the first reaction (2.1), it will produce a stoichiometric amount of Fe(III) which later precipitates to amorphous ferric oxyhydroxides as the pH is increased ferric oxyhydroxides production (which is the main disadvantage of the Fenton reaction). Some researchers had already explained the phenomena. The ferrous ions generated in the above redox reactions react with hydroxide ions to form ferric hydroxo complexes according to [Walling and Kato, 1971; Lin and Lo, 1997]:

$$[Fe(H_2O)_6]^{3+} + H_2O \leftrightarrow [Fe(H_2O)_5OH]^{2+} + H_3O^{+} \qquad (2.12)$$

$$[Fe(H_2O)_5OH]^{2+} + H_2O \leftrightarrow [Fe(H_2O)_4(OH)_2] + H_3O^{+} \qquad (2.13)$$

Within pH 3 and 7, the above complexes become:

$$2[Fe(H_2O)_5OH]^{2+} \leftrightarrow [Fe(H_2O)_8(OH)_2]^{4+} + 2H_2O \qquad (2.14)$$

$$[Fe(H_2O)_8(OH)_2]^{4+} + H_2O \leftrightarrow [Fe_2(H_2O)_7(OH)_3]^{3+} + H_3O^{+} \qquad (2.15)$$

$$[Fe_2(H_2O)_7(OH)_3]^{3+} + [Fe(H_2O)_5OH]^{2+} \leftrightarrow [Fe_2(H_2O)_7(OH)_4]^{5+} + 2H_2O \qquad (2.16)$$

which accounts for the coagulation capability of Fenton's reagent. Dissolved suspended solids are captured and precipitated. It should be noted that large amounts of small flocs are consistently observed in the Fenton oxidation step. Those flocs take a very long time, sometimes overnight, to settle out [Neyens and Baeyens, 2003].

Reaction (2.8), the so called Fenton-like processes which had been widely investigated

till now, showed that starting with the ferrous or starting ferric iron to initiate the chain reaction to decomposition H_2O_2 and generate the $^{\bullet}OH$ were different, though it is clear from reaction (2.1) to (2.5) that both Fe(II) and Fe(III) species are present simultaneously in the chain. It could be explained in which ferric ions react with hydrogen peroxide, reaction (2.6) is the rate-limiting step. When the pH is too low and the concentration of hydrogen ions is too high, it will slow down the formation of $FeOOH^{2+}$, which consecutively causes the production rates of ferrous ions and hydroxyl radicals to decrease as well. The earlier reactions may retard the Fenton reaction [Neyens and Baeyens, 2003]. Actually, Starting with Fe (II) can lead to an initial rapid degradation phase resulting from a burst of $^{\bullet}OH$ by reaction (2.1) [e.g., Bishop et al., 1968; Chen and Pignatello, 1997; Gallard and De Laat, 2000]. When H_2O_2 is in large excess the extent of this burst phase will depend on the Fe/contaminant molar ratio because that ratio determines the $HO^{\bullet}$/contaminant ratio in the burst phase [Hsueh, 2006]. While staring with the mix of Fe (II) and Fe (III) was also be investigated by some researchers [eg: Chen et al., 1997].

2.2.3 Mechanism of Iron-oxo iron and complexes in Fenton reaction

In 1946, Due to the work of Baxendale et a1., the earlier researchers including: Merz and Waters (1947), Barb et al.(1951), and Walling (1975) believed that there is little doubt that hydroxyl radicals are formed at low pH from the one-electron reduction of hydrogen peroxide by iron(II), presumably via an iron(II)-hydrogen peroxide, or iron(IV)-oxo intermediate. Actually, in 1932, the ferryl ion species FeO^{2+} had been firstly proposed by Bray and Gorin as one step in the ferric ion catalyzed decomposition of hydrogen peroxide. They connected the ferrous and ferric ion reaction through the postulated equilibrium:

$$2Fe^{3+} + H_2O = Fe^{2+} + FeO^{2+} + 2H^{+} \qquad (2.17)$$

With hydrogen peroxide in excess, oxygen evolution was proposed as follows:

$$Fe^{2+} + H_2O_2 \rightarrow FeO^{2+} + H_2O \qquad (2.18)$$

$$FeO^{2+} + H_2O_2 \rightarrow Fe^{2+} + H_2O + O_2 \qquad (2.19)$$

Thus their mechanism shows both ferrous and ferryl ions attacked by hydrogen peroxide, but not ferric ions.

Recently until the years 1999, a comprehensive reinvestigation of the reaction of ferrous ion with hydrogen peroxide had been published by Kremer. His mechanism for the iron(II) reaction was shown in Figure 2.2. In his mechanism with the iron(II) in excess, oxygen evolution is negligible. With hydrogen peroxide in excess, reaction with FeO^{2+} causes oxygen evolution in the initial stages, whereas in later stages the new species $\{FeOFe\}^{5+}$ is responsible.

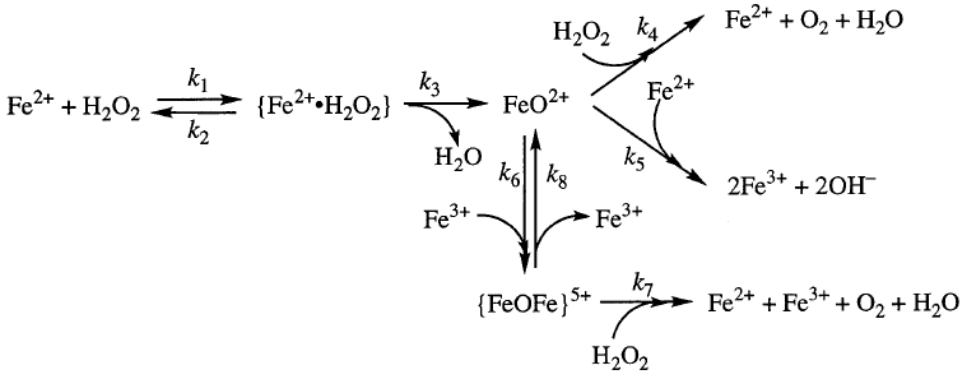

Figure 2.2 Mechanism of reaction of ferrous ion with hydrogen peroxide Kremer et al., 1999.

2.2.4. Main factors of Fenton reaction

2.2.4.1 Target organics

Reactions of $HO^{\bullet}$ with organic compounds lead to the formation of carbon-centered radicals. The hydroxyl radical always present in vanishingly small concentration reacts in many well known ways with organic compounds, principally by abstracting H from C—H, N—H, or O—H bonds, adding to C=C bonds, or adding to aromatic rings [Von Sonntag and Schuchmann, 1997; Buxton et al., 1988].

As shown in reaction (2.3), H_2O_2 can act as an $OH^{\bullet}$ scavenger as well as an initiator [reaction(2.1)]. Hydroxyl radicals can oxidise organics (RH) by abstraction of protons producing organic radicals ($R^{\bullet}$), which are highly reactive and can be further oxidised [Walling and Kato, 1971; Venkatadri and Peters, 1993; Lin and Lo, 1997]

$$RH + OH^{\bullet} \rightarrow H_2O + R^{\bullet} \rightarrow \text{further oxidation} \qquad (2.20)$$

Since k of (2.3) = $10^7 M^{-1}s^{-1}$ < k of (2.2) = 10^8, (2.7) can be made unimportant by maintaining a high [RH]/[H_2O_2] ratio [Neyens and Baeyens, 2003]. If the concentrations of reactants are not limited, the organics can be completely detoxified by full conversion to CO_2, water and in the case of substituted organics, inorganic salts if the treatment is continued [Neyens and Baeyens, 2003].

Walling (1975) simplified the overall Fenton chemistry [reaction (2.1)] by accounting for the dissociation water:

$$2Fe^{2+} + H_2O_2 + 2H^{+} \rightarrow 2Fe^{3+} + 2H_2O \qquad (2.21)$$

Due to the equation (2.21), it showed that the presence of H^+ is required in the decomposition of H_2O_2. This indicated the need for an acid environment to produce the maximum amount of hydroxyl radicals. Previous Fenton studies had shown that acidic pH levels near 3 are usually optimum for Fenton oxidations [Hickey et al. 1995]. In the

presence of organic substrates (RH), excess ferrous ion, and at low pH, hydroxyl radicals can add to the aromatic or heterocyclic rings (as well as to the unsaturated bonds of alkenes or alkynes).

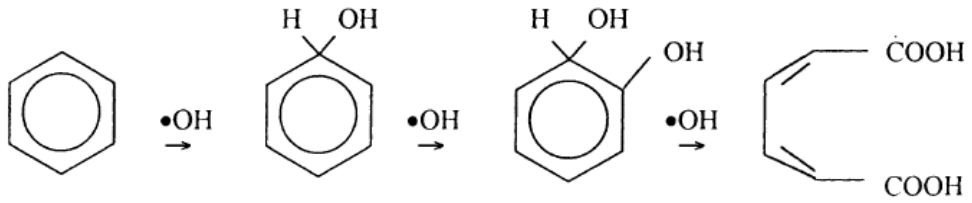

They can also abstract a hydrogen atom, initiating a radical chain oxidation [Walling, 1975; Lipczynska-Kochany et al. 1995]

$RH + OH^{\bullet} \rightarrow H_2O + R^{\bullet}$ (chain propagation) (2.22)

$R^{\bullet} + H_2O_2 \rightarrow ROH + OH^{\bullet}$ (2.23)

$R^{\bullet} + O_2 \rightarrow ROO^{\bullet}$ (2.24)

The organic free radicals produced in reaction (2.22) may then be oxidised by Fe^{3+}, reduced by Fe^{2+}, or dimerised according to the following reactions [Tang and Tassos, 1997]

$R^{\bullet} + Fe^{3+}\text{-oxidation} \rightarrow R^{+} + Fe^{2+}$ (2.25)

$R^{\bullet} + Fe^{2+}\text{-reduction} \rightarrow R^{-} + Fe^{3+}$ (2.26)

$2R^{\bullet}$—dimerization $\rightarrow$ R-R (2.27)

The sequence of reactions (2.1), (2.2), (2.22) and (2.25) constitute the present accepted

scheme for the Fenton's reagent chain.

2.2.4.2 Influence of pH

The pH is the key parameter of the treatment efficiency for Fenton's reagent, pH of the system has been observed to significantly affect the degradation of pollutants [Sedlak and Andren, 1991; Lin and Lo, 1997; Kang and Hwang, 2000; Nesheiwat and Swanson, 2000; Benitez et al., 2001a]. The optimum pH has been observed to be 3 in the majority of the cases [Venkatadri and Peters, 1993; Tang and Chen, 1996; Kwon et al., 1999; Benitez et al., 2001a] and hence is recommended as the operating pH at lower pH (pH < 3. 0). The scavenging effect of hydroxyl radicals by hydrogen ions becomes important at a very low pH [Tang and Huang, 1996] and also the reaction of Fe^{3+} with hydrogen peroxide is inhibited [Pignatello, 1992]. At operating pH of >4, the decomposition rate decreases because of the decrease of the free iron species in the solution, probably due to the formation of Fe (II) complexes with the buffer inhibiting the formation of free radicals and also due to the precipitation of ferric oxyhydroxides [Bigda, 1995; Lin and Lo, 1997; Nesheiwat and Swanson, 2000] which inhibit the regeneration of ferrous ions. Also, the oxidation potential of $HO^{\bullet}$ radical is known to decrease with an increase in the pH [Kwon et al., 1999].

A review of some works about the effect of pH on the Fenton reaction:

1. Hsueh et al. (2005) chose one kind of azo-dye named Red MX-5B as the modal pollutant in the experiment. The pH of this study focuses on the range of 1.5–6.5., the change of Red MX-5B concentration is significantly influenced by the solution pH. The optimum solution pH was observed at a pH of about 2.5–3.0 for the reactions. At pH 1.5, the dye decolorization rate dramatically decreased revealing that the scavenging effect of the $^{\bullet}OH$ by H^+ is severe at low pH. When at a pH higher than 3, it also showed low dye decolorization efficiency.

2. Carmen et al (2008) chose a kind of azo dye named Red H-EXL in his research. The experiments performed at different pH values between 2 and 5, His result showed that the maximum dye removal rate was reached for pH of 3.0. But the differences in the performances reached after 2 h are almost insignificant, whatever is the pH (3, 3.5 or other pH values).

3. Burbano et al. (2005) chose an organic chemical named methyl tort-butyl ether (MTBE) in the Fenton system. The experiments performed at different pH values between 3.0 and 7. This study was performed using solutions containing $[MTBE]_0$ of 11.4 and 22.7 mM, each one in individual experiments at pH values of 3.0, 3.6, 5.0, 6.3 and 7.0. FR means equimolar mixture of Fe^{2+} and H_2O_2 (i.e., $[Fe^{2+}]_0/[H_2O_2]_0$=1:1), and was added at a constant $[FR]_0$ /$[MTBE]_0$ molar ratio of 10:1 ($[FR]_0$ of 0.114 and 0.227 mM, respectively). The result showed that the maximum dye removal rate was reached for a pH of 3.0. Small variations were observed for the experiments at acidic pH values (between 3.0 and 5.0), while at neutral or close to neutral pH the extent of degradation was significantly lower.

From the foregoing, it appears that pH between 2 and 3 is the most effective in the degradation reactions. All these results showed were closely agreed with the literatures [Kuo, 1992; Sheng and Cho, 1997; Kang and Hwang, 2000; Sevimli and Kinacl, 2002]. This is also in agreement with the observation that complete mineralization of pentachlorophenol by Fenton's reagent [Watts et al., 1990].

2.2.4.3 Influence of Ferrous ion and H_2O_2

Amount of Ferrous ions

Usually, the rate of degradation increases with an increase in the concentration of ferrous ions [Lin and Lo, 1997; Kwon et al., 1999; Benitez et al., 2001a] though the extent of increase is sometimes observed to be marginal above a certain concentration as reported by Lin et al. (1999) and Kang and Hwang (2000) and Rivas et al. (2001).

But some report mentioned that the excessive use of ferrous ions in the solution will cause a negative effect of the oxidation of the pollutant, represented as the example followed.

Due to the work of Rodrigues et al. (2008), from their work, maximum dye removal levels are reached for a ferrous ion concentration of 0.27mM, the performance being worst for higher loads. Rodrigues (2008) reported that such detrimental effect of excessive catalyst dosages can be ascribed to other undesirable and competitive reactions that decrease the amount of radicals available to oxidize the organic matter, by reaction with excess iron ions, the reaction for ferrous ions they are represented may be as the reaction (2.2) and (2.4) mentioned above:

$$Fe^{2+} + HO^{\bullet} \rightarrow Fe^{3+} + OH^{-} \qquad (2.2)$$

$$Fe^{2+} + HO_2^{\bullet} \rightarrow Fe^{3+} + HO^{2-} \qquad (2.4)$$

Dosage of hydrogen peroxide

Concentration of hydrogen peroxide plays a crucial role in degradation process. Usually it has been observed that the percentage degradation of the pollutant increases with an increase in the dosage of hydrogen peroxide [Lin and Peng, 1995; Lin and Lo, 1997; Kwon et al., 1999; Lin et al., 1999; Kang and Hwang, 2000; Rivas et al., 2001]. However, hydrogen peroxide if presented in the solution in large quantities (excessive) will acts as a scavenger for the generated hydroxyl radicals. Thus, the loading of hydrogen peroxide should be adjusted in such a way that the entire amount is utilized, and this can be decided based on the laboratory scale studies with the total used amount of ferrous ions and the concentration of the pollutant. Some report below mentioned about the dosage of H_2O_2 in the reaction.

Due to the work of Dutta et al. (2001), the result showed that at a fixed Fe^{2+}

concentration of 3.58 $\times 10^{-5}$ mol dm^{-3}, the H_2O_2 concentration of 4.41×10^{-4} mol dm^{-3} was effected in degrading about 98% of dye in 30 min. The fractional conversion after 1 h remains almost same for H_2O_2 concentration of 4.41×10^{-4} to 2.94×10^{-2} mol dm^{-3}. Beyond 2.94×10^{-2} mol dm^{-3}, a decrease in fractional conversion of the dye was observed. Therefore, there is an optimum H_2O_2 concentration that is effective for the degradation of the dye. And also, data shown from the work of Rodrigues et al. (2008) put into evidence that in the tested range, dye removal efficiencies increase when the oxidant dosage is raised up to 5.9–8.8mM. Nevertheless, for higher concentrations oxidation performance remains practically unaffected, or even decreases.

This is a common behaviour in the Fenton's process, often attributed to the parallel and undesired reaction between excess hydrogen peroxide and hydroxyl radicals (scavenging effect) [Lin and Lo, 1997]. Consequently, the effective amount of these highly reactive species ($HO^{\bullet}$) that is available to degrade the dye and/or the intermediate compounds decreases. Although another radical is formed ($HO_2^{\bullet}$), it has an oxidation potential significantly smaller than that of the hydroxyl one [Bigda, 1995]. The excess amount of H_2O_2 is not recommended in the treatment of pollutant, it is costly, not very efficient, and to some points harmful to many of the microorganisms [Ito et al., 1998] when used as a pretreatment to biological oxidation.

Ferrous ions/ hydrogen peroxide ratio

Actually the $[Fe^{2+}]/[H_2O_2]$ ratio is an important factor about the dosage of ferrous ions and hydrogen peroxide in the Fenton oxidation. Some researchers had investigated about that, such as Yoon et al. [7], they studied these relationships and classified them into three categories according to the quantity of the $[Fe^{2+}]_0/[H_2O_2]_0$ ratio (initial concentration of Fe^{2+} versus initial concentration of H_2O_2). Their results are now summarized:

When the $[Fe^{2+}]_0/[H_2O_2]_0$ ratio is high (≥ 2). The Fenton reaction begins by producing

OH• from the reaction between ferrous ion and hydrogen peroxide [reaction (2.1)]. When the Fenton reaction in the absence of organics is initiated under $[Fe^{2+}]_0/[H_2O_2]_0$ (≥2), the consumption ratio of ferrous ion to hydrogen peroxide (□[Fe^{2+}]/□[H2O2]) becomes about 2, and radical chain reactions are quickly terminated. Yoon et al. explained that is because the OH• produced as a result of reaction (2.1) mainly reacts with the ferrous ion [reaction (2.2)] and not hydrogen peroxide [reaction (2.3)]. This explanation is supported by the fact that the reaction between OH• and the ferrous ion is ten times faster than that between OH• and hydrogen peroxide [$k_2 = 3.3 \times 10^8 M^{-1} s^{-1}$ [Buxton et al., 1988] and $k_7 = 2.7 \times 10^7 M^{-1} s^{-1}$ [Christensen et al., 1982].

When the $[Fe^{2+}]_0/[H_2O_2]_0$ ratio = 1, Regardless of the presence of organics, hydrogen peroxide rapidly converts all ferrous to ferric ion via reaction (2.1). In the absence of RH, hydrogen peroxide decomposes slowly through ferric ion induced radical chain reactions [reaction (2.6)] just after the rapid consumption of hydrogen peroxide. The reduction of the ferric ion [reactions (2.6) and (2.7)] is significantly lower than reaction (2.1) and is the rate-determining step. To have a continued decrease of hydrogen peroxide, ferrous ion must be formed by the reduction of ferric ion. Actually, from the result of Yoon et al., with or without RH, the ferrous iron will be consumed during first few minutes, and in 90 minutes the chain reaction can't decompose all H_2O_2.

When the $[Fe^{2+}]_0/[H_2O_2]_0$ ratio is low (≤1), In the absence of RH, a slow decomposition of hydrogen peroxide occurs caused by ferric ion, which induces radical chain reactions (ferric system) immediately after the initial rapid depletion of hydrogen peroxide. However, the presence of RH almost stops the decomposition of hydrogen peroxide by ferric ion (ferric system), the amount of hydrogen peroxide decomposition, induced by the initial ferrous ion (ferrous system) in the presence of RH, is smaller than in the absence of RH.

2.2.4.4 Influence of the pollutant concentration

Initial concentration of the pollutant: Usually lower initial concentration of the pollutants are favored [Kwon et al., 1999; Benitez et al., 2001a], but the negative effects of treating large quantity of effluent needs to be analyzed before the dilution ratio can be fixed.

In 2008 Lipczynska-Kochany and Kochany made a Table in their study to show the Concentrations of different pollutants and rates (*k*) of their reactions with $^{\bullet}OH$ radicals in some previous study (Table 2.2).

Table 2.2. Concentrations of pollutants of concern and rates (*k*) of their reactions with •OH radicals

Contaminants	Concentration (mg L^{-1})	K (M^{-1})(s^{-1})	Reference
Pollutants[a]			
Arsenic	9.2 ± 0.5	9×10^9	Buxton et al. (1988)
Cyanide	98.0 ± 0.5	7.6×10^9	Buxton et al. (1988)
Thiocyanate	460.0 ± 0.5	1×10^{10}	Buxton et al. (1988)
Phenol	41.0 ± 0.05	1×10^{10}	Buxton et al. (1988)
2,4-Diethylphenol	7.30 ± 0.06	1×10^{10}	Buxton et al. (1988)
Benzene	1.13 ± 0.05	7.8×10^9	Buxton et al. (1988)
Toluene	0.11 ± 0.02	3×10^9	Buxton et al. (1988)
o-Xylene	0.19 ± 0.03	6.7×10^9	Buxton et al. (1988)
m.p-Xylene	0.32 ± 0.065	7×10^9	Buxton et al. (1988)
Dichloromethane	0.09 ± 0.3	5.8×10^7	Buxton et al. (1988)
Anions			
Bicarbonate	238 ± 2	5.7×10^6	Kochany and lipczynska-kochany (1992)
Phosphate	9.8 ± 0.5	4.3×10^9	Kochany and lipczynska-kochany (1992)
Nitrate	12.0 ± 0.5		
Sulfate	33.0 ± 0.5		

[a] Contaminants of wastewater which were to be degraded by the Fenton reaction; in addition, the wastewater contained ammonia (890 mg L^{-1}) which was to be removed in the subsequent nitrification step (not described in this paper)

[b] Data for o-cresol.

In the work of Dutta et al. (2001), a dye solution of 3.13×10^{-5} mol dm^{-3} was stirred with 3.58×10^{-5} mol dm^{-3} Fe^{2+} and 4.41×10^{-4} mol dm^{-3} H_2O_2 solutions when a rapid

reaction occurred. After 10 min it came to a constant no more dye was decayed, rest of the reaction took about 2 h for practically complete degradation of the dye when the solution became colorless. The degradation reaction can be roughly divided into two phases: first 10 min of reaction occurs rapidly, and then sluggishly. It is clear that the lower concentration have a higher oxidation efficiency which is showed in the Table 2.3.

Table 2.3. Initial constant rates of degradation of methylene blue at different initial concentrations of dye.

Reactants	Initial concentration$\times 10^5$ ($moldm^{-3}$)	Initial rate $\times 10^5$ ($moldm^{-3}$ min^{-1})
Dye	3.13	0.81
	6.26	1.91
	9.39	3.23

2.2.4.5 Influence of temperature

In fact, Lin and Lo (1997) had reported an optimum temperature of 30 °C, whereas Rivas et al. (2001) reported that the degradation efficiency is unaffected even when the temperature is increased from 10 to 40℃, and also Rodrigues et al. (2008) reported that the degradation efficiency of the dye increased from 20 to 70℃. Nesheiwat and Swanson (2000) reported that if the reaction temperature is expected to rise beyond 40℃ due to exothermic reactions, cooling is recommended as above 40℃, efficiency of hydrogen peroxide utilization decreases due to accelerated decomposition of hydrogen peroxide into water and oxygen.

From the work of Dutta et al. (2001), the extent of degradation of the dye was observed when the reaction temperature was raised from 281 to 299 K. A further increasing in the reaction temperature from 299 to 313K resulted in the decrease in the extent of

degradation of the dye. Moreover, there was practically no difference in the rate and extent of degradation of the reaction in the temperature between 313 and 328 K. The author thought that at higher reaction temperatures, perhaps, the thermal decomposition of the hydrogen peroxide resulted in the reduction of its effective concentration towards making hydroxyl radicals, and this was possibly the reason behind lower conversion of the dye at higher reaction temperatures.

But, From the work of Rodrigues et al. (2008), under the catalyst dose of 0.27mM, the result illustrates that Fenton's process performance increases with temperature from 20 to 70℃, a trend that can be justified by the kinetic constants raise with that variable (Arrhenius law). However, such effect is much more pronounced on the mineralization rate (TOC removal). The author also pointed out that "For simple dye degradation temperatures of 20℃ are enough to provide fast decolourisation".

2.2.5 Disadvantages

Fenton's reagent over other oxidizing treatment methods are numerous, including high efficiency, simplicity in destroying the contaminants (eventually leaving no residues), stability to treat a wide range of substances, non-necessity of special equipment, etc. [Arnold et al., 1995]. Besides, operating conditions are usually mild (atmospheric pressure and around room temperature), and hydrogen peroxide is easy to handle and the excess decomposes to environmentally safe products [Kang and Hwang, 2000]. But the Homogeneously Fenton process has some significant disadvantages:

1. In the treatment of wastewater, it requires an application of acid and subsequently neutralization of the treated water what increases its salinity. In some cases, acidification of water may create gaseous emission problems when sulfides or cyanides are present. In the natural environment because of the strong buffering

capacity of groundwater and soil, acidification is often difficult and it could pollut the enviroment, and cause undesirable ecological impacts

2. During the reaction will generate the sludge. However, remove the sludge-containing Fe ions at the end of wastewater treatment are expensive and needs large amount of chemicals and manpower [Ramirez et al., 2007a].

3. Leads to high metal (iron or other transition metal) concentrations in the final effluent. Most of time the concentration was overcomes the legal limit of a country. Even though the metal recovery is possible, it would rise the costs and the complexity of the process [Duarte et al., 2009].

4. The catalyst used in the reaction can not be easily recovered by sedimentation or filtration for further uses.

2.3 Heterogeneous Fenton-like reaction

To overcome the disadvantages of the homogeneous Fenton process, some attempts have been made to develop heterogeneous catalysts, prepared by incorporating Fe ions or Fe oxides into porous supports [Gemeay et al., 2003; Ishtchenko et al., 2003; Letaief et al., 2003; Tachiev et al., 2000;]. In such cases, oxidation may potentially occur via iron ions released into solution or via reactions that take place between solutes and surface-bound species. Other transition metal complexes supported on several surfaces such as metal oxides, resins and mixed (Al-Cu) pillared clays have also been used as potentially active catalysts for the decomposition of H_2O_2 and for the oxidative degradation of organics [Carriazo et al., 2003; Ramirez et al., 2007a].

Thus, several studies have been made to find efficient heterogeneous systems, different types of solids can be used as heterogeneous catalysts. Among them iron powder and

different iron oxides have been tested [Hanna et al., 2008; Costa et al., 2008; Mecozzi et al., 2006; Lucking et al., 1998; Andreozzi et al., 2002a; Lu et al., 2002; Watts et al., 1999]. Solid catalysts can also be constituted by iron dispersed on different supports such as alumina [Al-Hayek and Dore, 1990], zeolite [Centi et al., 2000; Fajerwerg et al., 1996; Parkhomchuk (Kuznetsova) et al., 2008; Doocey et al., 2004], cation exchange resins [Liou et al., 2004] and clay [Barrault et al., 2000; Ramirez et al., 2008; Ramirez et al., 2007a], or carbons materials [Ramirez et al., 2007b]. All this process called heterogeneous Fenton-like or modified Fenton could avoid the initial acidification which may be costly and destructive for the *in situ* remediation of contaminated groundwater and soils, and also it could avoid other disadvantages of the classic Fenton reaction.

2.3.1 Iron oxides

Iron is the most abundant transition metal in the natural environment. It widely exists in the soil, fresh waters, ocean and atmosphere as mineral on the surface of the Earth. It plays a very important role in many biological and chemical processes. Its average concentration in the Earth's crust is around 5.6%. It usually exists in the form of oxides and hydroxides, which are hardly soluble in the aqueous solution. Since iron is one of the most abundant elements on the earth, many classes of iron metal, compounds, and mixtures are extensively used in industrial production and daily life, especially in chemical engineering as catalysts [Wu et al., 2006]. Different kinds of iron oxides, such as goethite, hematite, magnetite, and ferrihydrite, are among the most ubiquitous forms of iron species under environmental relative conditions (pH 4-9) [Kwan et al., 2002; Kwan et al., 2003; Petigara et al., 2002; Lin et al., 1998]. They show quite different catalytic activity due to the surface area or valence of iron [Kwan et al., 2003].

Several authors have reported that unlike the traditional Fenton's reagent, the reaction

of iron bearing minerals with hydrogen peroxide can effectively oxide the organic molecules at circumneutral pH, this systems can effectively oxidize pollutants at pH values from three to circumneutral through heterogeneous Fenton-like reactions [Lin and Gurol, 1998; Valentine and Wang, 1998; Watts et al., 1999; Kwan and Voelker, 2002; Kwan and Voelker, 2003; Matta et al., 2008; Hanna et al., 2008]. However, till now a consensus on the mechanism of this process does not exist [Barreiro et al., 2007]. Recent studies suggested that the process may be attributed to the generation of •OH radicals by H_2O_2 decomposition on surfaces of iron oxide particles [Lin and Gurol, 1998; Kwan and Voelker, 2002, 2004]. And the decomposition of H_2O_2 primarily takes place on the surface active sites of these iron oxides [Kwan et al., 2003; Petigara et al., 2002; Lin et al., 1998].

Heterogeneous Fenton-like process is a surface mineral-catalyzed system which can be explained by heterogeneous reactions occurring at the iron mineral surface [Lin and Gurol, 1998; Watts et al., 1999; Kwan and Voelker, 2002; Kwan and Voelker 2003]. The activity of the iron oxide used as catalyst depends on its characteristics such as crystallinity [Valentine and Wang, 1998; Miller and Valentine, 1999; Huang et al., 2001], surface area [Valentine and Wang, 1998; Miller and Valentine, 1999; Huang et al., 2001; Kwan and Voelker, 2004], iron content and/or iron oxidation sate [Matta et al., 2007; Hanna et al., 2008]. In surface-catalyzed mechanism, the interactions of H_2O_2 with iron oxide surface lead to the formation of $HO^{\bullet}$ radicals which attack the pollutants in either sorbed or aqueous phases [Lin and Gurol, 1998; Watts et al., 1999; Kwan and Voelker, 2002; Kwan and Voelker 2003]. Watts et al. [Watts et al., 1999] reported that different mechanisms may be occurred on the surface at high H_2O_2 concentration and the sorption rate could be a controlling factor of the whole catalytic oxidation reaction. The catalytic activity for hydrogen peroxide decomposition and/or organic compound oxidation were widely investigated using Fe^{III}-bearing minerals of different surface area [Lin and Gurol, 1998; Watts et al., 1999; Kwan and Voelker, 2002; Kwan and Voelker 2003; Valentine and Wang 1998; Miller and Valentine, 1999; Huang et al., 2001; Kwan and Voelker, 2004]. In these works, the authors proposed that

the surface area of the iron oxide accounts for the difference in reaction activity and the decomposition rates by goethite, ferrihydrite, and hematite were all relatively similar when normalized to surface area. So the decomposition of H_2O_2 on the surface may play a main role. But the authors such as Andreozzi et al. (2002a, b) suggested that the decomposition reactions occur through non-radical mechanisms. And also it was said that the consumption rate of H_2O_2 does not equal to the generation rate of $^{\bullet}OH$.

Another group of authors reported that the catalytic activity can be related to the activation of hydrogen peroxide by iron ions leached from the solid material and acting as homogeneous catalysts [Pera-Titus et al., 2004; Lucking et al., 1998]. Actually, in the presence of some natural ligands (oxalate, humic acid, et al.), however, iron is likely to be released from the oxide surface, increasing the contribution of solution phase reaction to the loss of H_2O_2 [Voelker et al., 1997; Kwan et al., 2002; Faust et al., 1984]. The authors [Fajerwerg et al., 1996; Kuznetsova et al., 2004] associated the catalytic activity to the combined and pH dependent effects of metal leaching and direct heterogeneous catalysis. In the latter case, the initiation step involves H_2O_2 adsorbed on the iron oxide surface [Kwan et al., 2003].

The disadvantage of using iron mineral is that the decomposition rate of organic contaminants is slower than in classic Fenton reaction using ferrous ions at acidic pH. In order to overcome these drawbacks of the homogeneous Fenton process, the Fe^{II}-bearing minerals have been used in the investigation of heterogeneous Fenton reaction. In this work, two kinds of iron oxides were chosen, both of them are iron (II, III) mixed oxide (Fe_3O_4). They were selected because of its FeII-structural content and its low solubility in reaction medium [Schwertmann and Cornell, 2000]. Experiments that evaluated different iron oxides under the same conditions exhibited differences in the degradation rates of hydrogen peroxide and contaminants. iron (II, III) mixed oxide (Fe_3O_4) was the most effective catalyst as compared to the other iron oxides [Tyre et al., 1991; Kong et al., 1998; Watts et al., 1999], because Fe_3O_4 contained FeII in it's structure, and the FeII-containing minerals are very interesting in the heterogeneous

Fenton reaction, FeII play an important role for the initiation of the Fenton reaction according to the classical Haber–Weiss mechanism [Hanna et al., 2005; Shiavello, 1987; Kwan and Voelker, 2003; Matta et al., 2008; Matta et al., 2007]. Iron oxide which had FeII in its structure can enhance the production rate of •OH.

2.3.2 Haber-Weiss (Haber and Willstätter) reaction

Haber and Willstätter believed that the mechanism by which enzymes reacted with substrates was via initiation of chain reactions, after which the enzyme played no direct role [Haber and Willstätter, 1931].

$$HO^{\bullet} + H_2O_2 \rightarrow H_2O + O_2^{\bullet-} + H^+ \quad (2.28)$$

$$O_2^{\bullet-} + H^+ + H_2O_2 \rightarrow O_2 + HO^{\bullet} + H_2O \quad (2.29)$$

The chain reactions (2.28) and (2.29) were originally proposed by Haber and Willstätter in a paper on radical reactions in organic chemistry and biochemistry, and specifically to explain the action of catalase [Haber and Willstätter, 1931]. The opinion of Haber and Willstätter was that enzymes initiated radical reactions, after which the chain reactions consumed the substrate. Iron just acted in the same way. Superoxide, hydrogen peroxide and the hydroxyl radical were proposed in the mid-twenties as chain carriers in combustion processes.

Haber and Weiss (1932) dismissed Fe_2O_5 and showed that even more hydrogen peroxide per iron(II) was consumed if the mixing of hydrogen peroxide with iron(II) was improved: they let one solution flow into the other from a rotating buret that was modified to have a horizontal tip. The interesting concept in their paper was that hydrogen peroxide was consumed by a chain reaction.

$Fe^{2+} + H_2O_2 \rightarrow Fe^{3+} + {}^{\bullet}OH + HO^{-}$ (chain initiation) (2.1)

Which is then followed by chain Reactions (2.28) and (2.29),

$HO^{\bullet} + H_2O_2 \rightarrow H_2O + O_2^{\bullet-} + H^{+}$ (2.28)

$O_2^{\bullet-} + H^{+} + H_2O_2 \rightarrow O_2 + HO^{\bullet} + H_2O$ (2.29)

while chain termination is caused by Reaction (2.30)

$Fe^{2+} + HO^{\bullet} + H^{+} \rightarrow Fe^{3+} + H_2O$ (2.30)

This is the so-called Haber-Weiss cycle. And Song et al. (2006) reported the mechanism of heterogeneous Fenton-like reaction may be happened like followed based on the Haber-Weiss cycle:

$\equiv Fe(II) + H_2O_2 \rightarrow \equiv Fe(III) + {}^{\bullet}OH + OH^{-}$ (2.31)

$\equiv Fe(III) + H_2O_2 \rightarrow \equiv Fe(II) + O_2^{\bullet-}/HO_2^{\bullet}$ (2.32)

$\equiv Fe(III) + O_2^{\bullet-}/HO_2^{\bullet} \rightarrow \equiv Fe(II) + O_2$ (2.33)

$\equiv Fe(II) + O_2^{\bullet-}/HO_2^{\bullet} \rightarrow \equiv Fe(III) + H_2O$ (2.34)

Some authors suggested an initial step of fast adsorption of the H_2O_2 molecule on (≡Fe(III)) sites [Dantas et al., 2006] and others the adsorption of the organics [Feng et al., 2006]. Even a consensus on the mechanism of this process does not exist, Nevertheless, the involvement of the these steps has been suggested in most of the works found in the literature, which correspond to Fe^{3+} reduction with generation of less oxidative $HO_2^{\bullet}$ radicals (reaction 2.32), followed by Fe^{3+} regeneration with

formation of the hydroxyl radicals. The symbol ≡ in the reaction (2.31) to (2.34) represents the surface of the catalyst. However, it must be remarked that the radicals can also be generated in the surface of the solid so they are actually ‘‘caged’’ in the solid structure, subsequently reacting with the adsorbed reagent(s) without radicals generation. Obviously, besides the indicated steps many other radical reactions occur, including those involving the reaction intermediates [Ramirez et al., 2007a].

The usage of heterogeneous Fenton-like reaction often combined with other AOPs technologies to improve the oxidation efficiency in recent years. It used to be named heterogeneous advanced Fenton process (AFP). Such as applied UV in the Fenton-like system, which was the so called Photo assist Fenton-like reaction, and also Ultrasonic, electrochemical methods, and so on. Table 2.4 showed some works recent years about using heterogeneous Fenton oxidation process to oxidize the pollutant including some works combined with other AOPs processes.

Table 2.4. The list of the chemicals degraded by heterogeneous Fenton oxidation in recent years.

Pollutants	Catalysis	Referance
1. Black 5 (RB5), Orange II	Fe_3O_4	Shin et al., 2008
2. Black 5 (RB5)	Fe^{3+}-containing ashes	Flores et al., 2008
3. Methylene blue	Fe^0/Fe_3O_4	Regina et al., 2008
4. Methyl red (MR)	Iron(III) / silica	Hanna et al., 2008
5. Pentachlorophenol (PCP)	Fe (II, III) oxide	Xiaofei et al., 2009
6. Methylene blue	Nb_2O_5/iron oxides	Oliveira et al., 2007
7. Orange II	$FeVO_4$	Deng et al., 2008
8. Dimethyl sulphoxide	α-FeOOH	Wu et al., 2006
9. Black 5 (RB5), EDTA	Zero Valent Iron (Fe^0)	Zhou et al., 2008
10. Methylene blue	Fe_{3-x}/Ti_xO_4	Yang et al., 2009
11. Propene	$FeSbO_4$	Zhang et al., 2008
12. Methane	CeO_2/Fe_2O_3	Li et al., 2008
13. Alcohols, olefins	Fe_2O_3	Shi et al., 2008
14. Phenol	Fe_2O_3	Zelmanov and Semiat, 2008
15. Methyl red	quartz/ iron(III) oxide quartz/maghemite quartz/magnetite	Hanna et al., 2008

	quartz/goethite	
16. 4-chlorophenol	Zero valent iron (Fe^0)	Zhou et al., 2008
17. Quinoline	α-FeOOH	Guimarães et al., 2008
18. Rhodamine B (RhB)	Fe (II, III) oxide	Xiaofei et al., 2008
19. 1,1-dimethylhydrazine	FeZSM-5	Makhotkina et al., 2006
20. Cinnamic acid	Fe/ montmorillonite	Tabet et al., 2006
21. Bisphenol A	Al_2O_3/Fe_2O_3	Li et al., 2007
22. Carbon tetrachloride	Valent iron metal (Fe^0)	Johnson., 2008
23. Orange II	Carbon/Fe	Ramirez et al., 2007
24. Polyacrylamide	$Fe(III)/SiO_2$	Liu et al., 2009
25. Reactive brilliant orange	Fe/Mt	Chen et al., 2009
26. Benzoic acid	Silica/ Fe_2O_3	Isabel Pariente et al., 2008
27. Remazol Brilliant Orange	Zeolite/ $Fe(NO_3)_3$	Tekbaş et al., 2008
28. Acid Blue 74	Fe-exchanged zeolite (Fe-ZSM5/ zeolite)	Kasiri et al., 2008
29. Quinoline	Goethite (αFeOOH)	Guimarães et al., 2008
30. Methylene blue	Tri-nuclear ferric acetate complex ion	León et al., 2008
31. Volatile organic compounds (industries)	Fe powder	Tokumura et al., 2008
32. Reactive black 5 (RB5)	Fe^{3+}-containing ashes	Flores et al., 2008
33. Phenolic wastewaters	Zero-valent iron (Fe^0)	Chakinala et al., 2007
34. Reactive brilliant red X-3B	Fe–Ce oxide	Zhang et al., 2007
35. Acid Violet 7	$Fe(III)oxalate/Al_2O_3$	Muthuvel et al., 2007
36. P-chlorophenol	Powder copper oxide (CuO) (Cu/Al), (Cu/Zn)	Kim et al., 2007
37. Phenol	SiO_2–Fe_2O_3 mixed oxide	Martínez et al., 2005
39. Pentachlorophenol (PCP)	Electric arc furnace	Mecozzi et al., 2006
40. Phenol	Fe-exchanged zeolite (Fe-ZSM5/ zeolite)	Kušić et al., 2006
41.Textile wastewater	Fe_2O_3/carbon	Dantas et al., 2006
42. Orange II	Fe/bentonite clay	Feng et al., 2006a
43. Indigo Carmine	Fe/bentonite clay	Feng et al., 2006b
44. Reactive Orange 4 (RO4)	Perrioxalate /TiO_2-P25 Perrous sulphate/ TiO_2-P25	Selvam et al., 2005
45. Phenol	Iron-containing SBA-15 Material	Martínez et al., 2005
46. 2,4-xylidine	Fe-exchanged zeolite (Fe-ZSM5/ zeolite)	Rios-Enriquez et al., 2004
47. Ethanol	Fe-containing zeolites	Kuznetsova et al., 2004
49. Reactive Red HE-3B	Laponite clay-based Fe	Feng et al., 2003

2.4 Model pollutant

The elimination of organics from industrial wastewater is an important environmental target. It is estimated that every year more than 1000 new organic compounds are commercialized [Seignez et al., 1992]. The big economic profits resulting from the utilization of new products have usually neglected the environmental risks inherent in their use. Because of an increasing social and political concern on environment, the research field of water purification has been extensively growing in the last decades, comprising both polluted wastewaters and groundwaters from seas, rivers and lakes, as water quality control and regulations against hazardous pollutants have become stricter in many countries [Pera-Titus et al., 2004]. In this work we had chosen two kinds of representative pollutants as our model pollutants, which are widely used chemicals all over the world, toxic, resistant to biodegradation and hard to degradation.

2.4.1 Pentachlorophenol (PCP)

Pentachlorophenol (PCP) belongs to Chlorophenols (CPs) which are environmental pollutants of great health concerning. Among the CPs there are 19 different chlorophenols, 2-chlorophenol (2-CP), 2,4-dichlorophenol (2,4-DCP), 2,4,6-trichlorophenol (2,4,6-TCP) and pentachlorophenol (PCP) have been listed by the US EPA as priority pollutants [Ormad, et al., 2001]. CPs is introduced into the environment as a result of several man-made activities. Because of their broad-spectrum antimicrobial properties, CPs has been used as preservative agents for wood, paints, vegetable fibers and leather and as disinfectants. In addition, they have been widely employed in many industrial processes as synthesis intermediates or as raw materials in the manufacturing of herbicides, fungicides, pesticides, insecticides, pharmaceuticals and dyes [Pera-Titus et al., 2004]. Chlorination of phenols during the disinfection of waste water also produces chlorophenols. CPs may be also generated as by-products during waste incineration, the bleaching of pulp with chlorine, and in the

dechlorination of drinking water [Ahlborg ad Thunberg, 1980].

Chlorophenols (CPs) constitute a particular group of priority toxic pollutants listed by the US EPA in the Clean Water Act [EPA, 2002; Hayward, 1998; Keith and Telliard, 1979] and by the European Decision 2455/2001/EC [EC Decision, 2001], because most of them are toxic and hardly biodegradable, and are difficult to remove from the environment—the half-life in water can reach 3.5 months in aerobic waters for PCP and some years in organic sediments [Abe and Tanaka, 1997]. Because of their numerous origins, they can be found in ground waters, wastewaters and soils [Wegman and Van den Broek, 1983] and even in the trophic chain of places with very low pollution levels [Paasivirta et al., 1980; WHO, 1989]. These result in contamination of many lakes and water streams by chlorophenols [Keating et al., 1978; Othmer et al., 1979; Prengle et al., 1976]. Due to their toxicity, they are consequently harmful to human, animal, and fish that are exposed to such contaminated environments. Thus, the removal or destruction of these compounds by other chemical or physical means must be required. They might produce disagreeable taste and odor to drinking water at concentrations below 0.1μg L^{-1} [Veschueren, 1983] and adverse effects on the environment [Folke and Birklund, 1986].

All CPs possess bactericidal activities, phytotoxicity and ability to bioaccumulate in organisms that increase with increasing the chlorination and substitution away from the ortho-(2-) position. The higher toxicity of the more chlorinated CPs may be ascribed to an increase in lypophility which leads to a greater potential for uptake into the organism. The ortho-substituted congeners are generally of lower toxicity than the meta-and para-ones, because ortho-substituted chlorine seems to shield $^{\bullet}OH$ group, which apparently interacts with the active site in aquatic organisms [Grimwood and Mascarenhas, 1997]. On the other hand, toxicity also depends on the extent to which CP molecules are dissociated, with an increasing toxicity when the pH decreases, because the more toxic non-dissociated forms predominate at lower pH [Pera-Titus et

al., 2004].

The presence of CPs has been detected in both surface and groundwaters [Howard, 1989]. Toxic reference values of 43.8, 36.5 and 13.0μg L^{-1} are, respectively, suggested for 2-MCP, 2,4-DCP and PCP in surface waters, and maximum average values should not exceed 2.020, 4.380 and 0.055 mgL^{-1} [EPA,1992b]. The limiting permissible concentration of CPs in drinking water should not exceed 10μg L^{-1} [Shulpin et al., 1997].

Nowadays, many kinds of AOPs processes were used to degradation and mineralization of CPs. Among the various AOPs proposed in the literature, there are four main kinds [Glaze, 1994; Prousek, 1996]. They are: (1) Photolysis (UV or VUV). (2) Hydrogen peroxide (H_2O_2) (classic Fenton/Fenton-like/Photo-Fenton), (3) Ozone (O_3) and (4) Heterogeneous catalysis + UV and photocatalysis. Pentachlorophenol (PCP) has been used as an industrial antiseptic and biocide for many decades since the 1960s. Some data concerned the degradation of several CPs by Fenton-like reagents involving different catalytic solids with ferrous ions are summarized in Table 2.5.

Table 2.5. Half-life times and pseudo-first kinetic constants for degradation of CPs by Fenton-like reagent for different initial concentrations of CP, H_2O_2 and Fe^{2+} charge on the surface of the solid at pH 3.0 [Pera-Titus et al., 2004].

CP congener	Solid	$[CP]_0$ (mM)	CP $t_{1/2}$ (min)	k_{CP} (min^{-1})	Reference
2-MCP	GAC-Fe	-	426	2.27×10^{-3}	Huling et al., 2000
2-MCP	Goethite	0.39	174	2.47×10^{-2}	Lu, 1999
2-MCP	Goethite	0.39	36	2.75×10^{-2}	Lu, 1999
2-MCP	Goethite	0.39	30	2.24×10^{-2}	Lu, 1999
2-MCP	Goethite	0.31	252	1.33×10^{-2}	Lu, et al., 2002
4-MCP	Iron powder	7.78	1.5	1.40×10^{-2}	Lücking et al., 1998
4-MCP	Graphite-Fe	7.78	Not reached	$5..38 \times 10^{-5}$	Lücking et al., 1998
4-MCP	GAC F-300	7.78	810	1.32×10^{-5}	Lücking et al., 1998
4-MCP	GAC GCW	7.78	311	3.30×10^{-5}	Lücking et al., 1998
4-MCP	GAC ROW	7.78	240	6.14×10^{-5}	Lücking et al., 1998
4-MCP	GAC RFZ	7.78	59	2.52×10^{-4}	Lücking et al., 1998
2,4,5-TCP	Nafion membrane	68.0[a]	Not reached	-	Sabhi and Kiwi, 2001

[a] Data referred to TOC.

Due to its proven carcinogenicity and toxicity, as well as the existence of a large number of known PCP contaminated sites, PCP has been designated as a "priority toxic pollutant" by the United States Environmental Protection Agency (EPA) under the guidance of the Clean Water Act in 1972 [Duan et al., 2008]. Pentachlorophenol (PCP) is a widespread environmental contaminant due to its use for wood preservation and as a pesticide. PCP contamination can be found in surface, ground waters and in soils, in the vicinities of past wood-treating facilities [Schellenberg et al., 1984; EPA, 1992a]. The relative resistance of PCP to biological degradation, the reason for its use as a preservative, creates a serious pollution problem. Mueller et al. [Mueller et al., 1991] and McAllister et al. [McAllister et al., 1996] found that only 42% of the PCP in groundwater was completely degraded after 14 days.

In recent years, Advanced Oxidation Processes (AOPs) has appeared as a logical alternative to biodegradation [Fukushima et al., 2001; Oturan et al., 2001; Hanna et al., 2004; Hanna et al., 2005]. As we mentioned before that these processes based on hydroxyl radical chemistry are currently used for the destruction of organic compounds. The hydroxyl radicals react in a non-selective way on organic compounds leading finally to the mineral end-products [Shiavello, 1987]. But till now there are not too much work about using iron oxides/H_2O_2 (heterogeneous Feton-like system) to degradation PCP. Actually, in recent years, the degradation of PCP by Fenton's reagent [Fukushima and Tatsumi, 2001; Oturan et al., 2001; Hanna et al., 2005] and Fenton-like system [Watts et al., 1993] was mainly reported at acidic conditions (pH = 3-5). In contrast, the Fenton-like degradation of PCP using iron minerals at neutral pH was scarcely investigated. Moreover that, the role played by the adsorption at solid surface in the oxidation of pollutant in heterogeneous Fenton reaction is poorly described. And the surface interactions of species with iron surface sites involving both sorption and decomposition reactions are scarcely investigated [Xiaofei et al., 2009]. Our work focused on using heterogeneous Fenton reaction at neutral pH, to investigate the mechanism of oxidation of PCP.

2.4.2 Rhodamine B (RhB)

Millions of various colored chemical substances have been generated within the last century or so, 10,000 of which are industrially produced [Zollinger, 1991]. On a global scale, over 0.7 million tons of organic synthetic dyes are manufactured each year mainly for use in the textile, leather goods, industrial painting, food, plastics, cosmetics, and consumer electronic sectors. A sizable fraction of this is lost during the dying process and is released in the effluent water streams from the above industries. Synthetic dyes exhibit considerable structural diversity (Figure 2.12). The chemical classes of dyes employed more frequently on industrial scale are the azo,

anthraquinone, sulfur, indigoid, triphenylmethyl (trityl), and phthalocyanine derivatives [Forgacs et al., 2004]. Therefore, decolorization and detoxification of organic dye effluents have taken an increasingly important environmental significance in recent years [Brown et al., 1993; Rajeshwar et al., 1997].

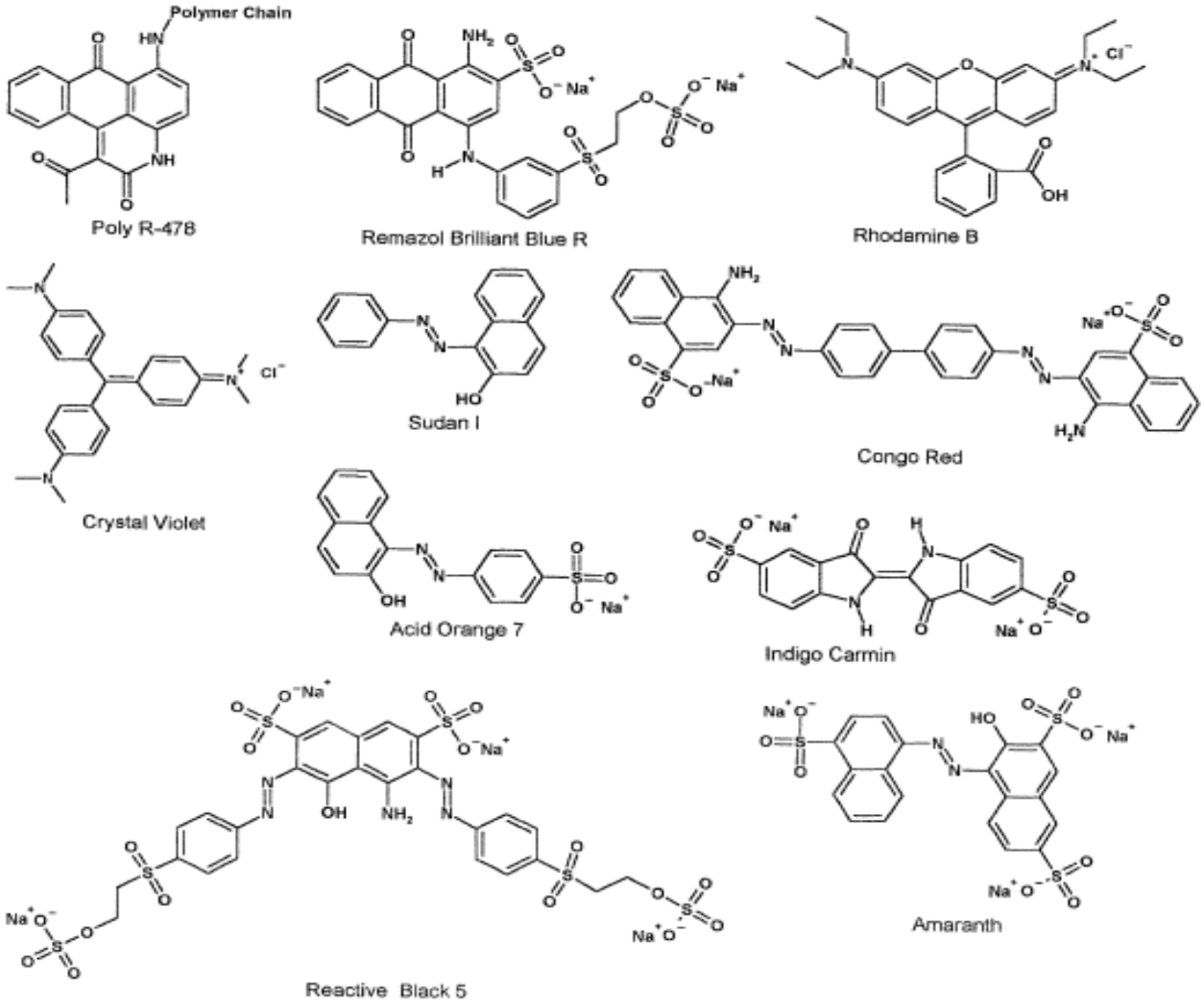

Figure 2.3. The chemical structure of synthetic dyes most frequently studied in degradation experiments [Forgacs et al., 2004]

Unfortunately, the exact amount of dyes produced in the world is not known. It is

estimated to be over 10,000 tons per year. Exact data on the quantity of dyes discharged in the environment are also not available. It is assumed that a loss of 1–2% in production and 1–10% loss in use are a fair estimate. For reactive dyes, this figure can be about 4%. Due to large-scale production and extensive application, synthetic dyes can cause considerable environmental pollution and are serious health-risk factors [Forgacs et al., 2004]. Color is one of the most hated pollutants, because of several reasons: (i) it is visible and even small quantities of dyes (≥0.005 mg/L) are not allowed [He et al., 2007]; (ii) color can interfere with transmission of sunlight into natural streams; (iii) many of the azo dyes and their intermediate products, such as aromatic amines, are toxic to aquatic life, carcinogenic and mutagenic to humans [Flores et al., 2008; Lucas and Peres, 2006; Ince et al., 1997; Chung et al., 1992]. Although, the growing impact of environmental protection on industrial development promoted the development of ecofriendly technologies [Desphande, 2001], reduced consumption of freshwater and lower output of wastewater [Knittel and Schollmeyer, 1996; Petek and Glavic, 1996], the release of important amounts of synthetic dyes to the environment causes public concern, legislation problems and are a serious challenge to environmental scientists.

A wide range of methods has been developed for the removal of synthetic dyes from waters and wastewaters to decrease their impact on the environment. Most conventional methods for the removal of dye pollutants such as adsorption on activated carbon, ultrafiltration, reverse osmosis, etc. are non-destructive and merely transfer pollutants from one phase (for example, aqueous) to the other (for example, adsorbent). Biodegradation is slow and inefficient for many azo dyes and does not work at all for others (for example, Acid Orange 7). Chlorination and ozonation are also relatively inefficient and have high operating costs [Rajeshwar et al., 2008]. Thus, Advanced Oxidation Processes (AOPs), which relies on the generation of hydroxyl and other radical species for environmental remediation, have been successfully deployed for the treatment of organic dye-laden waters [Brown et al., 1993; Legrini et al., 1993; Helz et al., 1994; Spadaro et al., 1994].

Rhodamine B (RhB), one of the most important xanthene dyes, which is highly water soluble, basic red dye of the xanthene class. It is found as a reddish violet power and comes under the trade name of D & C Red No. 19 [Jain et al. 2007]. It is widely used as a colorant in textiles and food stuffs, and is also a well known water tracer fluorescen [Richardson et al., 2004]. It is harmful if swallowed by human beings and animals, and causes irritation to the skin, eyes and respiratory tract [Rochat et al., 1978]. The carcinogenicity, reproductive and developmental toxicity, neurotoxicity and chronic toxicity towards humans and animals have been experimentally proven [Kornbrust and Barfknecht, 1985; IARC, 1987; Mirsalis et al., 1989; McGregor et al., 1991; Shimada et al., 1994]. Thus Rhodamine B, xanthene dye, has become a common organic pollutant. It is a very stable non-volatile dye usually used in factory, has a comparatively high resistance to photo and oxidation degradation [Mittal and Venkobachar, 1996; Ai et al., 2007]. It is needed to remove Rhodamine B from wastewaters using the efficiency way and it is meaningful to be chosen as the model pollutant in this work.

CHAPTER 3

CHAPTER 3. EXPERIMENTAL MATERIAL, METHODS AND PROCEDURES

3.1 Material

3.1.1 Iron oxides

Three kinds of Iron (II, III) oxide purchased from Aldrich (Chemical Co.), Prolabo (Chemical Co.) named M1 and M2 respectively.

3.1.2 Model pollutant

Pentachlorophenol (PCP)

Pentachlorophenol (PCP) was procured from Sigma-Aldrich (99% purity), C6HCl5O mol. wt. 266.34, which is Biocide (Wood preservative) Priority organic pollutant (EPA, 1980), Widespread in contaminated sites, Hydrophobic (very low water soluble), Weak acid (pKa = 4.75), Aqueous solubility and Kow depend on pH and ionic strength.

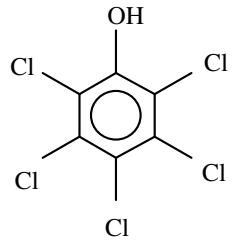

Rhodamine B (RhB)

Rhodamine B C28H31N2O3Cl; mol. wt. 479; IUPAC Name N-[9-(ortho-carboxyphenyl)-6-(diethylamino)-3H-xanthen-3-ylidene] diethyl ammonium chloride) was procured from Sigma-Aldrich (>99% purity), which is a common organic pollutant. As the chemical structure indicated above, it is a highly water soluble, basic red dye of the xanthene class. It is found as a red dish violet powder and

comes under the trade name of D & C Red No. 19. It is widely used as a colorant in textiles and food stuffs, and is also a well-known water tracer fluorescent [Richardson et al., 2004]. It is a very stable non-volatile dye usually used in factory, has a comparatively high resistance to photo and oxidation degradation.

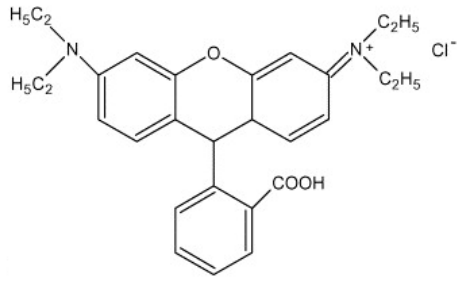

3.1.3 Reagents

Hydrogen peroxide (H_2O_2 35% w/w) Merck

Sodium hydroxide, Prolabo, > 97%

Ammonium acetate, Aldrich, > 98%.

Ferric chloride, Fluka, >99%.

Phosphoric acid, Sigma-Aldrich, > 85%

Acetic acid, Aldrich, > 99%.

Hydrochloric acid, Merck (0.1 M)

Perchloric acid, Merck, > 97%.

Acetonitrile Fluka, HPLC grade

1, 10-phenanthroline Sigma, > 99%.

Ferrous ammonium sulfate, Prolabo, >98%

Oxalic acid, Prolabo, > 99%

Ethylene Diamine Tetraacetic Acid (EDTA), Alfa Aesar, > 99%

Carboxymethyl-β-cyclodextrin (CMCD), Cyclolab, > 95%

Tartaric acid, Citric Acid, Succinic Acid, Sigma, > 99%.

N,N-diethyl-p-phenylenediamine, Sigma-Aldrich, > 99%

Horseradish peroxidase, Sigma-Aldrich, > 99%

Disodium hydrogen phosphate, Fischer Scientific

Sodium dihydrogen phosphate, Prolabo, > 99%

Ferrous sulfate, Alfa Aesar, > 99%

Ferric sulphate, Prolabo, > 99%

Ammonium acetate, Aldrich, > 98%

All solutions and suspensions were prepared from 18 MΩ/cm resistivity water (Mini-Q, Millipore)

3.2 Preparation of solution

3.2.1 Preparation the stock solution

(a) Pentachlorophenol (PCP) stock solution

0.1g of Pentachlorophenol was diluted to 1000 ml by using appropriate of Milli-Q water and set the pH of the stock solution at 10 at room temperature, protecting the light and stirring over night to get the desired concentration of Pentachlorophenol.

(b) Rhodamine B (RhB) stock solution

4.79g of Rhodamine B was diluted to 1000 ml by using appropriate of Milli-Q water into glass flask at room temperature, protecting the light and stirring until the total chemical dissolved.

(c) Ferrous iron stock solution

2.78g of ferrous sulfate ($FeSO_4 \cdot 7H_2O$) was diluted to 1000 ml by using appropriate volume of Milli-Q water into glass flask at room temperature, protecting the light and stirring until the total chemical dissolved.

(d) Ferric iron stock solution

3.998g of ferric sulphate $Fe_2(SO_4)_3$ was diluted to 1000 ml by using appropriate

volume of Milli-Q water into glass flask at room temperature, protecting the light and stirring until the total chemical dissolved.

(e) *N*,*N*-diethyl-*p*-phenylenediamine (DPD) stock solution

0.1g of N,N-diethyl-p-phenylenediamine dissolved by using appropriate volume of 0.1 M H_2SO_4 solution to make the stock solution, and then keep the solution immediately in the dark at 5□. The solution should be refreshed at most two weeks from the day prepared.

(f) Horseradish peroxidase (POD) stock solution

10 mg horseradish peroxidase was dissolved in 10 ml of Milli-Q water, the solution immediately in the dark at 5□. The solution should be refreshed at most two weeks from the day prepared.

(g) Phosphate buffer solution (pH 6)

12.3% of $Na_2HPO_4 \cdot 2H_2O$ (0.2mol/L) solution mixed with 87.7% of $NaH_2PO_4 \cdot 2H_2O$ (0.2mol/L) solution into glass flask at room temperature.

(h) Ammonium acetate buffer

24g $NH_4C_2H_3O_2$ was dissolved into 15ml of Milli-Q water mixed with 75ml of acetic acid solution into glass flask at room temperature.

(i) 1, 10-phenanthroline stock solution

0.1g of 1, 10-phenanthroline was diluted to 100 ml by using appropriate volume of acidification Milli-Q water (two drop of hydrochloric acid) into glass flask at room temperature, protecting the light and stirring until the total chemical dissolved.

(j) Ethylene Diamine Tetraacetic Acid (EDTA) stock solution

29.22g of ethylene diamine tetraacetic Acid was diluted to 1000 ml by using

appropriate volume of Milli-Q water.

(k) Carboxymethyl-β-cyclodextrin (CMCD) stock solution

7.4g of carboxymethyl-β-cyclodextrin was diluted to 50 ml by using appropriate volume of Milli-Q water.

(l) Oxalic acid stock solution

9.00g of ethylene diamine tetraacetic Acid was diluted to 1000 ml by using appropriate volume of a Milli-Q water.

(m) Tartaric Acid stock solution

15.01g of ethylene diamine tetraacetic Acid was diluted to 1000 ml by using appropriate volume of Milli-Q water.

(n) Citric Acid stock solution

19.21g of ethylene diamine tetraacetic Acid was diluted to 1000 ml by using appropriate volume of Milli-Q water.

(o) Succinic Acid stock solution

11.81g of ethylene diamine tetraacetic Acid was diluted to 1000 ml by using appropriate volume of Milli-Q water.

3.2.2 Preparation of the reaction solution

(a) Preparation of homogeneous Fenton-like solution

After calculation of each experiment, then take the appropriate volume of rhodamine B (RhB) stock solution or pentachlorophenol (PCP) stock solution, and after that add appropriate volume of ferrous iron stock solution or ferric iron stock solution, at the

end add appropriate amount of H_2O_2 into the mixed solution. The total amount of solution was fixed using Milli-Q water. The pH was set at 7. The reaction solution of each experiment was freshly prepared.

(b) Preparation of heterogeneous Fenton-like solution

After calculation of each experiment, then take the appropriate volume of rhodamine B (RhB) stock solution or pentachlorophenol (PCP) stock solution (The pH was set at 7), after that put appropriate amount of iron oxides into the solution and stirring for 1h to let the pollutant adsorbed onto the surface of iron oxides reach equilibrium. At the end add appropriate amount of H_2O_2 into the solution to start the reaction (check the pH and set at 7 again).

(c) Preparation of heterogeneous Fenton-like solution under using of chelating agent

After calculation of each experiment, the solution was prepared like the step: (a) take the appropriate volume of rhodamine B (RhB) stock solution or pentachlorophenol (PCP) stock solution, (2) put appropriate amount of iron oxides into the solution, (3) add appropriate amount of chelating agent, (4) pH was set at 7 and after that stir for 1h, (5) add appropriate amount of H_2O_2 to start the reaction (check the pH set at 7 again).

3.3 Reactor of the experiment

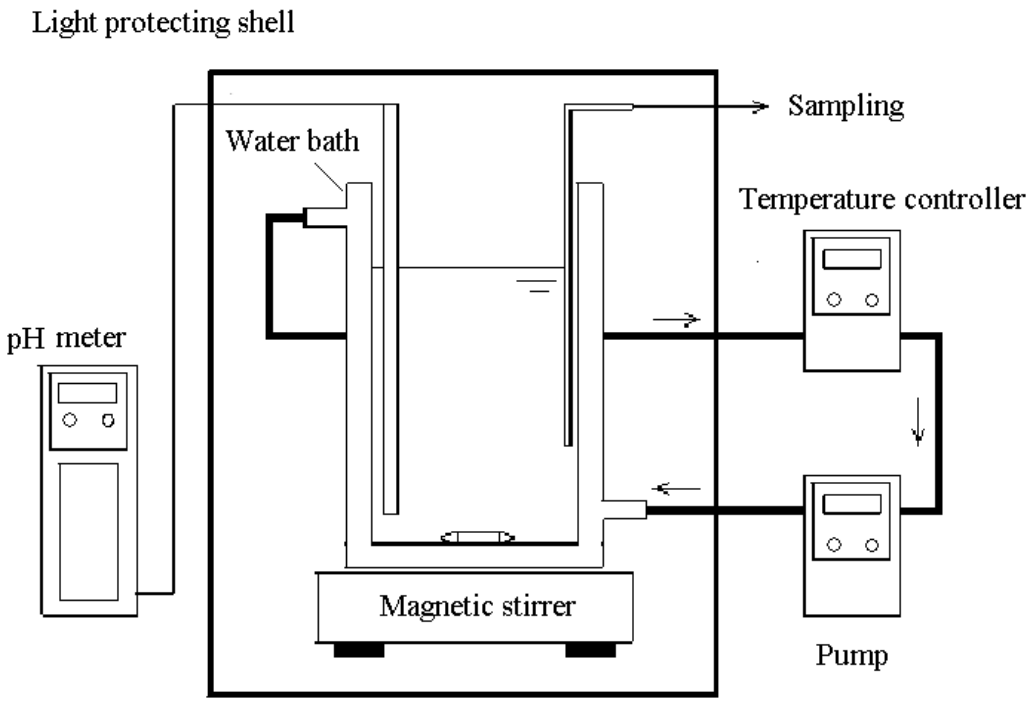

Firgue 3.1. The reactor of the experiment

It can be seen form Firgue 3.1, the experiment was carried out in a home-made reactor. Outside the reactor there is a water bath shell to keep the reaction solution at a fixed temperature. Out side the bottom of the reactor is a magnetic stirrer which used to let the reaction solution equal to any part. Outside all these there is a light protecting shell to protect any light from the reaction. The pH meter was used to check the pH of the solution periodically, and then modified the pH to 7.

3.4 Analytical method

3.4.1 PCP analysis by reversed phase liquid chromatography (HPLC)

The decay of PCP was followed by reversed phase liquid chromatography (HPLC) with a Waters HPLC Detector (486) fitted with a C-18 column (250 mm×4.6 mm i.d., 5 μm). The mobile phase was a mixture of water/acetonitrile (40:60 v/v) and pH at 3 (using acetic acid). The flow rate of the mobile phase was set at 2.5 mL min^{-1} in the isocratic mode. Detection was carried out at 238 nm. AT this machine condition the main peak of the PCP was shown at 2.5-3min, and the concentration of the PCP in the solution was determined by the peak area which calculated by the detector. The PCP degradation was used in the study, which is defined as follows:

PCP degradation ratio = $(1- C_t/C_0) \times 100\%$

where C_t and C_0 are the concentration of PCP at the reaction time t and 0 respectively. The calibration curve was prepared using different concentration of RhB, which was showed in Figure 3.2.

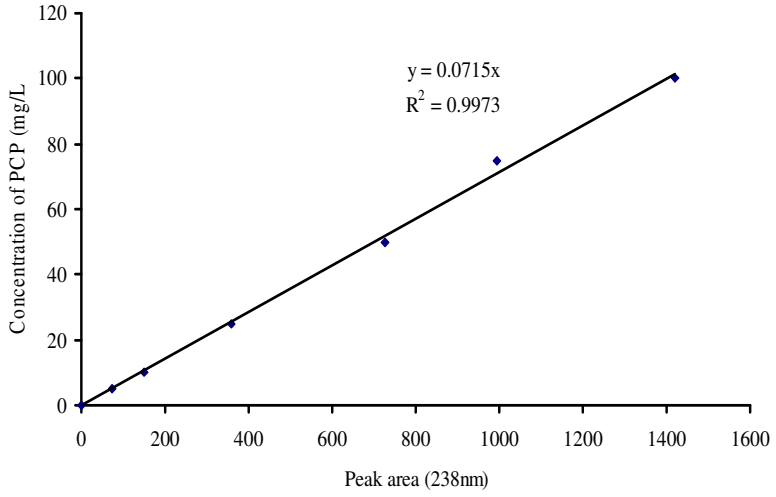

Figure 3.2. Calibration curve of PCP

3.4.2 RhB analysis by UV–Vis spectrophotometer

RhB concentration in solution was determined by measuring the absorbance using a UV-Vis spectrophotometer (Perkin-Elmer) at 554nm, using a 1 cm quartz cell.

The UV-VIS spectra of the RhB azo was recorded from 200 to 800nm using UV-Vis spectrophotometer (Perkin-Elmer). The concentration of RhB in water was determined by the absorption intensity at λ_{max}. The RhB degradation was used in the study, which is defined as follows:

RhB decolorization = $(1- C_t/C_0) \times 100\%$

where C_t and C_0 are the concentration of RhB at λ_{max} of the reaction time t and 0 respectively. The calibration curve was prepared by using different concentration of RhB, which was showed in Figure 3.3.

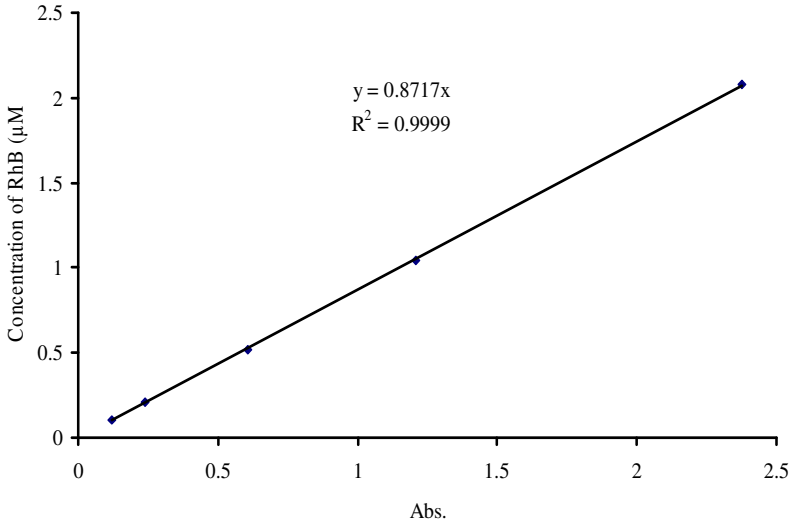

Figure 3.3. Calibration curve of RhB.

3.4.3 H_2O_2 analysis by UV–Vis spectrophotometer using modified N,N-diethyl-p-phenylenediamine (DPD) method

H_2O_2 was measured using the modified *N*,*N*-diethyl-*p*-phenylenediamine DPD method [Wu et al., 2006].

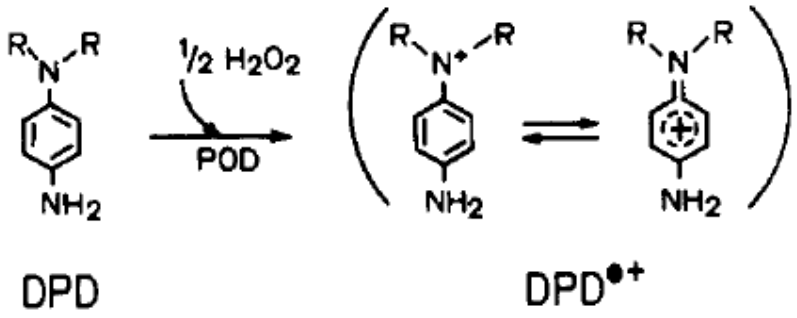

Figure 3.4. The reaction of the DPD method [Bader et al., 1988].

This method is based on the horseradish peroxidase (POD)-catalyzed oxidation by H_2O_2 of *N*,*N*-diethyl-*p*-phenylenediamine (DPD) Figure 3.4. This method measures H_2O_2 concentrations over the range 5–50 μmol L^{-1}. Because the H_2O_2 concentrations in the experimental reactors were above this range, each sample was diluted. The steps to prepare the solution and then to detected were shown from (1) to (6). Before the experiment all glassware was throughly washed hydrochloric acid and rinsed with Mini-Q water for dilution. Any contact of samples with metal surfaces was avoied and Eppendorf pipettes with plasitic tips were used.

(1) Dilute the samples.

(2) 0.5 ml of phosphate buffer (pH 6.0) and 5 ml aliquot of diluted sample was mixed in the reaction vial.

(3) An aliquot of 50 μL of DPD reagent (3.8×10^{-2} M in 0.1 M H_2SO_4)

(4) An aliquot of 50 µL (100 units mL^{-1}) horseradish peroxidase were then added to reaction vial.

(5) The cell was manually shaken for a minute for color development.

(6) Absorbance readings were taken at 551 nm using a UV–Vis spectrophotometer.

A series of iron standards is measured at wavelength of 551nm and a calibration plot of absorbance vs. concentration is prepared in the Figure 3.5:

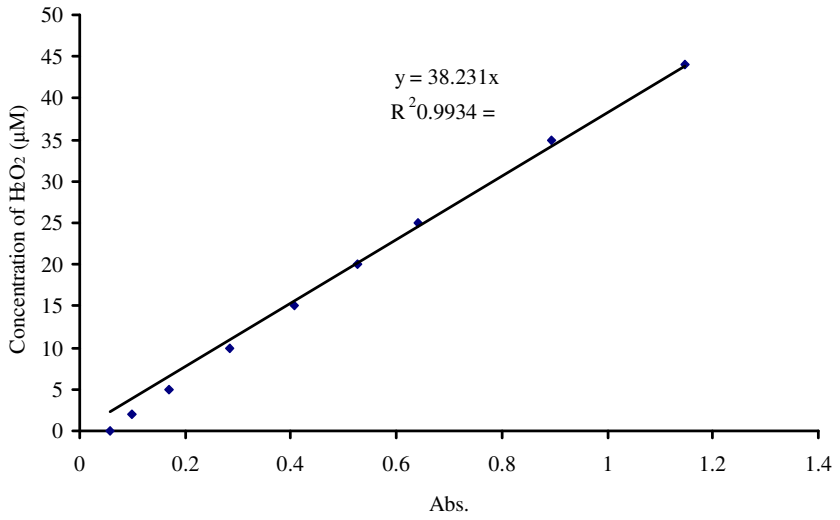

Figure 3.5. Calibration curve of H_2O_2

3.4.4 Dissolved ferrous iron (Fe^{II}) analysis by UV–Vis spectrophotometer using 1, 10-phenanthroline method

Ferrous iron was measured using the modified method 1, 10-phenanthroline. This experiment was determined by firstly, the ferrous iron react with 1, 10-phenanthroline to form a colored complex and then measuring the amount of light absorbed by this

complex using the machine Agilent 8543 spectrophotometer fixing λ at 510 nm. The ferrous iron of plotting the calibration curve was from the ferrous ammonium sulfate ($Fe(NH_4)_2(SO_4)_2\ 6H_2O$) salt.

The reaction ferrous iron complex with 1, 10-phenanthroline can be showed like the Figure 3.6:

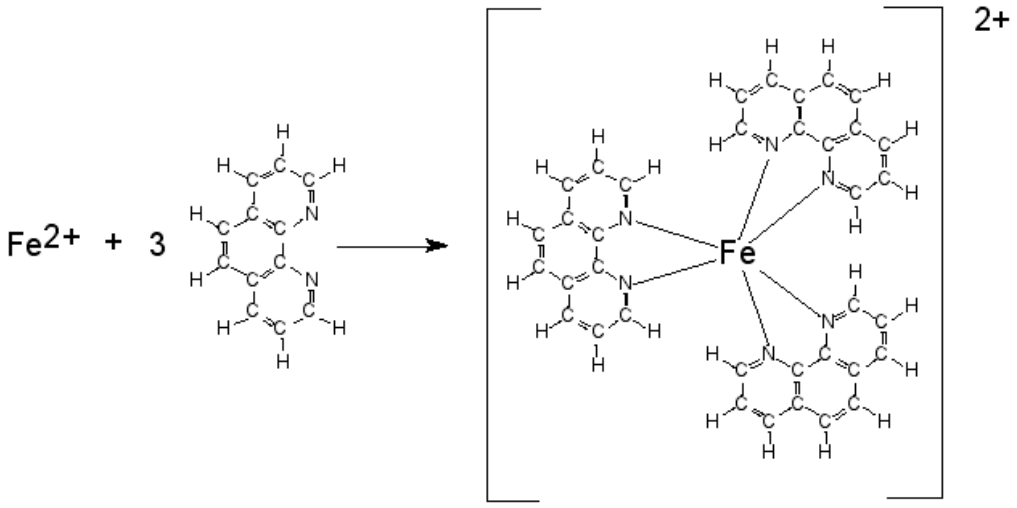

Figure 3.6. Reaction between Fe^{2+} and 1, 10-phenanthroline.

After the colored complex was formed, the wavelength of light which is most strongly absorbed is found by measuring the absorbance at various wavelengths between 400 -600 nm. The most suitable wavelength of the complex was taken at 510 nm. A series of iron standards is measured at this wavelength and a calibration plot of absorbance vs. concentration is prepared (Figure 3.7). The absorbance of the unknown sample is measured and the calibration curve is used to calculate the concentration of iron in the sample. The exact step to detect the ferrous iron in the solution is:

(1) Take the sample from the reactor

(2) Add appropriate volume of hydrochloric acid

(3) Add appropriate volume of 1, 10-phenanthroline stock solution.

(4) Add appropriate volume of ammonium acetate buffer.

(5) Fixed the total volume of the sample at 100ml

(6) Detect the sample by the UV-Vis spectrophotometer (Perkin-Elmer) at 510 nm

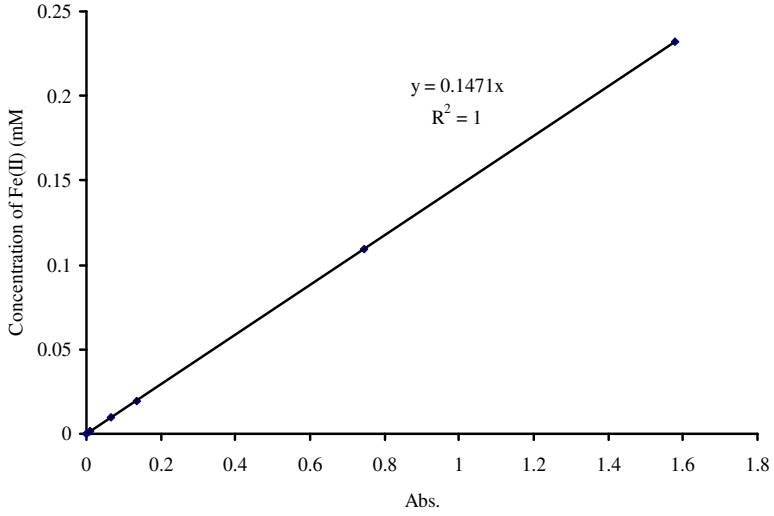

Figure 3.7. Calibration curve of the dissolved ferrous iron.

3.4.5 Total dissolved iron analysis by ICP

Total aqueous iron after dissolution was determined by inductively coupled plasma emission spectroscopy (ICP-AES) (Jobin Yvon-ULTIMA). The measured spectral element line was 259.941 nm. The RF power was set to 1000 W, the plasma gas was 15 L Ar min^{-1}, whereas the nebulizer gas was 600 mL Ar min^{-1}. The samples should be detected under the dissolved state and the sample introduction was performed by a peristaltic pump, connected to a Meinhard nebulizer which fitted into a cyclone spray chamber. Actually, the atoms in the plasma emit light with characteristic wavelengths for each element. This light is recorded by one or more optical spectrometers and when

calibrated against standards the technique provides a quantitative analysis of the original sample. The total dissolved iron in our experiment was detect follow the procedure: (1) Take the sample form the experiment reactor. (2) Filter the samples with the 0.22μm filter. (3) Add one drop of concentrated hydrochloric acid. (4) Diluted the samples by Mini-Q water. (4) Ddetected by the machine. The Figure showed the calibration curve of the total dissolved iron given by the machine.

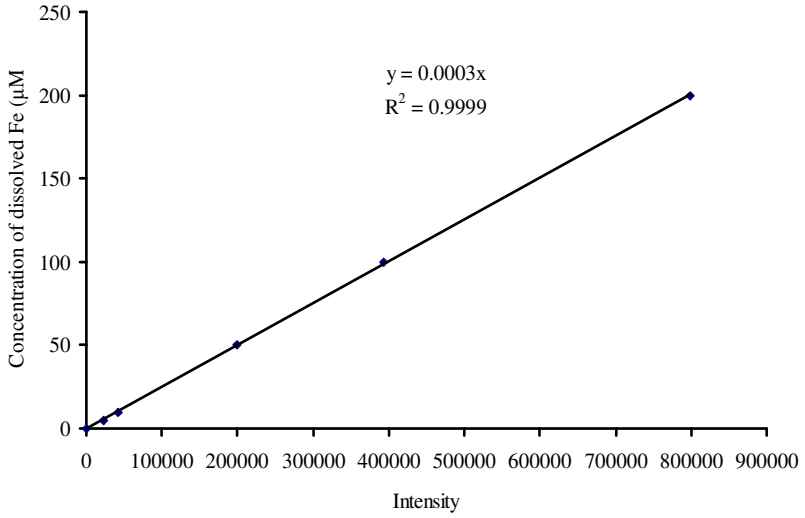

Figure 3.8. Calibration curve of the total dissolved iron in solution.

3.4.6 Total organic carbon (TOC) determination

Mineralization of pollutants was monitored by measuring the total organic carbon (TOC) via a Shimadzu Model TOC-5000 equipped with an automatic sample injector. The injection volume was 20 μL. Total organic carbon was determined with a Shimadzu Total Organic Carbon Analyzer.

3.4.7 Chloride analysis by ion chromatograph (IC)

The aqueous concentration of chloride ions released during electrolysis was measured

by ion chromatography (Dionex 200), fitted with an anionic exchange column (IonPack AS-14- Dionex) and coupled with a conductivity detector. The mobile phase was a mixture of 3.5 mmol L^{-1} sodium carbonate and 10 mmol L^{-1} sodium hydrogenocarbonate solution with a flow rate of 1.2 mL min^{-1}. The injection volume was 20 µL.

3.4.8 Short chain carboxylic acids analysis by ion exclusion chromatography

Short chain carboxylic acids were identified and quantified by ion exclusion chromatography fitted with a 300 × 6.5 mm i.d. column in conjunction with a Waters UV detector selected at λ = 204 nm. The mobile phase consisted of water containing 290 µg L^{-1} sulfuric acid at a flow rate of 0.6 mL min^{-1}.

3.4.9 pH measurement

The pH value of the suspension was adjusted with titrant solutions (HCl or NaOH) and recorded with the Orion pH meter model 710A having combination glass electrode.

3.4.10 Eelectrophoretic mobility

The electrophoretic mobility of the particles was measured with a Malvern Zetasizer (NanoZS) as a function of pH in 10 mM NaCl solution and then the zeta potential was calculated from the electrophoretic mobility.
The iso-electric point (IEP) of iron oxide is in agreement with the point of zero charge (PZC) determined by potentiometric titration.

3.4.11 Pollutant decomposition on the iron oxide surface analysis by Raman spectroscopy

Raman spectra were recorded with a triple-subtractive-monochromator Jobin Yvon T64000 spectrometer equipped with a confocal microscope. The detector was a charged-coupled device (CCD) cooled by liquid nitrogen. The Raman spectra were excited by a laser beam at 514 nm emitted by an Argon Laser (Stabilite 2017, Spectra Physics), focused on samples with a diameter of about 0.8 mm and a power of about 2.0mW on the sample. The Raman backscattering was collected through the microscope objective (x100, numerical aperture of 0.95) and dispersed by a 1800 groves/mm grating to obtain 2.7 cm^{-1} spectral resolution.

3.4.12 Pollutant sorbed analysis by FTIR

A Fourier transform infrared spectrometer Perkin-Elmer 2000, equipped with a KBr beam splitter and a MCT detector, was also used for sorption characterization by vibrational spectroscopy. The spectral resolution and the total acquisition time were respectively 4 cm^{-1} and 5 min. FTIR spectra in diffuse reflectance mode were collected using Harrick DRA-2CI equipment. To perform the analysis, the solid samples were first diluted in a KBr matrix (5 wt.%) which was spectroscopically pure dry KBr. The samples were mixed very gently with KBr in an agate mortar; so that these mixtures were not subjected to any elevated pressures. The reflectances (R_s) of the sample and (R_r) of pure KBr, used as a non-absorbing reference powder, were measured under the same conditions. The iron hydroxide reflectance is defined as $R = R_s/R_r$. The spectra is shown in pseudo-absorbance (-logR) mode.

3.5 Iron oxides characterization

3.5.1 Semi-quantitative surface composition and chemical state of iron oxides analysis by X-ray photoelectron spectroscopy (XPS)

X-ray photoelectron spectroscopy (XPS) was performed with a KRATOS Axis Ultra X-ray photoelectron spectrometer with a monochromatized Al Ka X-ray source (hn ¼ 486.6 eV) operated at 150W. XPS is sensitive to the outermost layer of solid sample and provides both semi-quantitative surface composition and chemical state information. In addition, the XPS analysis was very important in verifying the oxidation state of iron at the solid surface.

3.5.2 Specific surface area of iron oxides analysis by multipoint N_2–BET

The specific surface area of magnetite was determined by multipoint N_2–BET (Brunauer–Emmett–Teller) analysis using a Coulter (SA 3100) surface area analyzer. The particle size distribution was measured by a dynamic light-scattering method using Laser scattering particle size (HARIBA, LA 200). The site density or the concentration of the replaceable surface groups of magnetite was determined by measurement of the amount of fluoride adsorption on the surface [Sigg and Stumm, 1981]. Potentiometric titrations of the oxide were conducted in thermostated double walled pyrex cell at 293 K in 0.001, 0.01 and 0.1 M NaCl solutions according to the method of Parks and Bruyn [Parks and Bruyn, 1962]. The N_2 gas was constantly passed through the suspensions to bubble out the CO_2.

3.5.3 Characterization of iron oxides by Mössbauer spectra

The Mössbauer spectra were recorded with MIMOSII, which is designed and fabricated at the university Mainz in Germany [Klingelhöfer et al., 2004] and was originally developed for the exploration of the planet Mars. The instrument is operating in backscattering geometry measuring the scattered 14.41 keV Mössbauer radiation and the 6.4 keV Fe X-rays. The main parts of the instrument are the gamma and the X-ray detector, the ^{57}Co Mössbauer source (50 mCi), which is embedded in a rhodium metal matrix attached to a titanium holder, the Mössbauer drive and its control unit and the data acquisition and spectrometer control unit. Four Si-PIN-diodes were selected as detectors to detect backscattered radiation from the sample and was configured to select only 14.4 keV. Measurements were done by placing the detector head against the mylar window of a cell in Plexiglas which contains the sample. The spectra were fitted with the Recoil Software of Lagarec and Rancourt [Lagarec et al., 1997], using the Lorentzian model. The parameters resulting from any computer fitting must be mathematically and physically significant (chi^2 minimization).

3.5.4 Crystal structure of iron oxides analysis by X-ray powder diffraction (XRD)

In order to identify the crystal structure of mineral, sample of solid was analyzed by X-ray powder diffraction (XRD). The XRD data were collected with a D8 Bruker diffractometer, equipped with a monochromator and a position-sensitive detector. The X-ray source was a Co anode ($\lambda = 0.17902$ nm). The diffractogram was recorded in the 3-64° 2θ range, with a 0.0359° step size and a collecting of 3s per point.

3.6 Experimental Procedure

3.6.1 Sorption experiments

All equilibrium sorption experiments were conducted at 20°C in the dark at neutral pH. The solid samples were mixed with variable solute concentrations. Results of adsorption kinetic experiments indicated that sorption equilibrium was achieved within 2h. Before analysis, the suspensions were centrifuged and were filtered through 0.22 μm polyvinylidene fluoride (PVDF) syringe filters (Millipore) that were shown not to sorb PCP. The filtrate samples were analyzed by UV–visible spectroscopy and sorbed concentrations were calculated by difference according to:

$$q_e = \frac{(C_i - C_e)V}{M_s A} \qquad (3.1)$$

where q_e (mmol m^{-2}) is the sorbed concentration, C_e (mmol L^{-1}) is the equilibrium concentration at the end of the experiment, C_i (mmol L^{-1}) is the initial aqueous phase concentration, V (L) is the volume of solution, M_s (g) is the mass of solid sorbent, and A (m^2 g^{-1}) is the sorbent specific surface area. The sorption equilibrium experiments were performed in triplicate. The standard deviation of the three replicates was less than 4%.

3.6.2 Oxidation experiments

Firstly, iron oxide was added into the prepared solution, the pollutant and the iron oxide were stirred for 2h to ensure the adsorption equilibrium in the dark. After this period, 3 mL aliquot was withdrawn filtered to determine the concentration C_0 and then the oxidant was added to the suspension. The solution pH was adjusted to 7 and kept within 0.1 pH units of this value with diluted solutions of $HClO_4$ and NaOH during the experiments.

During all the oxidation reactions, 3 mL aliquots were withdrawn at selected time intervals, filtered and analyzed, and also the pH was adjusted to 7 with diluted solutions of $HClO_4$ and NaOH during the experiments periodic at the same time when take the samples. When H_2O_2 was used as an oxidant in the absence of catalyst, oxidation of the starting compound was always negligible. All experimental runs were performed within a temperature of 20°C in the absence of light. Each experiment was achieved in triplicates. All results were expressed as a mean value of the 3 experiments.

Raman spectroscopy was used to monitor the pollutant concentration on the oxide surface in magnetite/H_2O_2 aqueous suspension. Solid is easily removed from the reactor, and then put into a clean and dry glass flake, dried in the glove box (protecting the light) under N_2 and stored at ambient temperature.

3.6.3 Oxidation experiment in the presence of chelating agent

All equilibrium sorption experiments were conducted at 20°C in the dark at neutral pH. The solid samples were mixed with variable solute concentrations. Results of adsorption kinetic experiments indicated that sorption equilibrium was achieved within 2h. The sorption equilibrium experiments were performed in triplicate. The standard deviation of the three replicates was less than 4%.

Prior to oxidation experiments, the PCP solution and the oxide were stirred for 2h to ensure the adsorption equilibrium. After this period, 3 mL aliquot was withdrawn to determine the concentration C_0 and then the chelating agent or the oxidant was added to the suspension. The solution pH was adjusted to 7 and kept within 0.1 pH units with diluted solutions of HClO4 and NaOH during the experiments.

During all the oxidation reactions, 3 mL aliquots were withdrawn at selected time intervals, filtered and analyzed. When H_2O_2 was used as an oxidant in the absence of catalyst, oxidation of the starting compound was always negligible. All experimental runs were performed within a temperature of 20°C in the absence of light. Each experiment was achieved in triplicates, all results were expressed as a mean value of the 3 experiments.

In addition, the Fe leaching behavior from solids or magnetite dissolution was evaluated along the experiments under different conditions. Inductively coupled plasma emission spectroscopy (ICP/AES) (Jobin Yvon-ULTIMA) (detection limit 1.5µg L-1) was used to monitor the Fe concentration in reaction solution versus time.

CHAPTER 4

CHAPTER 4. RESULTS AND DISCUSSTION

4.1 Fenton-like oxidation of Rhodamine B in the presence of two types of iron (II, III) oxide

4.1.1 Introduction

In this work, two mixed iron (II, III) oxides were selected to study the heterogeneous Fenton-like reaction. In addition to their structural Fe^{II} content, these oxides were chosen because of their different crystallinity and surface area, which could affect their catalytic properties. The catalytic performance of iron (II, III) oxides was tested by taking into account their reactivity for oxidation of RhB used as model compound. In this study, the decolourization rate of RhB solution in an iron oxide/H_2O_2 system was investigated at different amounts of H_2O_2 and exposed surface area per unit volume.

In order to evaluate the role of adsorption in the disappearance of pollutant in heterogeneous Fenton reaction, sorption experiments were conducted under various chemical conditions (sorbate concentration, pH, ionic strength). FTIR analysis was also investigated to describe the binding mechanism of RhB on the surface of iron oxide.

In fact, the deactivation of surface catalytic sites may be caused by the adsorption/oxidation process and/or solid-dissolution reaction in medium [Valentine and Wang, 1998; Barrault et al., 2000]. For this reason, XRD analysis was used to analyze the iron oxide structure before and after exposure to H_2O_2. In addition, the dissolution of iron form oxide structure was tested by chemical analyses and the presence of residue of organic compound on the oxide surface was tested by FTIR

analysis.

4.1.2 Characterization of solid samples

The diffractograms of both iron oxides are shown in Figure 4.1. Five diffraction peaks at 2θ = 21.2°, 35°, 41.2°, 50.4° and 62.8° are shown in the XRD diffractogram (Figure 4.1), which could be assigned to Fe_3O_4, magnetite [Schwertmann and Cornell, 2000]. The d-space values of theses main peaks were 2.53, 2.96, 2.09, 4.85 and 1.71 Å which may correspond to the more intense lines 311, 220, 400, 111 and 422, respectively of magnetite [Schwertmann and Cornell, 2000]. Therefore, the spectra of solid M2 may correspond to that of the magnetite [Schwertmann and Cornell, 2000], which can be confirmed by Mössbauer analysis (Figure 4.2). It should be noted that the XRD pattern of M1 shows the same peaks which are less intense. The broad nature and low intensity of the peaks in the spectra of M1 can result from nanosized particles (Table 4.1) which may exhibit a poor crystallinity [Schwertmann and Cornell, 2000; Xuan et al., 2007]. Some surface properties of two iron oxides are reported in Table 4.1.

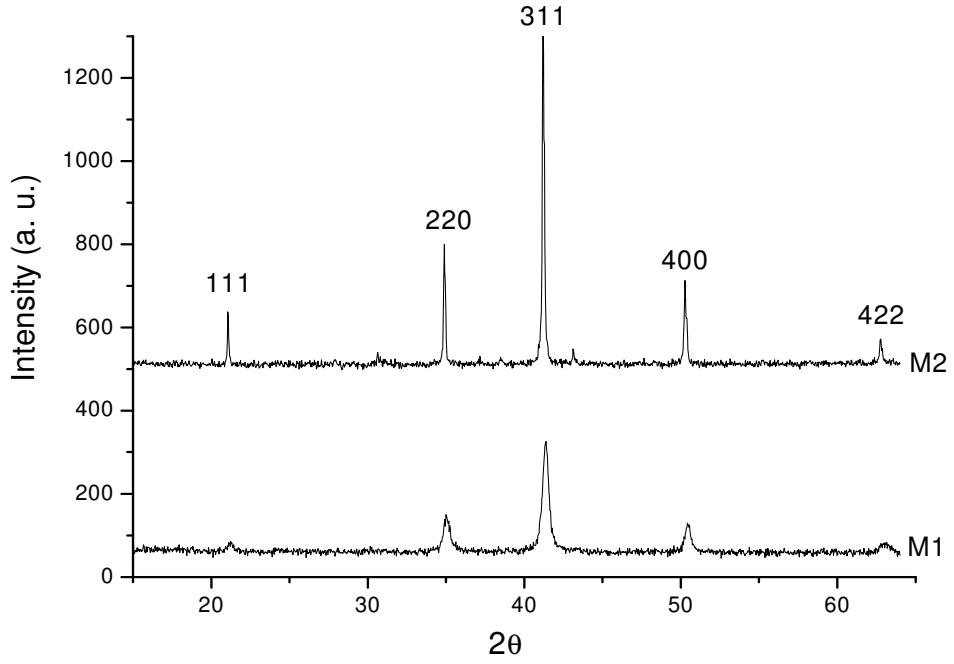

Figure 4.1. XRD of M1 and M2.

Table 4.1. Physicochemical properties of two investigated oxides

Solid	Fe_{tot} wt%	Fe^{II}/Fe^{III} ratio	Mean particle diameter	SSA m^2/g	Site Density $\mu mol/m^2$	PZC	IEP
M1	70 ± 2	0.24 ± 0.2	< 50 nm	40 ± 3	1.7 ± 0.1	7.8	8.0
M2	70 ± 2	0.43 ± 0.2	< 5 µm	2.4 ± 0.2	3.6 ± 0.2	7.4	7.2

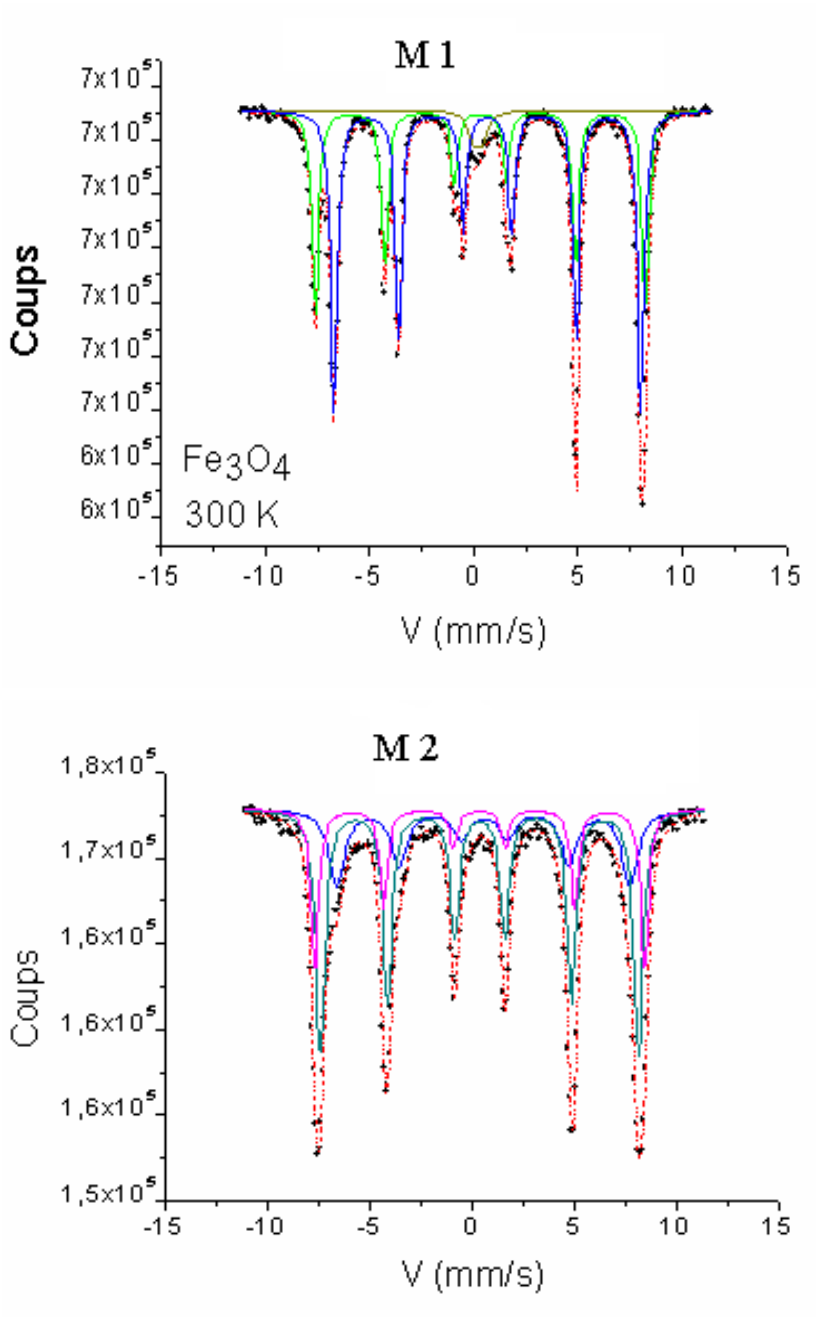

Figure 4.2. Mössbauer spectra data about two kinds of iron oxides used in this work (M1 and M2).

4.1.3 Sorption of RhB on M1 and M2

Sorption isotherms were determined to assess RhB distribution between solid and aqueous phases and to investigate the effect of contaminant sorption on the catalytic oxidation (Figure. 4.3). The experimental isotherm data were fitted to the equations of Langmuir, Freundlich and Tempkin by applying linear regression analysis. One way to asses the goodness of fit of experimental isotherm data to these equations is to perform an analysis of variance (ANOVA) with error calculation. On the basis of the statistic analysis, the curves were shown a best fit with Langmuir model for both solids. The linear form of the Langmuir equation is given by:

$$\frac{C_e}{q_e} = \frac{1}{K_L} + \frac{a_L}{K_L} C_e \qquad (4.1)$$

where a_L (L/mmol) and K_L (L/m^2) are the Langmuir isotherm constants. Langmuir monolayer sorption capacity (mmol/m^2) is numerically equal to K_L/a_L. An increasing in RhB concentration showed a progressive saturation of the surface sites. On surface area basis, the sorption intrinsic capacity of M2 is higher than of M1. The Langmuir isotherm constants obtained by plotting C_e/q_e against C_e are a_L = 36 L/mmol and K_L = 0.0095L/m^2 for M1, a_L =153.5L/mmol and K_L = 0.101 L/m^2 for M2.

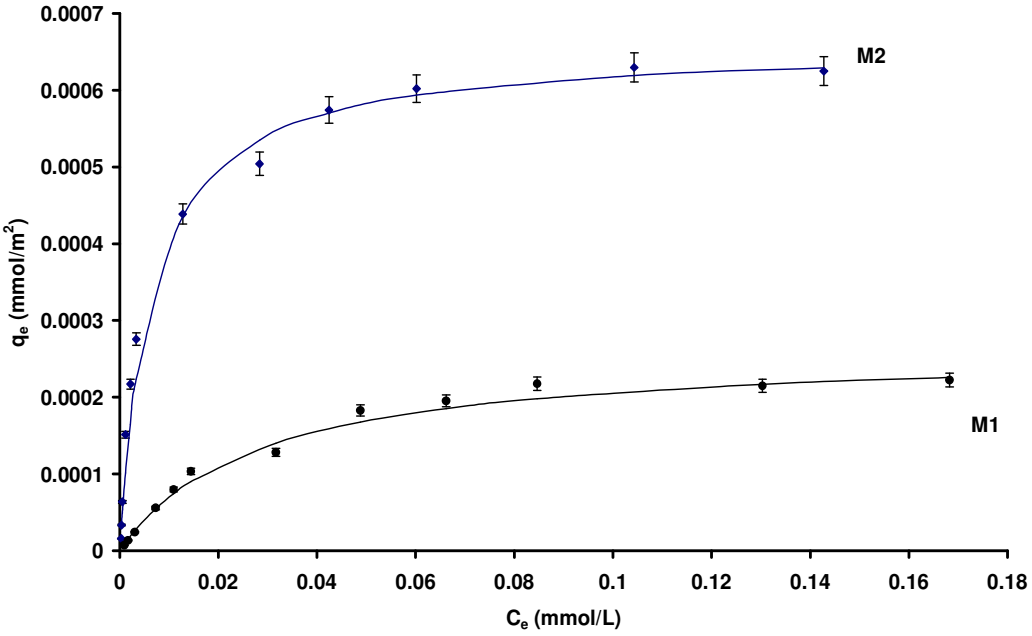

Figure 4.3. Sorption isotherms of RhB on the surface of M1 and M2 at pH7.

In general, the sorption behavior versus pH could be attributed to a combination of pH-dependent speciation of sorbate, surface charge characteristics of the mineral oxides. For M1, RhB sorption onto oxides slightly increased with increasing pH from 3 to 7, while it decreased with increasing pH for solid M2 (Figure 4.4a.). No electrostatic interactions between the carboxyl groups in the dye (pKa 6.41) and positively charged iron sites are expected. Above pH7, the sorption stayed almost constant for both solids, even though both sorbate and surface sorbent were negatively charged. The surface charge of solids deduced from the zeta potential curve varies from positive to negative, according to the point of zero charge due to deprotonation of surface hydroxyls (Figure 4.4b). Therefore, no electrostatic repulsions between the increasingly negative surface charge and the deprotonated carboxylic group of RhB are expected. This data was not consistent with some studies where the adsorption envelope of organic acids bound to iron oxide typically showed maximum adsorption at a pH near the pK_a [Hanna, 2007; Hanna and Carteret, 2007; refs cited in Hanna and Carteret, 2007].

(a)

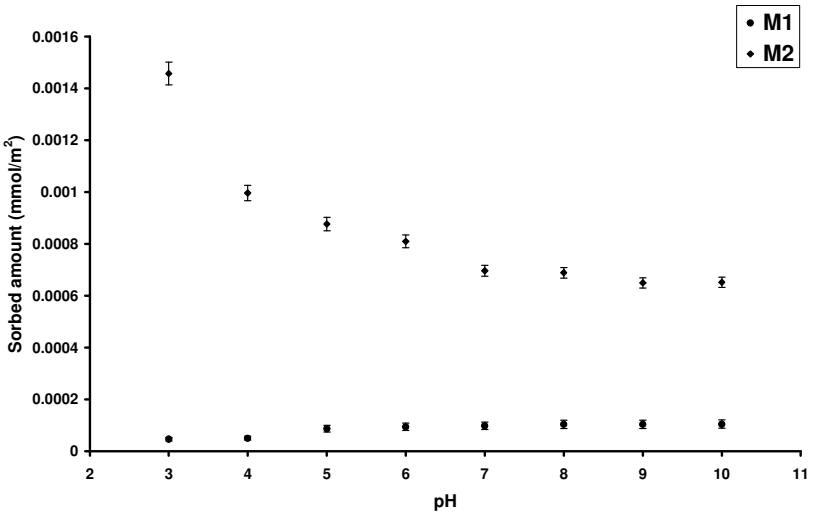

(b)

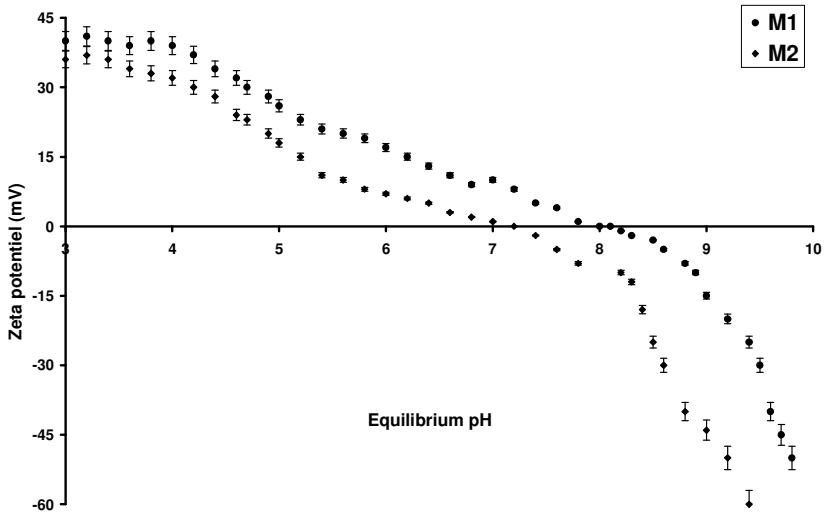

Figure 4.4. RhB sorption (a) and Zeta potential measurements (b) versus pH of both iron oxides.

Effect of ionic strength on RhB sorption was investigated by conducting sorption equilibrium experiment at different NaCl concentrations (from 1 to 100 mM of NaCl) at 20°C. Less than 5 % of sorption was decreased by the introduction of NaCl ions, implying that the ionic strength did not affect the sorption behavior to iron oxide surface. Because Cl^- can associate with the iron oxide surface as outer-sphere complexes and RhB sorption was independent on ionic strength including NaCl, it can be concluded that sorption mechanism of RhB on oxide surfaces was stronger than non-specific electrostatic interactions or outer-sphere complexes. In accord with all data listed above, the surface complexation mechanism was expected for RhB sorption on both iron oxides. By analogous structure with some carboxylate compounds, the adsorption of RhB expected to occur via the carboxylic group of RhB through the formation of a mononuclear monodentate complex with iron surface sites [Hanna and Carteret, 2007; refs cited in Hanna and Carteret, 2007]. The IR spectra of RhB equilibrated with iron oxide were recorded at wavelength range 2000-1000 cm^{-1} at two pH values 3 and 7 (Figure 4.5). The peaks at 1592 cm^{-1} and at around 1500 cm^{-1} correspond to aromatic ring vibrations, while the 1345 cm^{-1} peak attributes to C-aryl bond vibration. The peak at 1648 cm^{-1} is caused by vibrations of the C–N bond [Mittal and Venkobachar 1996]. The C=O is associated with the band at 1694 cm^{-1} and the C-OH bond with the group of bands in the range 1088-1300 cm^{-1} [Nakomoto, 1986]. In fact, it was not possible from the FTIR results to determine the preferred binding site for RhB sorption. The IR spectra of functional groups of RhB onto iron oxide surface is unchanged with the pH increasing. The overall intensity of adsorbate spectra depended on solid type and pH value, corroborating the batch sorption data. No significant difference of RhB sorbed spectrum was observed for M1 or M2, so the same type of surface complex may occur on the surface of both iron oxides. So, the sorption mechanism of RhB on both oxides seems to be identical at both studied pH even though the sorption edges did not revealed a similar trend.

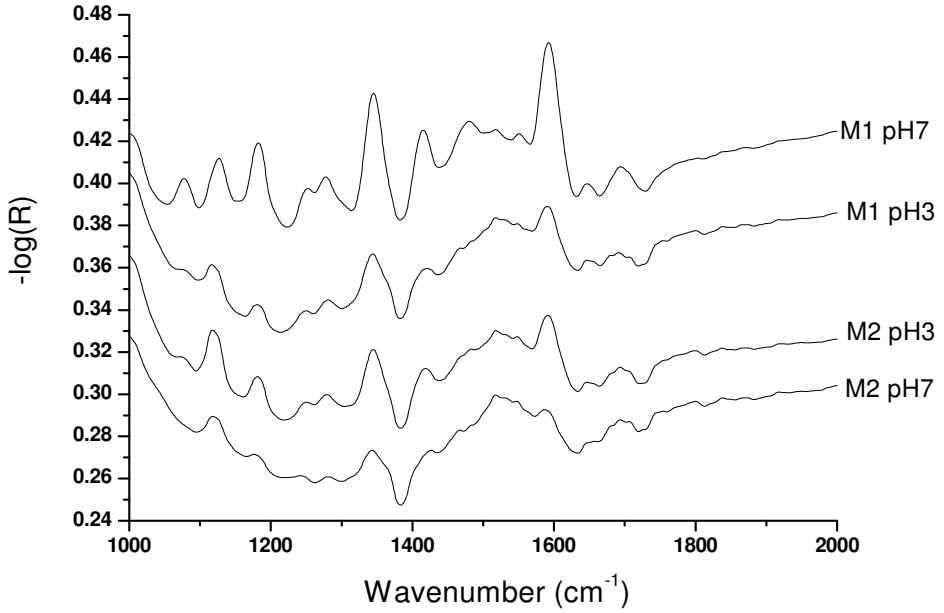

Figure 4.5. Infrared spectra of solid samples equilibrated in the dark in RhB (5mM) at two pH values (pH 3, pH 7).

4.1.4 Effect of H_2O_2 dose on decolorisation rate of RhB solution at neutral pH

The oxidation kinetics was studied to quantitatively characterize the decolourization at neutral pH in the presence of 2g/L of iron oxide. Preliminary test showed no significant photochemical reaction of RhB was observed by natural light under our experimental conditions.

Hydroxyl radical can be generated by the reaction between hydrogen peroxide and iron surface leading to a decolourization of RhB solution. The degradation of organic compounds by $HO^{\cdot}$ is typically described as a second-order reaction:

$$\frac{dC}{dt} = -kC\left[HO^{\cdot}\right] \tag{4.2}$$

where C and [$HO^{\cdot}$] are concentrations of RhB in water and hydroxyl radical, respectively, k is the second-order rate constant, and t is the reaction time. By assuming that $HO^{\cdot}$ instantaneous concentration is constant, the kinetics of decolourization of RhB in water can be described according to the pseudo-first-order equation as given below :

$$C_t = C_0 \exp(-k_{app} t) \qquad (4.3)$$

Where C_0 is the initial concentration of RhB and k_{app} is the pseudo-first-order apparent rate constant (min^{-1}). The k_{app} constants were obtained from the slopes of the straight lines by plotting $-\ln(C_t/C_0)$ as a function of time t, through regression.

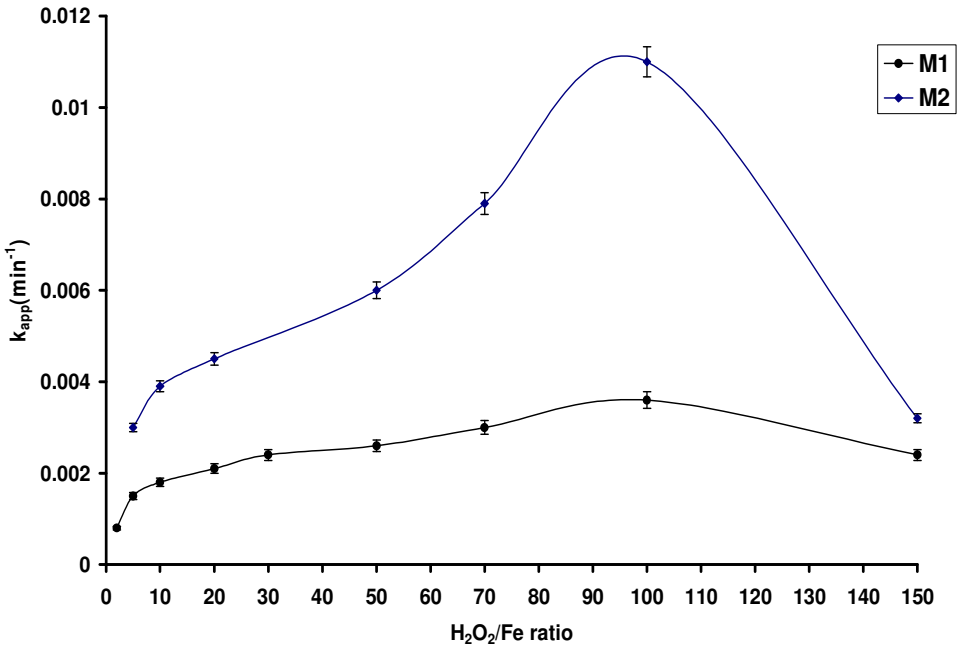

Figure 4.6. Effect of H_2O_2 /Fe ratio on the decolourization kinetic constant of RhB. H_2O_2/Fe (molar ratio) = 5-150, [RhB] = 5 mg L^{-1}, [Iron (II, III) oxide] = 2g L^{-1}, 20°C, pH7.

The kinetic constants rate k_{app} were determined at different H_2O_2 concentrations (Figure 4.6). At all range of H_2O_2/Fe ratio, M2 exhibits better oxidation capacity than M1. From the figure it is clear that when the H_2O_2 /Fe ratio was 5, the k_{app} were 0.0015 and 0.003 for M1 and M2 respectively. The oxidation efficiency of M2 was two times bigger compared with M1. While, when the H_2O_2 /Fe ratio rise up and reach to 100, the k_{app} were 0.00326 and 0.011 for M1 and M2 respectively. So at the ratio 100, the degradation efficiency of RhB when using the M2 is more than 3 times bigger than using the M1. That indicated the higher ratio the better degradation efficiency it will reached compared M2 with M1.

Since the decolourization of RhB solution is directly related to the concentration of the hydroxyl radicals produced by the catalytic decomposition of hydrogen peroxide, more RhB decomposition is expected when hydrogen peroxide dosage increases. Usually it has been observed that the percentage degradation of the pollutant increases with an increase in the dosage of hydrogen peroxide (Lin and Peng, 1995; Lin and Lo, 1997; Kwon et al., 1999; Lin et al., 1999; Kang and Hwang, 2000; Rivas et al., 2001). However, in our experiment it is clear that a decrease in the values of k_{app} was observed at a much higher H_2O_2 concentration (Figure 4.6). The occurrence of this optimum H_2O_2 concentration for the effective degradation of the dye could be explained by the scavenging effect of hydroxyl radicals by hydrogen peroxide. The excessive dosage of H_2O_2 will make a competition between decomposition of RhB and H_2O_2 it self. Similar observation was noted earlier for the degradation of organic compounds by Fenton-like reactions using goethite as catalyst [Wu et al., 2006]. At low H_2O_2 concentration, the HO. radicals preferentially attack the substrate molecules, whereas at higher H_2O_2 concentration, there is a competitive reaction between the substrate and H_2O_2. The $^{\bullet}OH$ radical may react with hydrogen peroxide producing superoxide/hydroperoxy radicals according to Eq. (4.4):

$$^{\bullet}OH + H_2O_2 \quad \rightarrow \quad HO_2^{\bullet}/O_2^{\bullet-} + H_2O \qquad (4.4)$$

Buxton et al. [Buxton et al., 1988] have determined the reaction rate of H_2O_2 with hydroxyl radical (k= $2.7x10^7$ $M^{-1}s^{-1}$). Because the pKa of $HO_2^{\bullet}/O_2^{\bullet-}$ is 4.8, generation of hydroperoxide anion $HO_2^{\bullet}$ may be neglected at neutral pH. The generated radicals $O_2^{\bullet-}$ are much less reactive and do not contribute to any oxidation of RhB [Lin and Gurol, 1998]. $O_2^{\bullet-}$ plays an important role in the redox cycle of Fe^{2+} and Fe^{3+} in aqueous phase and generates oxygen as a byproduct but the interactions of superoxide/hydroperoxy radicals with the iron mineral surface are not yet well argued :

$$O_2^{\bullet-} + Fe^{3+} \rightarrow O_2 + Fe^{2+} \quad (4.5)$$

$$HO_2^{\bullet} / O_2^{\bullet-} + Fe^{2+} \rightarrow HO_2^{-} + Fe^{3+} \quad (4.6)$$

4.1.5 H_2O_2 decomposition and RhB removal versus exposed surface area per unit volume

The H_2O_2 decomposition versus time at various surface area for M1 (A) and M2 (B) is presented in Figure 4.7. Good linear plot obtained with the expressions of $\ln([H_2O_2]/[H_2O_2]_0)$ as a function of the reaction time, indicates that the H_2O_2 decomposition is the first order reaction.

$$\frac{d[H_2O_2]}{dt} = -k_{app}[H_2O_2] \quad (4.7)$$

Where $k_{app} = k[SSA]$

[SSA] means the amount of specific surface area par unit volume (m^2/L). The H_2O_2 decomposition rate k_{app} (min^{-1}) was plotted as a function of [SSA] (Figure 4.9). The good linear relationship (R^2=0.99) between the rate constant and [SSA] indicates that the H_2O_2 decomposition is the first order reaction with oxide surface area. The results clearly indicate that this is the surface reaction because the increase of surface area

provides more active sites for catalytic oxidation. The second order rate constant (k) obtained from the plot of observed first-order rate constant for H_2O_2 decomposition versus [SSA] is 3.10^{-4} min^{-1} $(m^2/L)^{-1}$ for M2 and 8.10^{-5} min^{-1} $(m^2/L)^{-1}$ for M1. The H_2O_2 decomposition versus time at 1g/L for both oxides is shown in Figure 4.8. As for sorption rate, the H_2O_2 decomposition rate was higher for M2 than M1 based on surface area basis, while the trend is opposite based on mass basis.

(a)

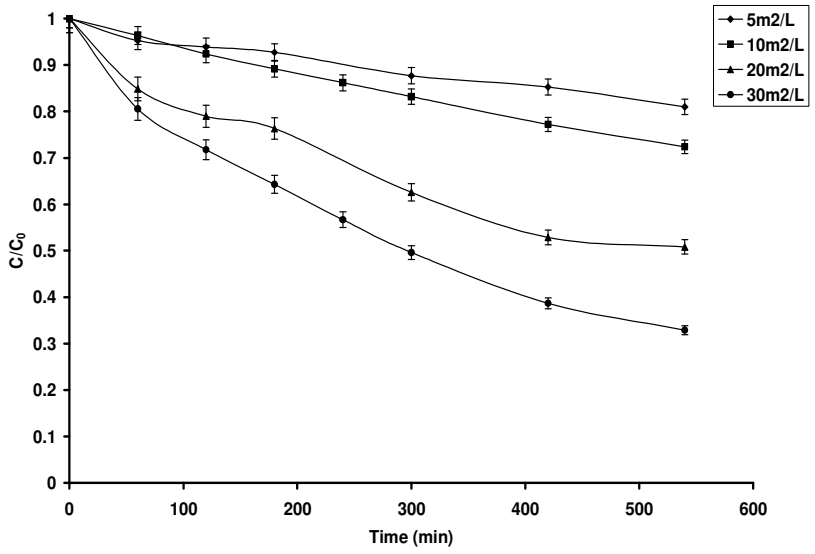

(b)

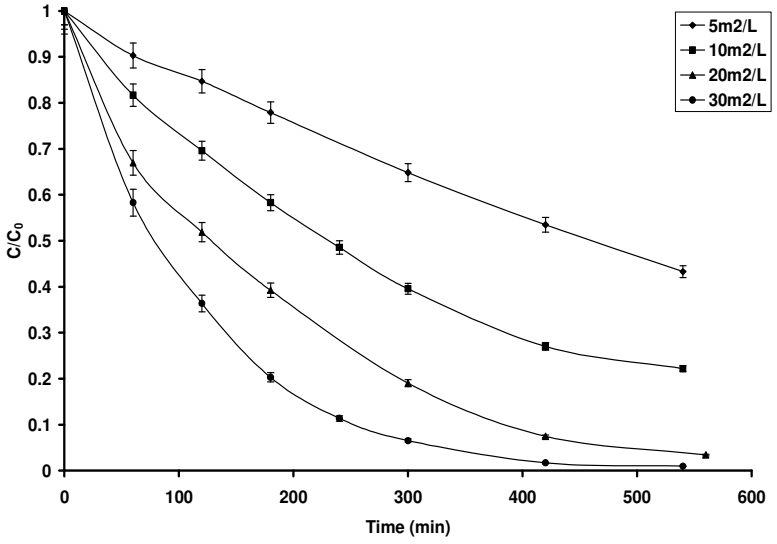

Figure 4.7. H_2O_2 decomposition at various [SSA] of M1 (a) and M2 (b). $[H_2O_2]$ =1

mM, 20°C, pH7.

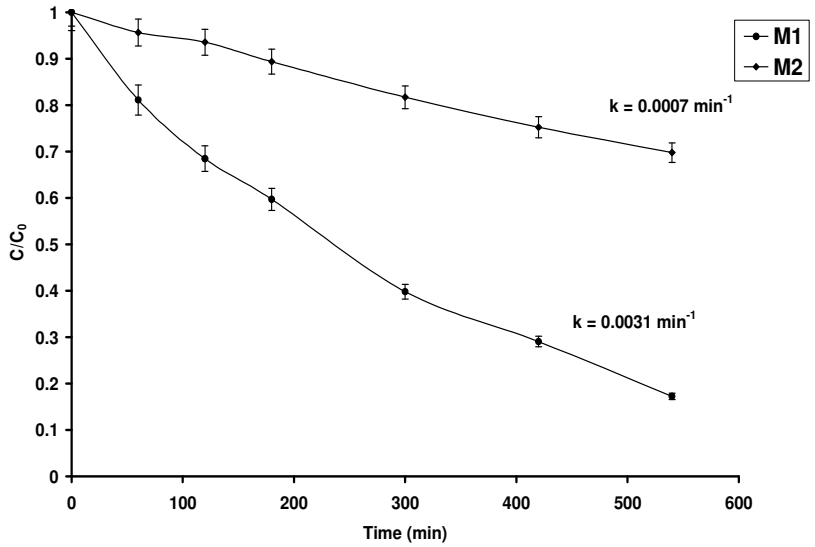

Figure 4.8. H_2O_2 decomposition at 1g/L of both solids (M1, and M2). [H_2O_2] = 1 mM, 20°C, pH7.

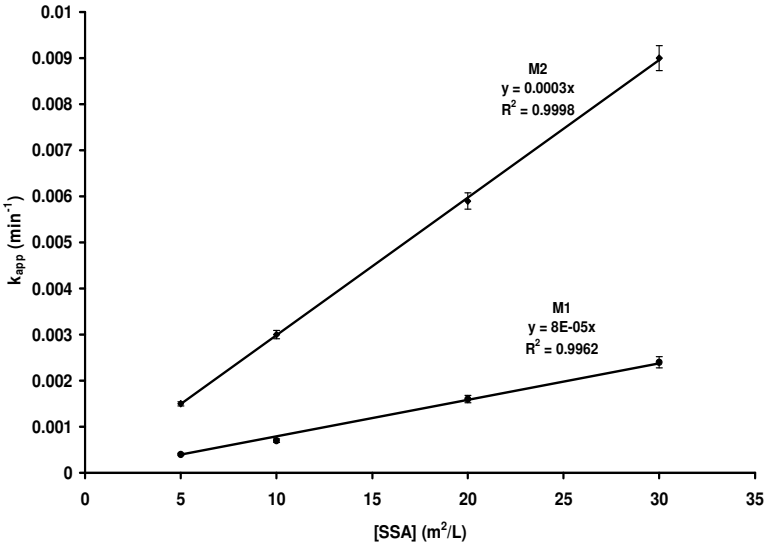

Figure 4.9. H_2O_2 decomposition rate versus [SSA]. [H_2O_2] = 1 mM, 20°C, pH7.

The decolourization of RhB solution was also investigated at various [SSA]. The good

linear plot obtained with the expressions of ln([RhB]/[RhB]$_o$) as a function of the reaction time, allows determining the first order kinetic constant:

$$\frac{d[RhB]}{dt} = -k_{app}[RhB] \qquad (4.8)$$

A plot of observed first order rate constant k_{app} (min^{-1}) for dye removal as a function of [SSA] is shown in Figure 4.10. In contrast with the result of Figure 4.9, the RhB removal was not proportional to the oxide surface area. The observed first order rate constant for dye removal firstly increased with [SSA] increasing and then reduced. This phenomenon can be explained from the assumption that OH radical generated by the reaction between hydrogen peroxide and iron oxide is scavenged by iron surface. Miller and Valentine [Miller and Valentine,1999] reported that OH radical is very reactive with natural iron oxide-coated sand (k = 8 x 10^{11}(g/ml) $^{-1}$ s^{-1}). Regarding this data (Fig. 4.10), M2 exhibits better oxidation performance than M1 at full range of studied [SSA] (3-40 m^2/L). Furthermore, M_1 seems to be more radical scavenger than M2, where the SSA optimum occurred at about 17m^2/L for M1 and at 32m^2/L for M2.

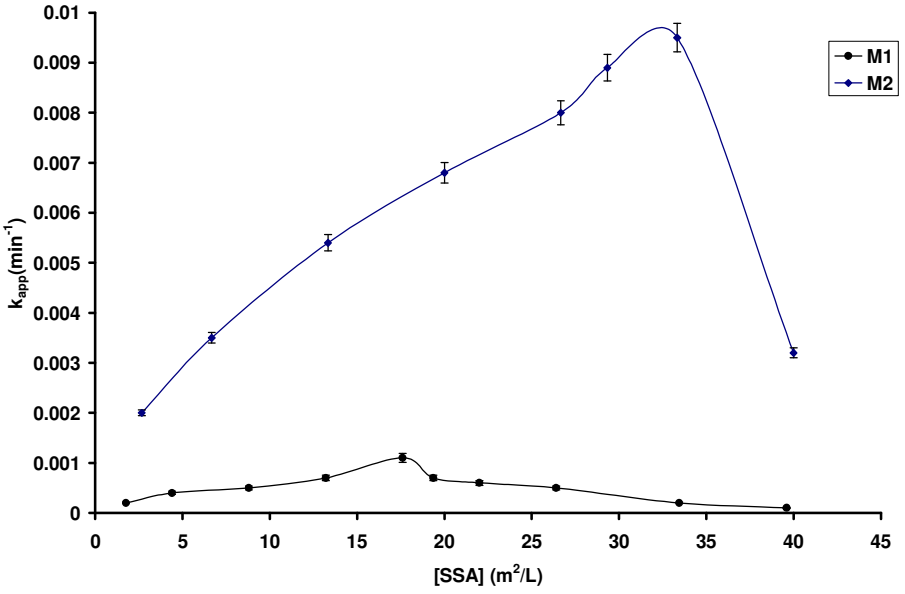

Figure 4.10. Effect of [SSA] on the decolourization kinetic constant of RhB. H_2O_2 = 150mM; 20°C, pH7.

Oxidation efficiency was assessed by the following equation:

$$E(mole/mole) = \frac{\Delta[RhB]}{\Delta[H_2O_2]} \quad (4.9)$$

Where E(mole/mole) is the stoichiometry efficiency while Δ[RhB] and Δ[H_2O_2] represent the variation in molar concentration of RhB and H_2O_2 as a function of [SSA]. A high E value means a high reaction yield between RhB and hydroxyl radicals. Figure 4.11 shows that E for dye removal is inversely proportional to the amount of oxide surface area, corroborating that iron surface can act as an OH radical scavenger. A sharply decreases of oxidation efficiency (E) was observed for M1, while a first rise in the E value before a slow decrease was observed for M2. On the basis of this data, M1 seems to be less reactive and more $HO^{\cdot}$ scavenged in comparison with M2. This difference in oxidation efficiency might be due to difference in mineral structural properties (crystallography, Fe^{II} content). Valentine and Wang [Valentine and Wang, 1998] reported that an amorphous iron oxide has more vacant Fe sites and OH groups able to scavenge hydroxyl radicals than crystallized iron oxides. Valentine and Wang [Valentine and Wang, 1998] and Huang et al. [Huang et al., 2001] showed that the hydrogen peroxide decomposition rate was the highest for ferrihydrite, less for semicrystalline oxide, and much less for goethite or hematite (high crystallized oxide). However, they also affirmed that the catalytic activity for organic compound oxidation exhibited a converse series for these iron oxides, corresponding to the inverse sequence of specific surface area. Indeed, an amorphous iron oxide with high surface area may improve the decomposition of H_2O_2 via non-radical pathway [Kwan and Voelker, 2002; Kwan and Voelker, 2003]. However, it should be noted that the reaction of H_2O_2 decomposition would not be expected to yield a simple dependence of HO. generation rate.

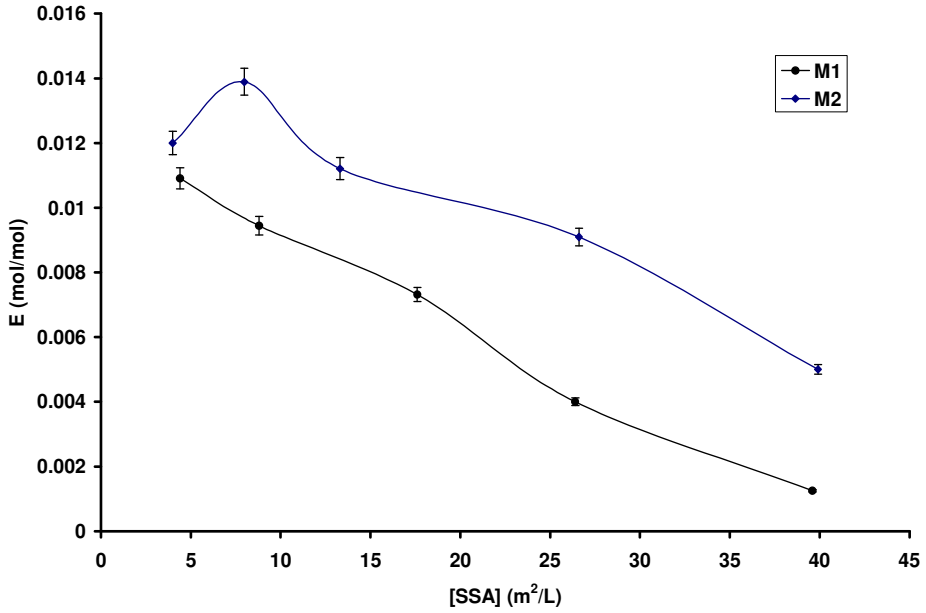

Figure 4.11. Oxidation efficiency (E) versus [SSA].

In the present study, the H_2O_2 decomposition rate was higher for M2 than M1 when normalized to the oxide surface area. However, the trend is inversed when based on oxide mass basis (M1 ($40 m^2/g$) > M2 ($2.4 m^2/g$)). Based on both mass and surface area basis, the dye decolourization rate was higher for M2 (high crystallinity, $2.4 m^2/g$) than for M1 (low crystallinity, $40m^2/g$). This discrepancy may be probably due to the fact that the surface reactivity of the mixed oxides depended on surface properties such as structural Fe^{II} content. Firstly, Fe^{II} play an important role for the initiation of the Fenton reaction according to the classical Haber–Weiss mechanism and therefore the enhancement of the production rate of $^{\cdot}OH$ [Lin and Gurol, 1998; Haber and Weiss, 1934]. Heterogeneous reactions analogous to the solution phase reactions were used to explain the interactions between oxidant and iron surface:

$$\equiv Fe^{II} + H_2O_2 \rightarrow \equiv Fe^{III} + HO^- + HO^{\cdot} \quad (4.10)$$

$$\equiv Fe^{III} + H_2O_2 \rightarrow \equiv Fe^{III}(H_2O_2) \quad (4.11)$$

$$\equiv Fe^{III}(H_2O_2) \rightarrow (\equiv Fe^{II}.O_2H) + H_2O \quad (4.12)$$

$$(\equiv Fe^{II}.O_2H) \rightarrow \equiv Fe^{II} + HO_2^{\cdot} \quad (4.13)$$

In mineral catalyzed reaction, the dominant reaction is first a chain of reactions occurring on the mineral surface. If only Fe^{III} is originally present, Fe^{II} is slowly generated by reactions (4.11-4.13) initiating oxidation reaction (12). In the case of mixed Fe^{II}-Fe^{III} bearing mineral, reactions involving both Fe^{II} and Fe^{III} may occur. Therefore, the presence of iron (II) in the Fe-bearing minerals can enhance the production rate of $HO^{\cdot}$ [Lin and Gurol, 1998; Haber and Weiss, 1934; Matta et al., 2008a; Matta et al., 2008b].

4.1.6 Structural and catalytic stabilities

The action of H_2O_2 on the oxide surface can transform the oxide particles into a only Fe^{III}-bearing mineral or into a amorphous iron oxide which may be less stable and more soluble. This mineralogical transformation may lead to a substantial change in the surface characteristics of the mineral, causing a different kinetic behavior and decomposition rate for H_2O_2. The very low dissolved iron concentration measured in all our studied systems did not expect the formation of more soluble iron oxide. Furthermore, chemical analysis, XRD analysis of both oxides was conducted before and after exposure to H_2O_2. The chemical analyses of the solid after reaction revealed no significant change in the total Fe loading. In addition, XRD patterns recorded at the end of oxidation reaction was found to be similar to that recorded before reaction (Figure 4.1).

The reusability of the solids has been evaluated under identical oxidation conditions as explained in our previous work [Hanna et al., 2008]. At the end of the oxidation process, the solid is easily removed from the reactor, dried in the glovebox under N_2

and stored at ambient temperature. The FTIR spectrum of the recovered solid was recorded at wavelength range 2000-1000 cm^{-1}. It is noted that the absorption peaks for sorbed RhB in the range 1000-1700cm^{-1} (Figure 4.5) almost disappeared and there is no residue of organic compounds on the surface of the solid. The H_2O_2 decomposition and RhB decolourization on the recovered catalyst were then investigated as for previous experiments and showed a slight difference with the first oxidation cycle. The excellent stability of the catalytic activity could be attributed to the low loss of iron content during oxidation cycles and to the structural stability of the solid.

4.1.7 Conclusion

The removal rate of organic compound by Fenton-like oxidation firstly increased with the dosage of H_2O_2 or with the amount of exposed surface area, reached an optimum value and then decreased. The occurrence of these optimums values for the effective degradation of the dye could be explained by the scavenging and parasite reactions with (i) H_2O_2 or (ii) iron oxide surface. Only heterogeneous Fenton reaction happened for the decolourization of Rhodamine B (RhB) because Fe leaching from the oxide surface is negligible at neutral pH. M2 exhibits important intrinsic reactivity for RhB decolourization or H_2O_2 decomposition. On surface area basis, RhB sorption and H_2O_2 decomposition rates on the surface of oxide were higher for M2 (high crystallinity and Fe^{II}/Fe^{III} ratio) than for M1 (low crystallinity and Fe^{II}/Fe^{III} ratio). M2 exhibits better oxidation efficiency for dye removal than M1 based on both mass and surface area basis. The decomposition of RhB on M2 is higher than M1 even though the sorption mechanism of RhB on the surface of both oxides revealed a similar trend. The site density and sorption ability of RhB on catalyst surface may also influence the oxidation performance in iron oxide/H_2O_2 system. The iron oxides catalysts exhibited low iron leaching, good structural stability and no loss of performance in second reaction cycle. The sorption on the surface of iron oxide with catalytic oxidation using hydrogen peroxide would be an effective oxidation process for the contaminants.

4.2 Adsorption and oxidation of PCP on the surface of magnetite: Kinetic experiments and spectroscopic investigations

4.2.1 Introduction

In this part of work, the apparent degradation rate of PCP in magnetite/H_2O_2 system was determined under various experimental conditions and correlated with the intrinsic chemical reactions on the oxide surface. Because in the Fenton-like system where iron solid mineral was used instead soluble iron, adsorption of the species on the oxide surface and oxidation by hydroxyl radicals coming from surface-catalyzed reaction could occur simultaneously, the surface reaction may play a very important role. Actually, in TiO_2-photocatalysis process, the importance of adsorption was widely pointed out in several studies [Herrmann et al., 1999; Lu et al., 1993; Chen and Ray, 1998; Daneshvar et al., 2004]. However, the role played by the adsorption at solid surface in the oxidation of pollutant in heterogeneous Fenton reaction is poorly described. Furthermore, the surface interactions of species with iron surface sites involving both sorption and decomposition reactions are scarcely investigated.

In this part, the oxidation kinetic was operated at various initial PCP concentration, H_2O_2 dose, magnetite loading and temperature. The Langmuir and Langmuir–Hinshelwood models were used to describe the surface interactions with PCP in the absence and the presence of oxidant, respectively. The surface reactivity of magnetite was evaluated by conducting H_2O_2 decomposition experiments, FTIR spectroscopy and Raman analysis. The PCP mineralization rate was also determined by monitoring both TOC abatement and chloride formation along the oxidation reaction.

In fact, the deactivation of surface catalytic sites may be caused by the adsorption/oxidation process and/or leaching effects of iron in reaction medium

[Valentine and Wang, 1998; Barrault et al., 2000]. For this reason, X-ray powder diffraction (XRD), X-ray photoelectron spectroscopy (XPS), and Mossbauer spectroscopy were used to analyze the magnetite structure before and after exposure to H_2O_2. In addition, the dissolution of iron form oxide structure was tested by chemical analyses and the presence of residue of organic compound on the oxide surface was tested by Raman analysis.

4.2.2 Characterization of iron oxides

The diffractogram of solid powder are shown in Figure 4.12. Five diffraction peaks at 2θ = 21.2°, 35°, 41.2°, 50.4° and 62.8° are shown in the XRD diffractogram, which could be assigned to Fe_3O_4, magnetite [Schwertmann and Cornell, 2000]. The d-space values of theses main peaks were 2.53, 2.96, 2.09, 4.85 and 1.71 Å which may correspond to the more intense lines 311, 220, 400, 111 and 422, respectively of magnetite [Schwertmann and Cornell, 2000]. So in this part of work we can call this type of iron oxide (M2) (which purchased from Prolabo) magnetite.

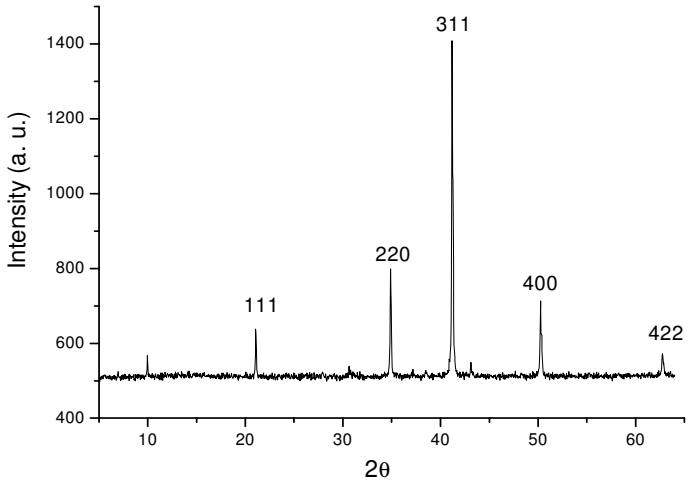

Figure 4.12. XRD spectra of solid sample.

Magnetite (Fe_3O_4) is the only pure oxide of mixed valence. At Room Temperature (RT)

it has a cubic spinel structure with iron in both tetrahedral and octahedral sites. It is usually represented by the formula $(Fe^{3+})_{tet}[Fe^{3+}Fe^{2+}]_{oct}O_4$. Its Mössbauer spectrum at RT is constituted by a superposition of two subspectra associated to the distribution of the iron in the octahedral and tetrahedral sites. The two valence states on octahedral sites are not distinguishable (valence $Fe^{2.5+}$) due to a fast electron hopping between Fe^{2+} and Fe^{3+} in octahedral sites. Thus, the ideal magnetite has only two distinct sextets at RT [Murad and Johnston, 1987] in 1:2 intensity ratio corresponding to tetrahedral iron (A sites) with H (magnetic hyperfine field) = 498 kOe, isomer shift δ = 0.31 $mm.s^{-1}$, and octahedral iron (B site) with H = 465 kOe and δ = 0.67 $mm.s^{-1}$.

Table 4.2. Hyperfine parameters of magnetite at room temperature. δ ($mm.s^{-1}$): isomer shift (Relative to room temperature -iron foil), H (kOe): magnetic hyperfine field, Δ or ϵ ($mm.s^{-1}$): quadrupole splitting or quadrupole shift , RA (%): relative area.

Sample	Component	δ (mm/s)	Δ or ϵ (mm/s)	H (kOe)	RA (%)
Before reaction	D	0.32	0.3		2.3
	S1	0.31	0	490	38.8
	S2	0.66	0	456	58.9
After reaction	D	0.4	0.47		1.6
	S1	0.31	0	492	39.9
	S2	0.66	0	457	58.5

In our sample, the Mössbauer spectrum at RT (Figure. 4.13) has been adjusted with

two sextets and their resulting hyperfine parameters (Table 4.2) are in agreement with literature values for magnetite [Da costa et al., 1995]. The relative area ratio of the two spectral components is close to 1:1.5; it is not exactly 1:2 as would be expected in the stoichiometric magnetite. Otherwise the Mössbauer spectrum shows in the central part a ferric doublet which accounts for 2% of the total absorption and its origin could not be established. Storage of the sample for many years without any particular protection against oxidation could explain the ferric doublet observed in the central part of the spectrum.

The XPS spectrum of the solid material was taken over the entire energy range (data not shown). A detail of the Fe peaks (Fe $2p_{1/2}$ and Fe $2p_{3/2}$) can be seen in Figure 4.14. Deconvolution of the Fe $2p_{3/2}$ peak shows only those corresponding to Fe^{III} component, indicating that the outermost surface of solid sample is already oxidized. This may be probably due to the conditions storage of this commercial sample. It should be noted that XPS is sensitive to the outermost layer of sample, while the Mössbauer spectroscopy detects the iron state in the bulk solid. Some surface properties of solid sample are reported in Table 4.3.

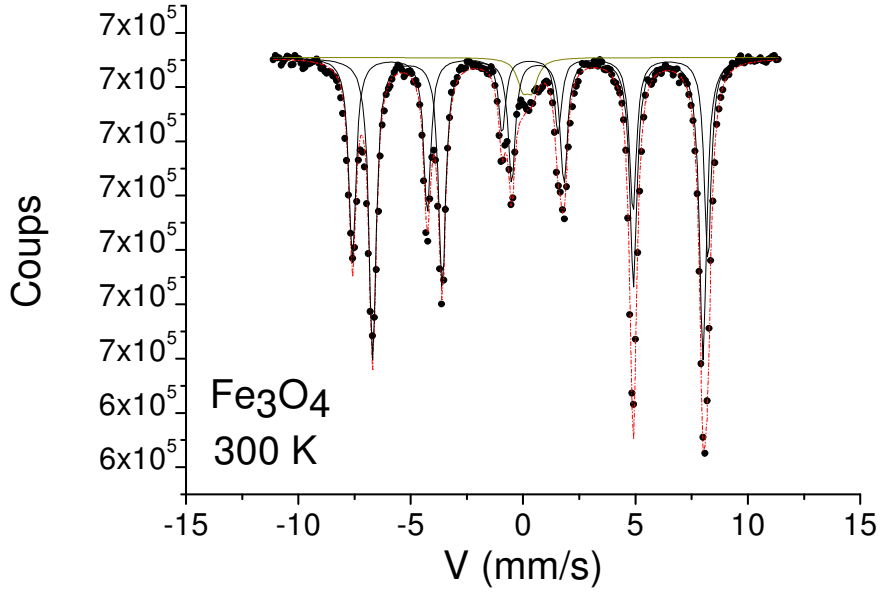

Figure 4.13. Mössbauer spectra of solid sample.

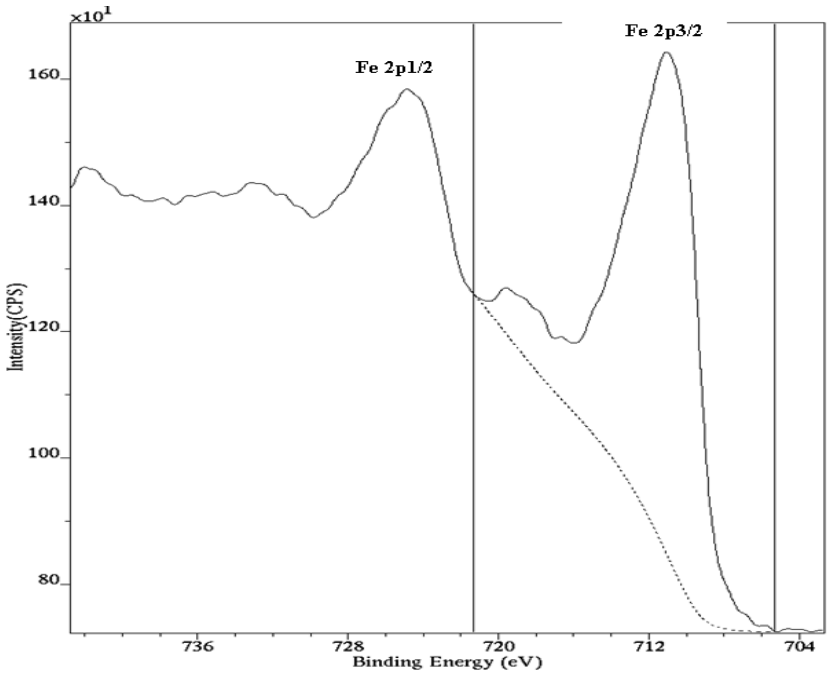

Figure 4.14. XPS spectra of solid sample.

4.2.3 Sorption of PCP on magnetite

Sorption isotherms were determined to investigate the effect of contaminant sorption on the catalytic oxidation (Figure 4.15). The experimental isotherm data were fitted to the equations of Langmuir, Freundlich and Tempkin by applying linear regression analysis. One way to asses the goodness of fitting the experimental isotherm data to these equations is to perform an analysis of variance (ANOVA) with error calculation. On the basis of the statistic analysis, the curves were shown a best fit with Langmuir model. The linear form of the Langmuir equation is given by:

$$\frac{C_e}{q_e} = \frac{1}{K_a q_m} + \frac{1}{q_m} C_e \qquad (4.14)$$

where q_m (mmol m^{-2}) is Langmuir maximum sorbed amount and K_a (L $mmol^{-1}$) is the Langmuir isotherm constant. An increasing in PCP concentration showed a progressive saturation of the surface sites. The Langmuir isotherm constants obtained by plotting C_e/q_e against C_e are q_m = 0.023 mmol m^{-2} and K_a = 10.5 L $mmol^{-1}$. The Langmuir maximum sorbed amount is 6-times greater than the site density of solid (Table 4.3), supposing that more than one molecule might be fixed per iron site (i.e. solute aggregation at oxide surface). A hydrophobic adsorption directly to the iron surface does not seem likely since this is presumed to yield an almost linear isotherm [Chiou et al., 1983]. However, the lack of resistance to desorption when methanol was used to remove the solute sorbed from solid, may signify some hydrophobic interactions rather than a strong phenolate-Fe bond. Kung and McBride [Kung and McBride 1991] reported that while a chemisorption of monochlorophenol (CP) onto goethite (inner-sphere complexation) was identified from FTIR spectroscopy, the mechanism of PCP sorption can not be easily described.

Table 4.3. Physicochemical properties of the investigated magnetite

Solid	Fe_{tot} (wt%)	Fe^{II}/Fe^{III} ratio	Mean particle diameter (µm)	Specific Surface Area (SSA) ($m^2\ g^{-1}$)	Site Density (µmol m^{-2})	Point of Zero Charge (PZC)	Iso-Electric Point (IEP)
Magnetite Fe_3O_4	70 ± 2	0.48 ± 0.2	4 ± 1	2.4 ± 0.2	3.6 ± 0.2	7.4	7.2

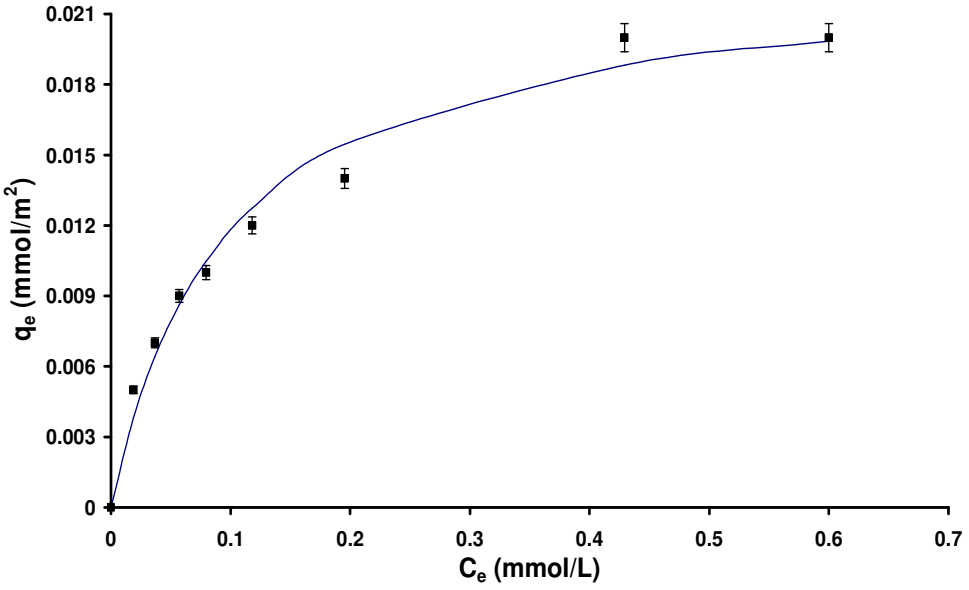

Figure 4.15. Sorption isotherm of PCP at pH 7. Solid line represents Langmuir model.

4.2.4 Effect of H_2O_2 dose on PCP degradation

Hydroxyl radical can be generated by the reaction between hydrogen peroxide and iron surface leading to PCP degradation. The degradation of organic compounds by $HO^{\cdot}$ is typically described as a second-order reaction:

$$\frac{d[PCP]}{dt} = -k[PCP][HO^{\cdot}] \qquad (4.15)$$

where $[HO^{\cdot}]$ is steady-state concentration of hydroxyl radical, [PCP] is concentration of PCP in water, k is the second-order rate constant, and t is the reaction time. By assuming that $HO^{\cdot}$ instantaneous concentration is constant, the kinetics of degradation of PCP in water can be described according to the pseudo-first-order equation as given below:

$$[PCP]_t = [PCP]_0 \exp(-k_{app} t) \qquad (4.16)$$

where k_{app} is the pseudo-first-order apparent rate constant (h^{-1}). The k_{app} constants were obtained from the slopes of the straight lines by plotting $-\ln(C_t/C_0)$ as a function of time t, through regression.

The kinetic constants rate k_{app} were determined at different H_2O_2 concentrations (Figure. 4.16). Since the PCP degradation is directly related to the concentration of the hydroxyl radicals produced by the catalytic decomposition of hydrogen peroxide, more PCP decomposition is expected when hydrogen peroxide dosage increases. When the molecule concentration of H_2O_2 was 0.086 M, the kinetic constants rate k_{app} was 0.048 min^{-1}. When the molecule concentration of H_2O_2 reached to 0.86 M, the k_{app} was 0.12 min^{-1}. However, a decrease in the values of k_{app} was observed at a much higher H_2O_2 concentration (Figure. 4.16). When the concentration reached to 1.29 M, the k_{app} went down to 0.045 which was even lower than the first one. The occurrence of this maximum H_2O_2 concentration for the effective degradation of PCP could be explained

by the scavenging effect of hydroxyl radicals by hydrogen peroxide. Similar observation was noted earlier for the degradation of organic compounds by Fenton-like reactions using goethite as catalyst [Kung and McBride, 1991]. The $HO^{\cdot}$ radicals preferentially attack the PCP molecules at low H_2O_2 concentration, whereas at much higher H_2O_2 concentration, there is a competitive reaction between the PCP and H_2O_2. The $^{\bullet}OH$ radical may react with hydrogen peroxide producing superoxide/hydroperoxy radicals according to:

$$^{\bullet}OH + H_2O_2 \rightarrow \quad HO_2^{\bullet}/O_2^{\bullet -} + H_2O \qquad (4.4)$$

Buxton et al. [Buxton et al., 1988] have determined the reaction rate of H_2O_2 with hydroxyl radical (k= 2.7×10^7 $M^{-1}s^{-1}$). Because the pKa of $HO_2^{\bullet}/O_2^{\bullet -}$ is 4.8, generation of hydroperoxide anion $HO_2^{\bullet}$ may be neglected at neutral pH. The generated radicals $O_2^{\bullet -}$ are much less reactive and do not contribute to any oxidation of organic compound [Lin and Gurol, 1998].

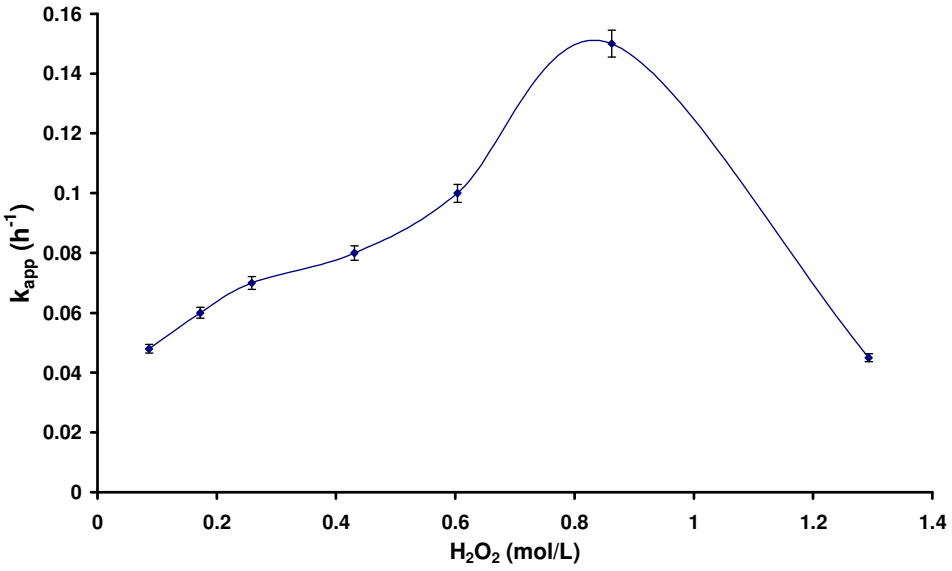

Figure 4.16. Degradation kinetic constant of PCP versus H_2O_2 dose. [PCP] = 50 mg L^{-1},

[Magnetite] = 2g L^{-1}, 20°C, pH 7.

4.2.5 H_2O_2 decomposition and PCP removal versus exposed surface area per unit volume

The H_2O_2 decomposition was monitored versus time at various exposed surface area of magnetite per unit volume. Good linear plot obtained with the expressions of $\ln([H_2O_2]/[H_2O_2]_0)$ as a function of the reaction time, indicates that the H_2O_2 decomposition is the first order reaction:

$$\frac{d[H_2O_2]}{dt} = -k_{app}[H_2O_2] \qquad (4.7)$$

where $k_{app} = k[SSA]$

[SSA] means the amount of specific surface area (BET method) par unit volume (m^2 L^{-1}). The H_2O_2 decomposition rate k_{app} (min^{-1}) was plotted as a function of [SSA] (Figure. 4.17). The good linear relationship (R^2=0.99) between the rate constant and [SSA] indicates that the H_2O_2 decomposition is the first order reaction with oxide surface area. The results clearly indicate that this is the surface reaction because the increase of surface area provides more active sites for catalytic oxidation. The second order rate constant (k) obtained from the plot of observed first-order rate constant for H_2O_2 decomposition versus [SSA] is 3.10^{-4} min^{-1} $(m^2 L^{-1})^{-1}$.

The PCP degradation was also investigated at various [SSA]. A plot of observed first order rate constant k_{app} (h^{-1}) for PCP removal as a function of [SSA] is shown in Figure. 4.17. In contrast with the result of H_2O_2 decomposition rate vs [SSA], the PCP removal was not proportional to the oxide surface area. The observed first order rate constant

for PCP oxidation firstly increased with [SSA] increasing. As shown in the figure that when [SSA] was 1 m^2L^{-1}, the k_{app} (h^{-1}) of PCP degradation was 0.035 h^{-1}, and k_{app} increased during the increasing of [SSA] until it reached to 25 m^2L^{-1} (k_{app} = 0.109), after that the k_{app} reduced to 0.09 (30 m^2L^{-1}) . This phenomenon can be explained from the assumption that $^{\bullet}OH$ radical generated by the reaction between hydrogen peroxide and iron oxide is scavenged by iron surface. Miller and Valentine [Miller and Valentine, 1999] reported that OH radical is very reactive with natural iron oxide-coated sand (k = 8 x 10^{11} (g mL^{-1}) $^{-1}$ s^{-1}). And also Rodrigues (2008) reported that such detrimental effect of excessive catalyst dosages can be ascribed to other undesirable and competitive reactions that decrease the amount of radicals available to oxidize the organic matter, by reaction with excess iron ions. The reaction or ferrous ions they are represented may be as the reaction (4.7) and (4.8) mentioned above:

$$Fe^{2+} + HO^{\bullet} \rightarrow Fe^{3+} + OH^{-} \qquad (4.17)$$

$$Fe^{2+} + HO_2^{\bullet} \rightarrow Fe^{3+} + HO^{2-} \qquad (4.18)$$

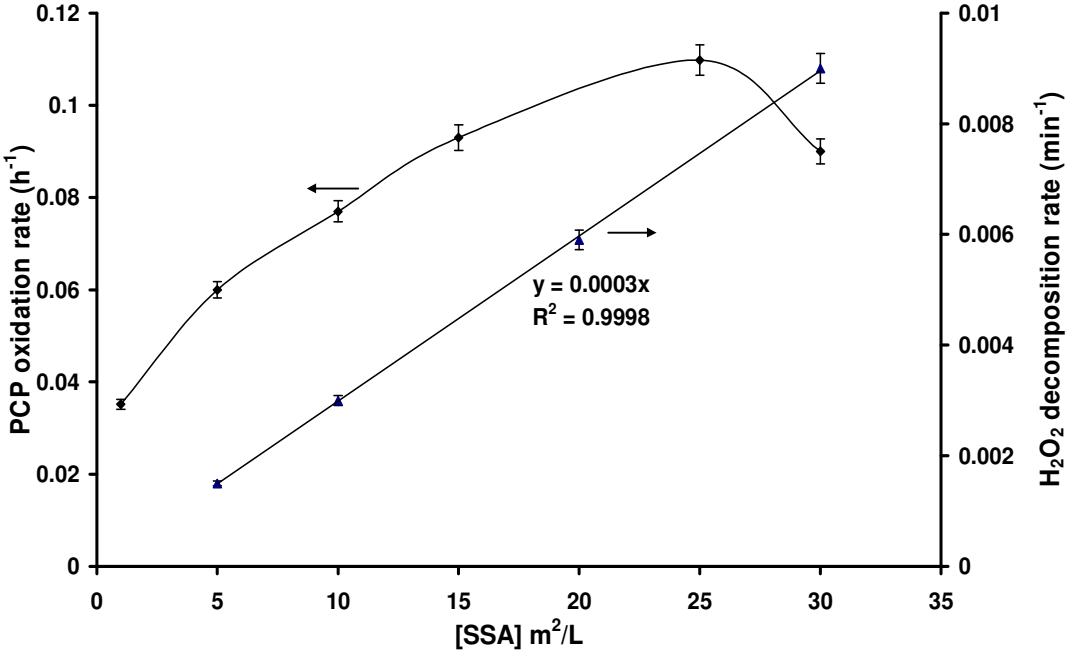

Figure 4.17. Degradation kinetic constant of PCP and H_2O_2 decomposition rate versus [SSA]. [H_2O_2] = 150 mM, 20°C, and pH 7 for the PCP degradation. [H_2O_2] = 1 mM, 20°C, and pH 7.

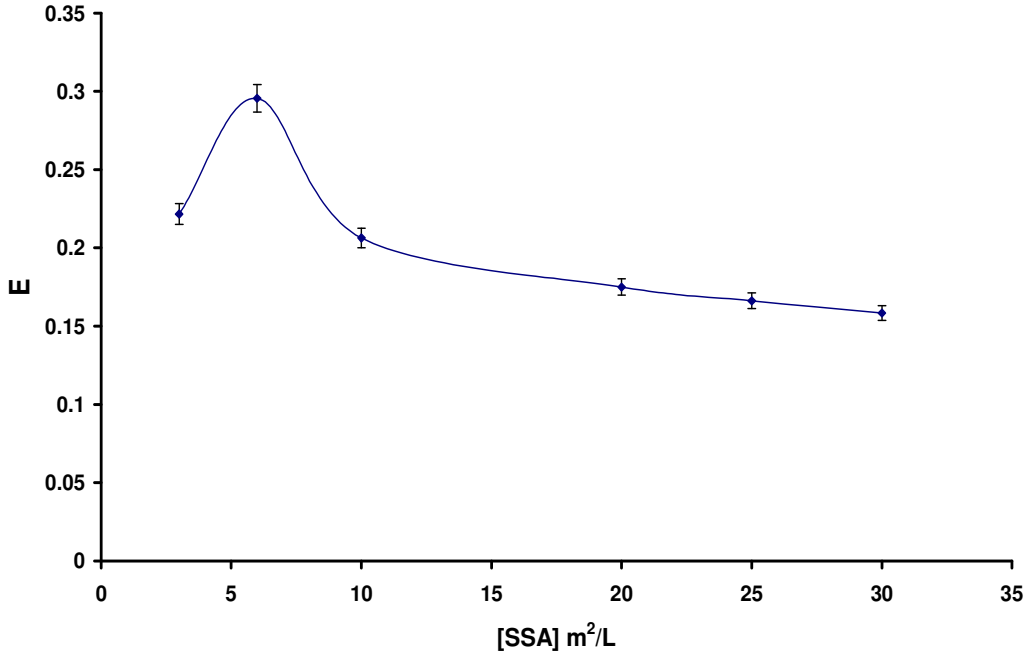

Figure 4.18. Oxidation efficiency (E) versus SSA. [PCP] = 50 mg L^{-1}, [H_2O_2] = 150 mM, 20°C, and pH 7 for the PCP degradation. [H_2O_2] = 1 mM, 20°C, and pH 7 for H_2O_2 decomposition.

Oxidation efficiency can be assessed by the following equation:

$$E(mole/mole) = \frac{\Delta[PCP]}{\Delta[H_2O_2]} \quad (4.19)$$

Where E(mole/mole) is the stoichiometry efficiency while Δ[PCP] and Δ[H_2O_2] represent the variation in molar concentration of PCP and H_2O_2 as a function of [SSA]. A high E value means a high reaction yield between PCP and hydroxyl radicals. Figure 4.18 shows that PCP oxidation efficiency increased with [SSA] increasing and then reduced. At low [SSA], the generated $HO^{\cdot}$ radicals preferentially react with PCP molecules, whereas at high [SSA], the iron surface can act as an OH radical scavenger.

4.2.6 Effect of initial PCP concentration

The pseudo-first-order apparent rate constant was determined at various initial PCP concentration (Figure 4.19). The pseudo-first-order degradation rate constant of PCP decreased when the initial concentrations of PCP increased from 10 to 100 mg L^{-1}. Increased amount of pollutant may occupy a greater number of iron active sites of the surface of the iron oxide, which become unavailable for H_2O_2 and result in lower $HO^{\cdot}$ generation rate. More PCP sorbed on the magnetite surface and less H_2O_2 interacted with iron surface and so that less hydroxyl radical formed at the surface. These results are consistent with many photocatalysis studies where activation by photon absorption is typically the first step for reaction, reaction rates were lowered with the higher initial concentration [Herrmann, 1999; Chen and Ray 1998; Daneshvar et 2004; Ollis et al., 1989]. The Langmuir-Hinshelwood model that is widely used in heterogeneous catalysis was tested [Chen and Ray 1998; Ollis et al., 1989]. In this case, the species present in the reaction compete with each other for adsorption on a fixed number of active sites. This Langmuir-Hinshelwood model postulates that the rate of reaction of two species adsorbed on the surface is the rate-limiting step:

$$k_{app} = \frac{k_{\text{int}} K_s}{1 + K_s [PCP]_i} \tag{4.20}$$

and linear expression :

$$\frac{1}{k_{app}} = \frac{1}{k_{\text{int}}} . [PCP]_i + \frac{1}{k_{\text{int}} K_s} \tag{4.21}$$

Where k_{app} is the initial pseudo-first-order rate constant (h^{-1}), k_{int} is the intrinsic reaction rate constant (mmol L^{-1} h^{-1}), and K_s is the adsorption constant of PCP over magnetite surface (L $mmol^{-1}$). The linear correlation (r^2 ~ 0.98) between $1/k_1$ and $[PCP]_i$ is relatively good, indicating that surface reactions of PCP including sorption and oxidation by surface $^{\cdot}OH$, play an important role in determining rate of the whole reaction. k_{int} and K_s were obtained as 0.022 mmol L^{-1} h^{-1} and 5.40 L $mmol^{-1}$. This K_s

value is lower than the sorption constant determined in the absence of oxidant by Langmuir model, suggesting an adsorption competition for the magnetite surface.

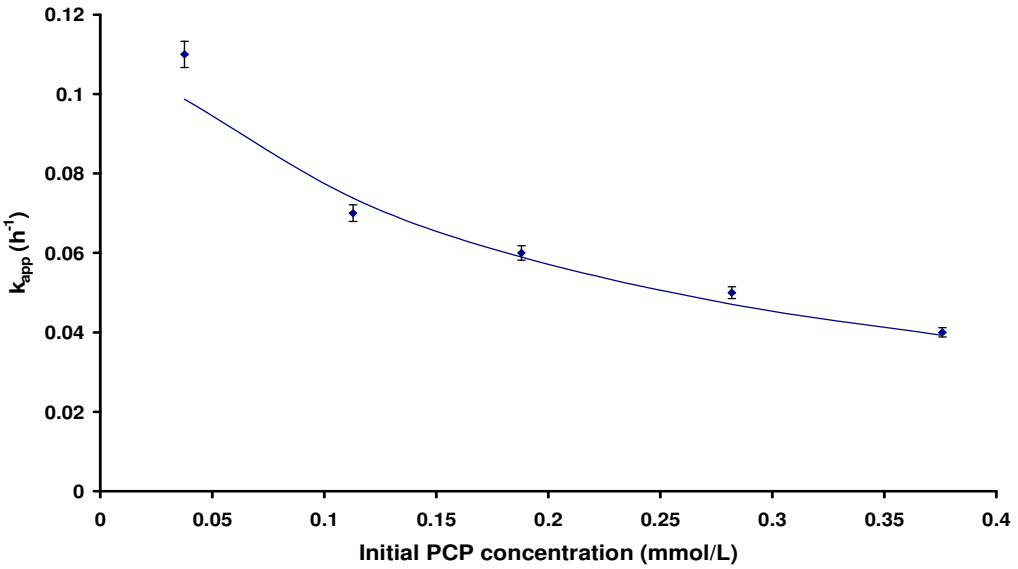

Figure 4.19. Degradation kinetic constant of PCP vs initial concentration of PCP. [Magnetite] = 2g L^{-1}, H_2O_2 =150 mM, 20°C, pH 7. Solid line represents Langmuir-Hinshelwood model.

In order to verify the competition between species and the implications of iron surface sites in the decomposition of these species, H_2O_2 decomposition and PCP oxidation experiments are operated in the presence of fluoride ions at pH7. Magnetite and fluoride solution were stirred for 1h to reach equilibrium sorption, after that H_2O_2 or PCP was added. Fluoride exhibits a strong chemical affinity for iron oxide surfaces and is capable of forming both inner and/or outer sphere complexes with iron oxide surfaces, with an intrinsic surface complexation constant of $\log K_{int}$ = 9,3 [Dzombak and Morel, 1990]. This might reduce the surface sites available for chemically-specific interactions with H_2O_2 or PCP, and lead to inactivation of iron mineral surfaces. Coherently, decrease in H_2O_2 decomposition rate value was observed with fluoride (Figure. 4.20a).

The observed decrease in PCP oxidation rate in the presence of fluoride (F^-) (Figure. 4.20b) may be due to several factors: (i) the decrease in H_2O_2 decomposition rate and so decrease in hydroxyl radical generation rate; (ii) the decrease in PCP sorption rate because of the competition with F^- for adsorption on surface active sites or (iii) the scavenging effect of fluoride ions towards hydroxyl radical in solution. Batch experiments showed that the presence of fluoride resulted in PCP adsorption decreasing on magnetite (around 50%). Furthermore, the scavenging of hydroxyl radical by chloride or fluoride is operational in acidic solution only and not at neutral to basic pH [Lipczynska-Kochany et al., 1995]. The increase of fluoride concentration to 1 mM did not significantly reduce more the oxidation performance observed at 0.1mM, corroborating that the scavenging effect of hydroxyl radical by fluoride is not significant under our experimental conditions. These observations confirm that the Fenton-like oxidation of PCP is controlled by surface mechanism reaction and adsorption of H_2O_2 or PCP on the surface of magnetite can affect the whole degradation reaction rate.

(a)

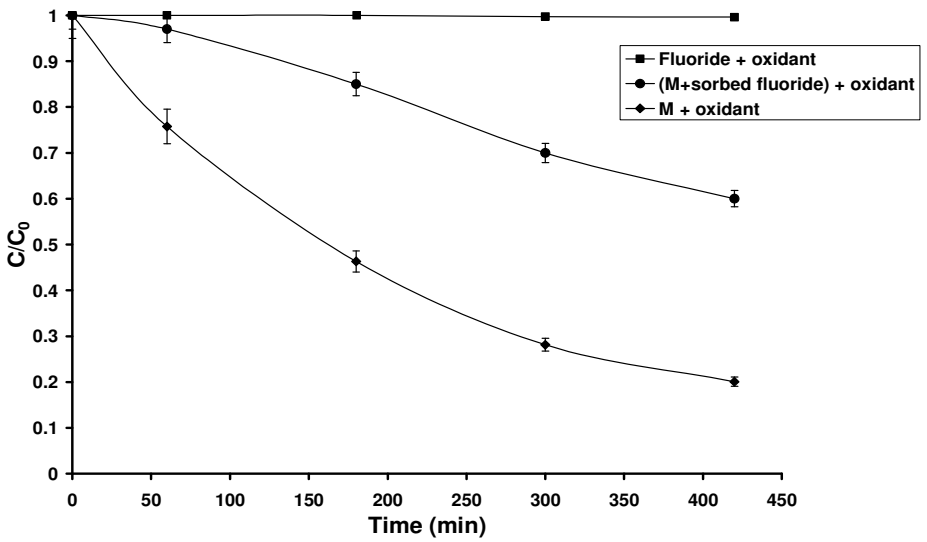

(b)

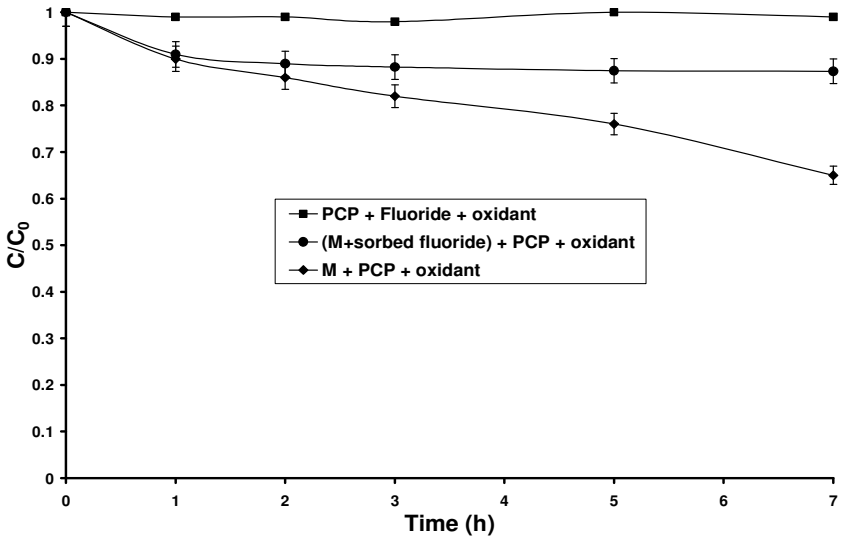

Figure 4.20. H_2O_2 decomposition versus time after F^- sorption and PCP removal versus time after F^- sorption. [H_2O_2] = 1 mM, F^- = 0.1 mM, [Magnetite (M)] = 10 $m^2 L^{-1}$, 20°C, and pH 7 for H_2O_2 decomposition. [Magnetite (M)] = 2 g L^{-1}, H_2O_2 =150 mM, F^- = 0.1 mM, 20°C and pH 7 for the PCP degradation.

4.2.7 Mass transfer rate of species

The apparent rate of a heterogeneous reaction is usually dominated by either the rate of intrinsic chemical reactions on the surface or the rate of diffusion of the solutes to the surface. Since the solid used in this study was not porous, the diffusion rate through the liquid film (external mass transfer resistance) was only considered.

Assuming that the entire surface is equally accessible, the rate of flow of substrate to the surface has been found to be proportional both to the surface area (A) and the difference in substrate concentration ([S]) between the bulk of the solution and the microenvironment next to the surface. The mass transfer coefficient k (cm s^{-1}) which depends upon the diffusivity of the substrate and the effective distance between the surface and the bulk phase can be written as:

$$k = \frac{D}{L} \tag{4.22}$$

D is the diffusion coefficient (cm^2/s), and L is the thickness of the stagnant liquid film (cm).

The rate of diffusion can be expressed as:

$$\alpha = \frac{D}{L^2} \tag{4.23}$$

The diffusion coefficient of the solutes in liquids is typically ~10^{-5} cm^2/s, and the stagnant layer thickness of the liquid film can be estimated by the Film theory as ~10^{-3} cm [Sherwood et al., 1975]. So, the mass transfer coefficient was estimated as 10^{-2} cm s^{-1} and the rate of diffusion as 10 s^{-1}.

The maximum observed rate for the PCP oxidation and for the decomposition of hydrogen peroxide is ~ 3.8×10^{-5} s^{-1} and 1.5×10^{-4} s^{-1}, respectively. So, the rate of diffusion is much faster than the reaction rate of either H_2O_2 or PCP on the iron oxide surface. Furthermore, the intrinsic reaction rate constant determined by Langmuir-Hinshelwood model was 6.1×10^{-6} mmol L^{-1} s^{-1}. Therefore, the intrinsic

reactions on the oxide surface including sorption and oxidation are expected to be the rate-limiting steps.

The kinetic rate constant of PCP degradation was also determined at different temperatures (10, 20, 30, and 40°C) to determine the activation energy of the PCP oxidation on the oxide surface ([PCP] = 50 mg L^{-1}, [Magnetite] = 2 g L^{-1}, H_2O_2 = 0.8 M, pH7). A correlation can be established by plotting the data from temperature and kinetic degradation rate (k_{app}) using linear form of Arrhenius equation:

$$\ln k_{app} = \ln A + (\frac{-E_a}{RT}) \quad (4.24)$$

where A is a constant and E_a is the activation energy. The activation energy of the reaction was determined as 47 ± 3.2 kJ mol^{-1}. This value is close to that reported by Seung and Veriansyah [Seung et al., 2007] for the oxidation activation energy of PCP in supercritical water (43.56 ± 1.47 kJ mol^{-1}).

The activation energy value of PCP degradation is higher than that of the diffusion-controlled reactions, which usually ranges within 10-13 kJ mol^{-1} [Stumm et al., 1996]. These results corroborates that the apparent reaction rate is dominated by the rate of intrinsic chemical reactions on the oxide surface rather than the rate of mass transfer.

4.2.8 Removal of PCP in aqueous or sorbed phase

The interactions between oxidant and iron surface can be explained by heterogeneous reactions analogous to the solution phase reactions [Barb et al., 1951; Pignatello, 1992; Walling and Cleary, 1977], where the dominant reaction is first a chain of reactions occurring on the mineral surface:

$$\equiv Fe^{II} + H_2O_2 \rightarrow \equiv Fe^{III} + HO^- + HO^\cdot \quad (4.10)$$

$$\equiv Fe^{III} + H_2O_2 \rightarrow \equiv Fe^{III}(H_2O_2) \quad (4.11)$$

$$\equiv Fe^{III}(H_2O_2) \rightarrow (\equiv Fe^{II}.O_2H) + H_2O \quad (4.12)$$

$$(\equiv Fe^{II}.O_2H) \rightarrow \equiv Fe^{II} + HO_2^{\bullet} / O_2^{\bullet -} \quad (4.13)$$

$HO_2^{\bullet}$ / $O_2^{\bullet -}$ plays an important role in the redox cycle of iron in aqueous phase and generates oxygen as a byproduct but the interactions of superoxide/hydroperoxy radicals with the iron mineral surface are not yet well argued :

$$\equiv Fe^{III} + O_2^{\bullet -} \rightarrow \equiv Fe^{II} + O_2 \quad (4.25)$$

$$\equiv Fe^{II} + HO_2^{\bullet} / O_2^{\bullet -} \rightarrow \equiv Fe^{III} + HO_2^{-} \quad (4.26)$$

Other competitive reactions may be occurred such as the auto-decomposition of H_2O_2 to oxygen and water, the recombination of OH radicals to generate H_2O_2. However, the disproportionation of hydroperoxy radical (combination of two hydroperoxy radicals to H_2O_2 and O_2) is not expected because generation of hydroperoxide anion $HO_2^{\bullet}$ may be neglected at neutral pH.

On the other hand, the interactions between PCP and iron surface sites (≡Fe) can be described as equilibrium reaction between sorbed and aqueous species:

$$\equiv Fe + PCP_e \leftrightarrow \equiv Fe(PCP)_s \quad (4.27)$$

The hydroxyl radicals formed by the reaction between hydrogen peroxide and iron surface can probably attack the sorbed species as well as the aqueous species leading to the degradation and mineralization of PCP:

$$HO^{\cdot} + \equiv Fe\ (PCP)_s \rightarrow \equiv Fe + (PCP\ byproducts)_{solution} \rightarrow Cl^- + CO_2 \quad (4.28)$$

$$HO^{\cdot} + PCP_e \rightarrow PCP\ byproducts \rightarrow Cl^- + CO_2 \quad (4.29)$$

Raman spectra show the PCP sorbed on the surface of magnetite along the oxidation reaction (Figure. 4.21). Prior to Raman analysis, oxidation experiment of PCP at neutral pH was conducted versus time in 2 g L^{-1} of magnetite with the optimum value of H_2O_2 dose (Figure. 4.22). During the oxidation reaction, a few milligrams of magnetite were sampled from oxidation reactor at selected time intervals and immediately analyzed by Raman spectroscopy without drying (Figure. 4.21). The PCP amount was also quantified in aqueous phase and in solid phase after extraction by chromatography analysis.

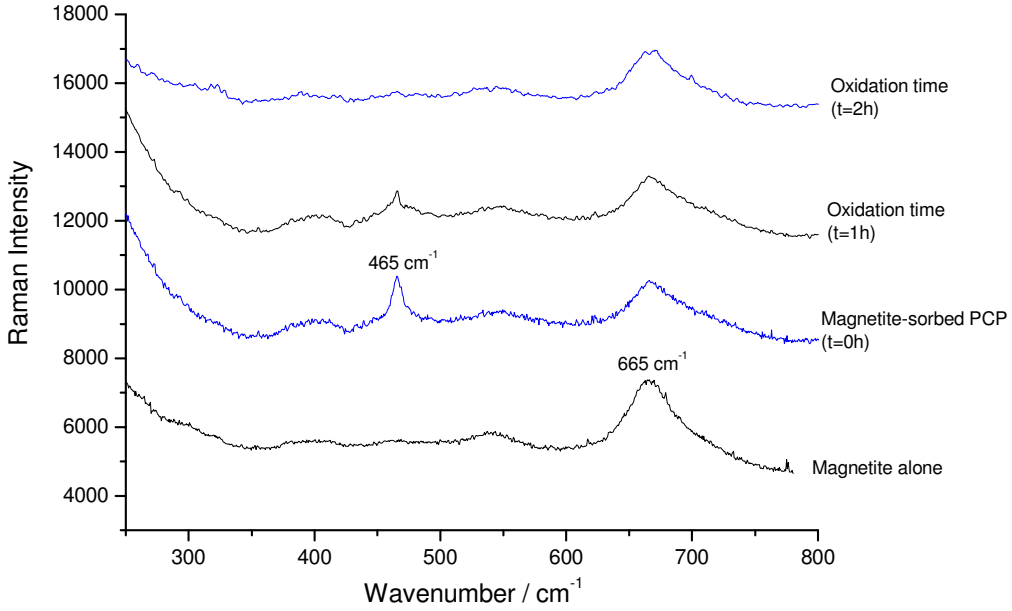

Figure 4.21. Raman spectra of sorbed PCP on magnetite before and after exposure to H_2O_2. [PCP] = 50 mg L^{-1}, [Magnetite] = 2 g L^{-1}, H_2O_2 = 0.8 M, 20°C, pH 7.

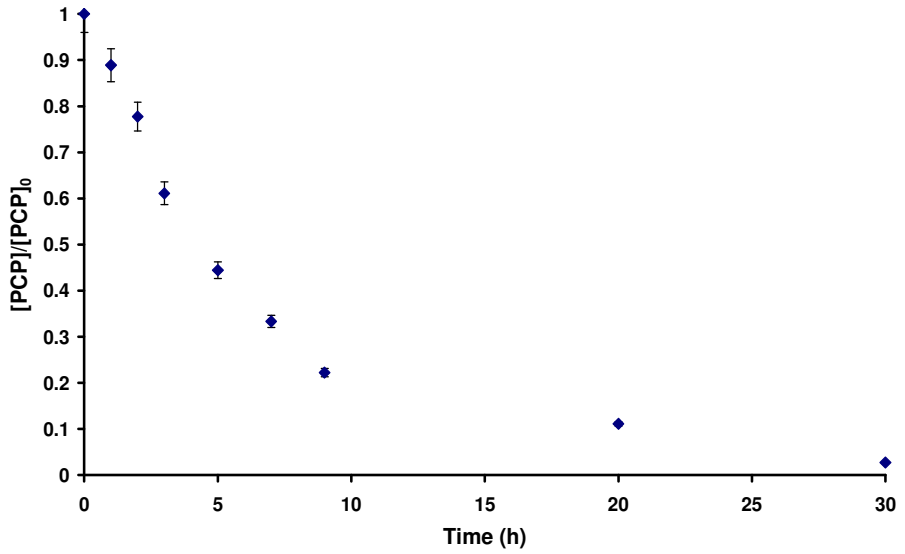

Figure 4.22. PCP decay versus time. [PCP] = 50 mg L^{-1}, [Magnetite] = 2 g L^{-1}, H_2O_2 = 0.8 M, 20°C, pH 7.

Based on the Raman signature, the band at 665 cm^{-1} could be assigned to magnetite (Fe_3O_4) [Neff et al., 2006], while the stronger band of PCP is around 465 cm^{-1} (Figure 4.21). The sorbed PCP disappeared from the surface of magnetite at 2h treatment time before the total removal of PCP in aqueous solution (occurred at around 30h as shown in Figure 4.22). Both degradation and desorption processes could explain the disappearance of PCP from magnetite surface at the first stage of reaction. In the case of degradation, the OH radicals generated from the surface reaction between hydrogen peroxide and surface active sites may preferentially react with surface sorbed PCP. In the case of desorption, H_2O_2 competed with PCP for the fixation on magnetite active sites as previously shown by Langmuir-Hinshelwood model, and displaced it from surface to aqueous phase.

4.2.9 Kinetic of PCP mineralization

Complete degradation of PCP does not imply that the PCP was completely oxidized into CO_2, H_20 and inorganic ions. Reaction intermediates are usually formed and enter solution during degradation. It is known that reaction intermediates can form during the oxidation of pollutant and some of them could be long-lived and even more toxic than the parent compounds. Therefore, it is necessary to realize the mineralization of PCP. So in our work the PCP mineralization was determined by both TOC and chloride formation measurements (Figure 4.23).

The first reaction of PCP oxidation should be the dechlorination since 90% of chloride was formed at the first 30 hours corresponding to the total disappearance of parent compound (Figure 4.22). It indicated that after 30 hours, not only most of the PCP was degraded, but also most type of common intermediates under Fenton-reaction such as: mixtures of tetrachlorobenzoquinone, tetrachlorohydroquinone, and tetrachlorocatechol [Benitez et al., 2003; Hirvonen et al., 2000; Luo et al., 2008; Mills and Hoffman, 1993] were degraded. After then, the total dechlorination increasesed slowly even though a complete degradation of PCP is achieved. Actually the further oxidation induces ring cleavage and leads to the formation of organic acids such as formic, acetic, and oxalic acids [eg: Pignatello et al., 2006].

Total dechlorination (chloride mass balance corresponding to 50 mg L^{-1} of PCP) was achieved at 4d treatment time and complete mineralization measured by TOC abatement occurred after 7d. The remained TOC after total dechlorination at 4d (28%), 5d (18%) and 6d (10%) could be attributed to organic acids accumulated in the solution. So it is clear that the oxidation of PCP undergoes a fast reaction rate than the mineralization of it under the same experiment conditions. In order to identity the end products, aliquots sampled at 4d, 5d and 6d treatment times were analyzed by ion exclusion chromatography (results not reported). Two major peaks corresponding to

oxalic acid and formic acid were identified by comparison of their retention time with those of authentic standards. Note that oxalic and formic acids have been well described as by products of the aromatic ring cleavage and often detected in solution after Fenton treatment [Hanna et al., 2005; Matta et al., 2008].

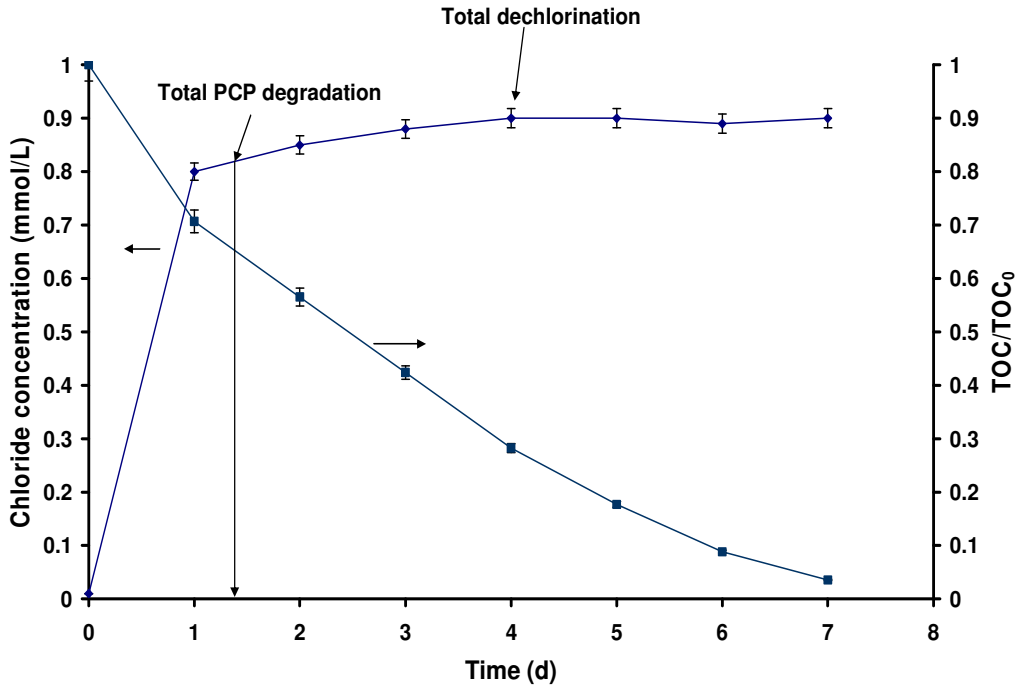

Figure 4.23. TOC abatement and chloride formation versus time. [PCP] = 50 mg L^{-1}, [Magnetite] = 2 g L^{-1}, H_2O_2 = 0.8 M, 20°C, pH 7.

In order to confirm the role played by ·OH in the degradation of PCP in the Fenton-like reactions, the reaction with magnetite was repeated with the addition of excess 2-propanol as an ·OH scavenger. 2-propanol is rapidly oxidized by hydroxyl radicals ($k_{OH\cdot} = 3 \times 10^9$ M^{-1} s^{-1}) but is less reactive with superoxide $O_2^{\bullet-}$ ($k_{O2\bullet-} = 1 \times 10^6$ M^{-1} s^{-1}) [Teel and Watts, 2002]. Addition of 2-propanol (2% v/v) in the magnetite/H_2O_2 system inhibited the oxidation of PCP which confirms the predominant role of hydroxyl radical in the dechlorination and mineralization of PCP and corroborates with a Fenton-like reaction taking place in this system.

4.2.10 Structural and catalytic stabilities

For the iron oxides/H2O2 system, the stability of a catalyst is a very important factor for its application, If when reuse the iron oxides that the oxidation efficiency was not as good as the first round of usage, it means that the stability of the catalyst is poor and easy to be deactivation, then the catalyst will be useless in a realistic pollutant treatment application. Thus, it is necessary to check the structural and catalytic stabilities of the iron oxide after the reaction.

The action of H_2O_2 on the oxide surface can transform the oxide particles into an only Fe^{III}-bearing mineral or into an amorphous iron oxide which may be less stable and more soluble. This mineralogical transformation may lead to a substantial change in the surface characteristics of the mineral, causing a different kinetic behavior and decomposition rate for H_2O_2. The very low dissolved iron concentration measured (< 0.05 mM) did not expect the formation of more soluble iron oxide. The chemical analyses of the solid after reaction revealed no significant change in the total Fe loading. In addition, XRD diffractogram recorded at the end of oxidation reaction was found to be similar to that recorded before reaction (i.e. Fig.4.12). Furthermore, the hyperfine parameters of Mössbauer spectra shown in Table 4.2 are unchanged after reaction, indicating a strong structural stability of solid.

The reusability of the solid has been evaluated under identical oxidation conditions as for the first oxidation cycle. At the end of the oxidation process, the solid is easily removed from the reactor, dried in the glovebox under N_2 and stored at ambient temperature. The H_2O_2 decomposition and PCP degradation on the recovered catalyst were then investigated as for previous experiments and showed a slight difference with the first oxidation cycle. Indeed, $k_{app/H2O2}$ and $k_{app/PCP}$ are found to be respectively 0.058 h^{-1} and 0.0040 min^{-1} for the first batch oxidation, and 0.060 h^{-1} and 0.0039 min^{-1} for the second oxidation cycle. So, no deactivation of surface catalytic sites was caused by the adsorption/oxidation process. The excellent stability of the catalytic

activity could be attributed to the low loss of iron content and to the structural stability of magnetite during oxidation cycles at neutral pH. However, the oxidative transformation of magnetite to maghemite and goethite may be possible at high pH conditions as reported by He and Traina [Thomas He and Traina, 2005]. In this work, the authors stated that the possible transformation mechanism of magnetite at alkaline conditions is through the dissolution and re-precipitation process [Thomas He and Traina, 2005].

4.2.11 Conclusion

The degradation rate of PCP by Fenton-like oxidation firstly increased with the dosage of H_2O_2 or with the amount of magnetite, reached a maximum value and then decreased. The occurrence of these maximums values for the effective degradation of PCP could be explained by the scavenging reaction with H_2O_2 or iron oxide surface. The PCP mineralization determined by TOC was completed after 7days, while total dechlorination was achieved at 4d treatment time. The first reaction of PCP oxidation should be the dechlorination since 90% of chloride was formed at the first 30 hours corresponding to the total disappearance of parent compound. The magnetite catalyst exhibited low iron leaching, good structural stability and no loss of performance in second reaction cycle. The apparent reaction rate for heterogeneous Fenton reaction is dominated by the rate of intrinsic chemical reactions on the oxide surface rather than the rate of mass transfer. All batch experiments indicate that Fenton-like oxidation of PCP is mainly controlled by surface mechanism reaction and the species compete with each other for adsorption on a fixed number of magnetite active sites. Raman analysis suggested that the sorbed PCP was removed form magnetite surface at the first stage of oxidation reaction. Due to the complex nature of chemical surface species, it is difficult to fully understand the multiple interactions that occur on the oxide surface. Spectroscopic characterization *in situ* of surface active sites and solute surfaces complexes during the oxidation reaction are required for this purpose.

4.3 Effect of chelating agent on the oxidation rate of PCP in the magnetite /H_2O_2 system at neutral pH

4.3.1 Introduction

In this part of work, magnetite was selected as iron bearing mineral. Six kinds of chelating agents were chosen including Ethylene Diamine Tetraacetic Acid (EDTA), Carboxy-methyl-cyclodextrin (CMCD), oxalate, tartarate, citrate and succinate, based on their different chelating ability of iron ion. Pentachlorophenol (PCP) was selected as model pollutant. The effect of chelating agents on the Fenton heterogeneous oxidation rate of pentachlorophenol in the presence of magnetite (Fe_3O_4) was investigated in opened batch reactor at neutral pH. The PCP oxidation rate in the Fenton-like system was significantly improved by using chelating agents at neutral pH. The kinetic rate constant was increased by 5.7, 4, 3.2, 2.4, 2.5 and 1.7 times with oxalate, EDTA, CMCD, tartarate, citrate and succinate, respectively. This observation was supported by the increased concentration of chloride generated by the degradation of PCP. The enhancement factor of heterogeneous oxidation rate was found to be correlated with that of iron dissolution rate except for oxalate.

The chelating agents (CA) have strong complexing ability with multivalent cation and have been widely used to enhance the efficiency of Fenton's reaction [Matta et al 2008a; Sun and Pignatello, 1992; Ferraz et al. 2007; Matta et al., 2008b; Seol and Javandel, 2008; Li et al., 2005]. Many of these chelating agents are naturally occurring organic acid such as low molecular weight organic compounds [Kayashima and Katayama, 2002; Li et al., 2008]. However, EDTA remains the mostly used CA in the Fenton-chelate based studies at ambient pH when iron is complexed with EDTA or an EDTAanalog [Nowack et al., 1996; Blesa et al., 1984]. EDTA is similar to other organic ligands in that it has the ability to accelerate the dissolution of oxide minerals. In previous studies, the effect of CA on the enhancement of degradation efficiency was

tested in either homogeneous or heterogeneous system [Matta et al 2008a; Sun and Pignatello, 1992; Ferraz et al. 2007; Matta et al., 2008b; Seol and Javandel, 2008; Li et al., 2005; Li et al., 2008; Nowack et al., 1996; Blesa et al., 1984; Strathmann and Stone et al., 2002; Naka and Kim et al., 2006]. In Fenton homogenous system at near neutral pH, the CA could maintain iron in soluble form preventing its precipitation and thus enhance the production of hydroxyl radical and the degradation efficiency [Li et al., 2008; Strathmann and Stone et al., 2002; Naka and Kim et al., 2006]. In Fenton heterogeneous system, the CA could dissolve iron form the solid surface and then the propagation of homogeneous reaction by the dissolved iron contributes to the improvement of the whole oxidation rate [Matta et al 2008a; Sun and Pignatello, 1992; Ferraz et al. 2007; Matta et al., 2008b; Seol and Javandel, 2008; Li et al., 2005]. In these studies, the implication of the surface interactions with the heterogeneous catalyst in the enhancement of pollutant oxidation was poorly investigated. Furthermore, the competition between all species toward iron surface sites in heterogeneous oxidation reaction was scarcely described.

Our research goals of this part are: 1) to test heterogeneous Fenton reaction by adding chelating agent to make it more suitable at circumneutral pH environment; 2) to find out the role played by the CA in heterogeneous Fenton system compared to the homogeneous one; 3) to understand the kinetic and mechanism of the chelate-based Fenton reaction in heterogeneous system and to determine the rate-limiting step 4) to highlight the multiple surface reactions involving sorption, oxidant decomposition and oxidation processes.

4.3.2 Effect of chelating agents on the heterogeneous oxidation rate of PCP

The effect of chelating agent (CA) on the PCP heterogeneous oxidation was pointed out through the determination of kinetic constant rate and the chloride formation. The oxidation of PCP was investigated versus time in the presence of six types of chelating agents (Figure. 24a). The degradation of organic compounds by $HO^{\cdot}$ is typically described as a second-order reaction:

$$\frac{d[PCP]}{dt} = -k[PCP][HO^{\cdot}] \qquad (4.15)$$

where [PCP] and [$HO^{\cdot}$] are concentrations of PCP in water and hydroxyl radical, respectively, k is the second-order rate constant, and t is the reaction time. By assuming that $HO^{\cdot}$ instantaneous concentration is constant, the kinetics of degradation of PCP in water can be described according to the pseudo-first-order equation as given below:

$$[PCP]_t = [PCP]_0 \exp(-k_{app} t) \qquad (4.16)$$

where k_{app} is the pseudo-first-order apparent rate constant. The k_{app} constants were obtained from the slopes of the straight lines by plotting $-\ln(C_t/C_0)$ as a function of time t, through regression. The kinetic constants rate k_{app} (h^{-1}) determined in the presence of different CA follow the sequence: oxalate (0.23) > EDTA (0.16) > CMCD (0.13) > citrate (0.1) > tartarate (0.098) > succinate (0.07) > without chelating agent (0.04). The kinetic rate constant was increased by 5.7, 4, 3.2, 2.4, 2.5 and 1.7 times with oxalate, EDTA, CMCD, tartarate, citrate and succinate, respectively. As indicator of PCP mineralization, the increase of chloride concentration was also measured versus time

(Figure. 24b). The extent of chloride generation follows the same order as for the oxidation rate constant: oxalate > EDTA > CMCD > citrate > tartarate > succinate > without chelating agent. At 21 hours treatment time, 90, 82 and 78 % of dechlorination (chloride mass balance corresponding to 50 mg L^{-1} of PCP) was achieved for oxalate, EDTA and CMCD, respectively. The enhancement factor of PCP dechlorination in the presence of CA was 2.1, 1.9, 1.8 for oxalate, EDTA and CMCD, respectively.

(a)

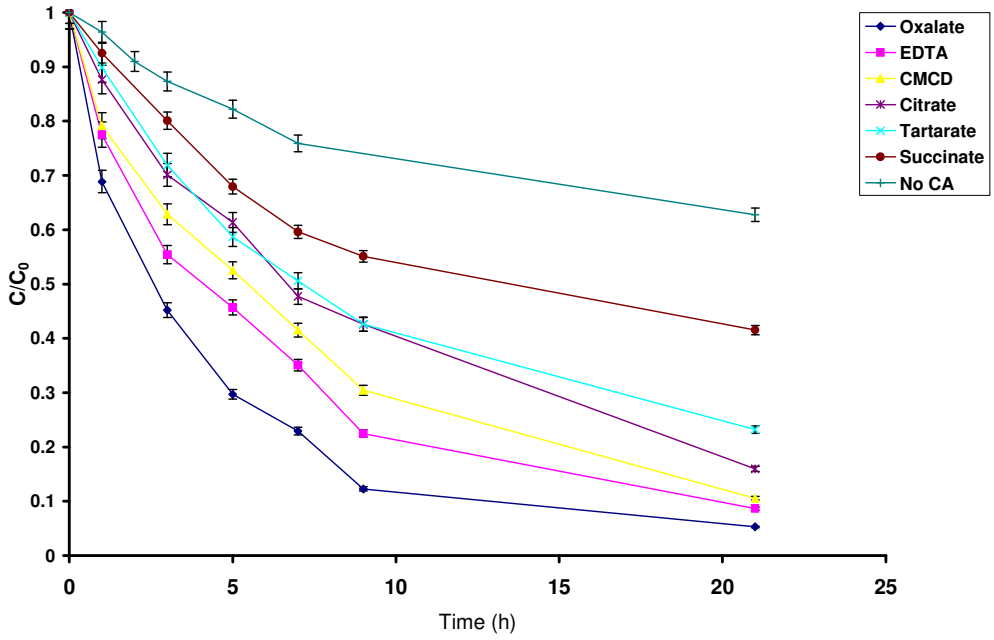

(b)

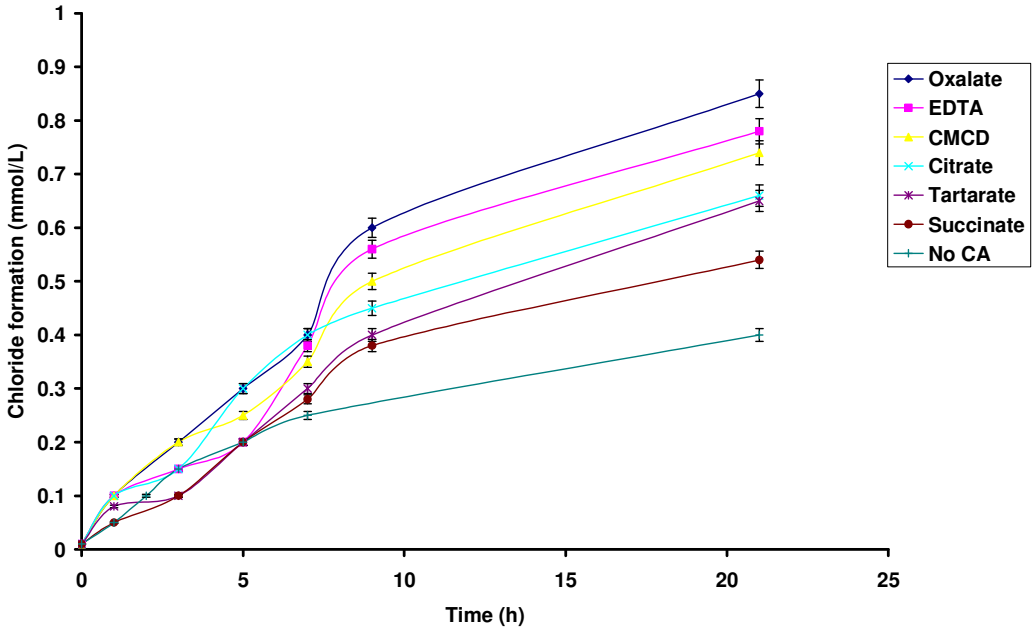

Figure 4.24. Effect of chelating agents on the PCP degradation rate (a) and chloride formation (b). [PCP] = 50 mg L^{-1}, [Magnetite] = 2g L^{-1}, H_2O_2/Fe (molar ratio) = 100, [Chelating Agent (CA)]] = 1mM, 20°C, pH7.

Because the chelating agents contain a high density of functional groups, they can accelerate the dissolution of oxide minerals [Seol and Javandel, 2008; Li et al., 2005]. The CA-promoted dissolution involves the Fenton reaction to be propagated in solution by the dissolved iron. Consequently, the Fenton-chelate based system becomes more active in generating $^{\bullet}OH$ and decomposing of the pollutant. In order to determine the contribution of homogenous Fenton reaction or the extent of magnetite dissolution, the total dissolved iron concentration was measured versus time in magnetite/CA/ H_2O_2 solutions. Results are reported in Figure 4.25 and showed that the total dissolved iron in the solution increased firstly versus time and then reduced. The total amount of dissolved iron followed the sequence: EDTA > CMCD > tartarate > citrate > oxalate > succinate. This sequence was in the same order as for the oxidation rate constant k_{app} (h^{-1}) except for oxalate. Generally, all used CA contributed to the increase in iron oxide dissolution rate. Consequently, homogeneous Fenton's reaction was assumed to be in part responsible for the improvement of PCP degradation.

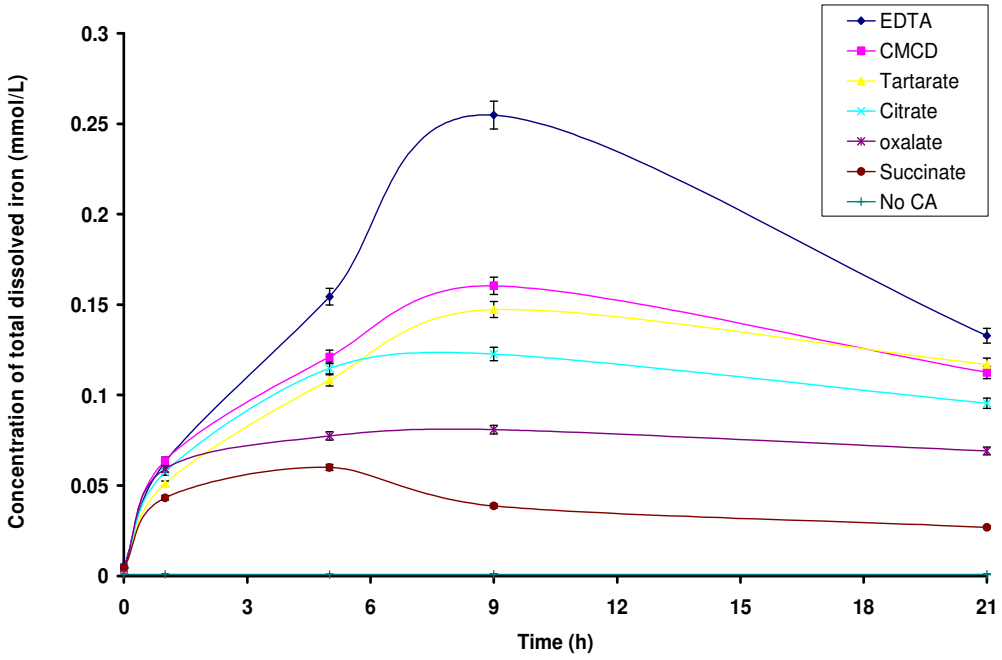

Figure 4.25. Total dissolved iron vs reaction time. [PCP] = 50 mg L^{-1}, [Magnetite] = 2g L^{-1}, H_2O_2/Fe (molar ratio) = 100, [CA] = 1mM, 20°C, pH7.

Despite their iron chelating ability, the oxidation enhancement factor using citrate, tartarate or succinate was found to be relatively low. Burkitt and Gilbert [Zepp and Faust, 1992] reported that citrate, tartrate and succinate were shown to be relatively poor catalysts of the Haber-Weiss cycle. In addition, the hydroxyl radical reaction rates with these organic acids are relatively high: k (citrate /$HO^{\cdot}$) = 3.2×10^8 (L mol^{-1} s^{-1}) at pH = 6.6; k (tartrate/ $HO^{\cdot}$) = 1.4×10^9 (L mol^{-1} s^{-1}) at pH = 9; k (succinate/ $HO^{\cdot}$) = 7.6×10^8 (L mol^{-1} s^{-1}) at pH = 9) [33, 34]. So, these compounds compete actively with PCP for the reaction with hydroxyl radical and can act as $HO^{\cdot}$ scavenger.

On the other hand, EDTA, CMCD and oxalate showed a good catalytic activity in the Fenton-chain reaction. The oxidation rate constant of PCP in magnetite/H_2O_2 system

was then determined versus CA concentration (0.5mM to 5 mM) (Figure 4.26a). Oxalate, CMCD and EDTA which showed the highest enhancement factor of oxidation rate are chosen for this experiment. At all tested concentration range, the oxidation rate constant k_{app} (h^{-1}) with oxalate is higher than with EDTA or CMCD. However, EDTA was the most able to dissolve iron from magnetite surface (Figure 4.26b).

(a)

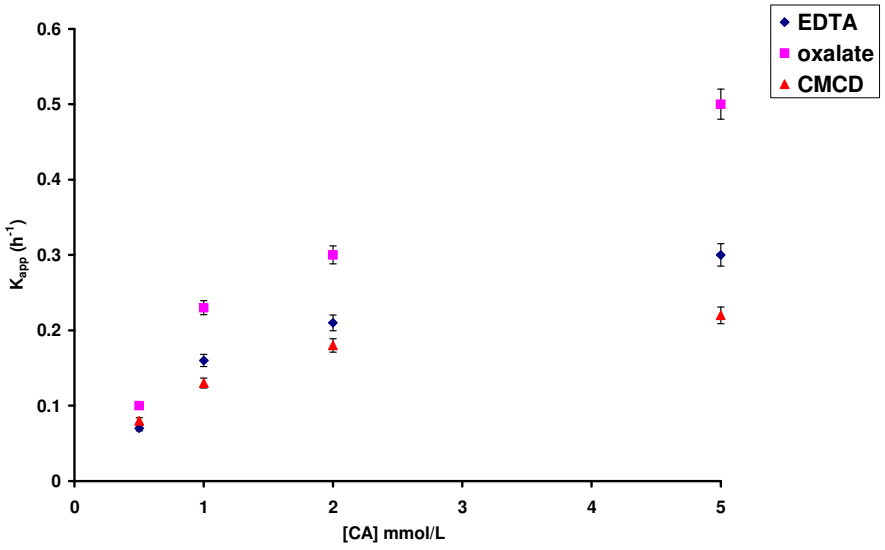

(b)

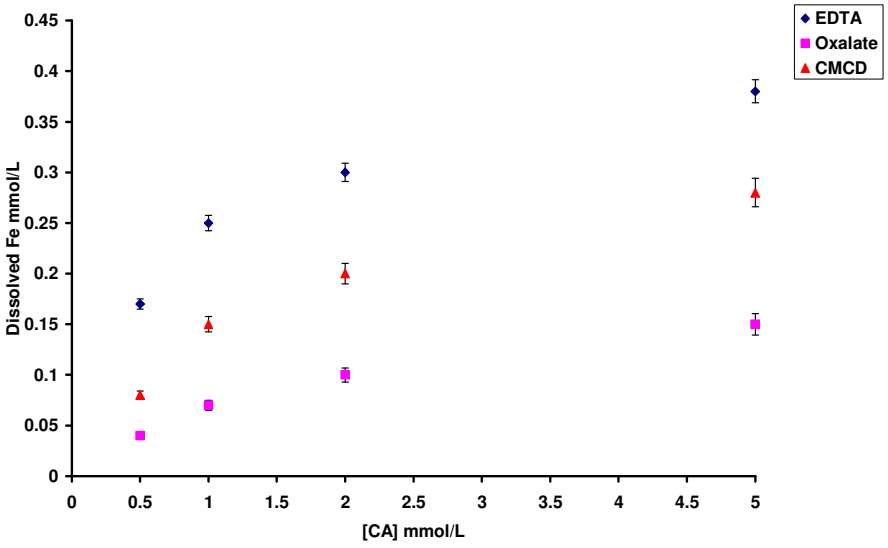

Figure 4.26. Degradation kinetic constant of PCP (a) and total dissolved iron (b) versus different concentration of chelating agents. [PCP] = 50 mg L^{-1}, [Magnetite] = 2g L^{-1}, H_2O_2/Fe (molar ratio) = 100, 20°C, pH7.

The variation of k_{app} (h^{-1}) against CA concentration is not linear (Figure 4.26a), which may be due to the radical scavenging effect of CA when it is used at high concentration. This phenomenon is more pronounced for EDTA or CMCD, probably due to the high reaction rate with hydroxyl radical [Hanna et al., 2005; Zhou et al., 2008]. k (EDTA /$HO^{\cdot}$) = 4.0×10^8 (L mol^{-1} s^{-1}) at pH = 4.0 and k (EDTA /$HO^{\cdot}$) = 2.0×10^9 (L mol^{-1} s^{-1}) at pH = 9.0) [Noradoun and Cheng, 2005]; k (β-CD /$HO^{\cdot}$) = 4.2×10^9 (L mol^{-1} s^{-1}) at pH ~7 and k (HPCD /$HO^{\cdot}$) = 8.8×10^9 (L mol^{-1} s^{-1}) at acidic pH) [Hanna et al., 2005; Deeble et al., 1989]. EDTA and cyclodextrin can easily be oxidized and acted like a scavenger of $^{\cdot}OH$ under the Fenton reaction [Zhou et al., 2008; Li et al., 2007; Noradoun and Cheng, 2005; Englehardt et al., 2007]. EDTA and CMCD could be oxidized by hydroxyl radicals and derivated low molecule weight (LMW) organic acids in the solution [Hanna et al., 2005; Zhou et al., 2008]. However, the reaction of hydroxyl radical with oxalate was found to be relatively low (i.e. k (oxalate/$HO^{\cdot}$) = 1.4×10^6 (L mol^{-1} s^{-1}) [Getoff et al., 1971; Hag and Yao, 1992]. This value is lower than that of other CA and so EDTA and CMCD have a higher reactivity than oxalate against hydroxyl radicals.

The increase of dissolved iron amount versus CA concentration was reported in Figure 4.26b. The ligand-promoted dissolution of oxide minerals is a surface-controlled reaction occurring in steps [Stumm, 1997]. The first step is the adsorption of the ligand on the oxide surface, most commonly by a ligand exchange mechanism. This step is very fast compared to the dissolution reaction. Upon adsorption, the surface complex weakens the metal-oxygen bonds on the surface of the crystal lattice. Thus, the overall dissolution rate is proportional to the rate of breaking a metal-oxygen bond [Stumm, 1997; Miller et al., 1986] compared the effectiveness of thirteen organic acids to dissolve crystalline iron oxy-hydroxides. They found that EDTA completely dissolved the noncrystalline oxides and partially dissolved the crystalline ones. The EDTA-promoted dissolution was found to be greater than for other organic acids such as oxalate, tartrate and succinate [Miller et al., 1986].

Inspection of figures 3a and 3b showed that the performance of Fenton-chelate based reaction can not be correlated with the extent of magnetite dissolution. Despite its strong chelating ability, EDTA is less reactive than oxalate in heterogeneous Fenton reaction. So, an additional mechanism than iron dissolution could take place and would be discussed below. Moreover, the Fenton-chelate based reaction in solution must be also different for each CA type. The evaluation of the homogeneous Fenton reaction in the presence of oxalate, EDTA and CMCD will be the aim of the following section.

4.3.3 Effect of chelating agents on the homogeneous oxidation rate of of PCP (dissolved Fe^{II} and Fe^{III}).

In order to highlight the effect of oxalate, EDTA and CMCD on the homogeneous Fenton degradation rate of PCP, oxidation experiments were performed with the dissolved iron (Fe^{2+} or Fe^{3+}). The chosen concentration (0.5mM) was higher than the maximum value obtained in magnetite dissolution experiments (Figure 4.27). The kinetic of degradation of PCP can be described according to the pseudo-first-order equation. The k_{app} constants (min^{-1}) obtained from the pseudo-first-order fit are shown in Table 4.4. For both Fe^{II} and Fe^{III}, the kinetic oxidation rate can be ranked as: EDTA >> Oxalate > CMCD > without chelating agent.

(a)

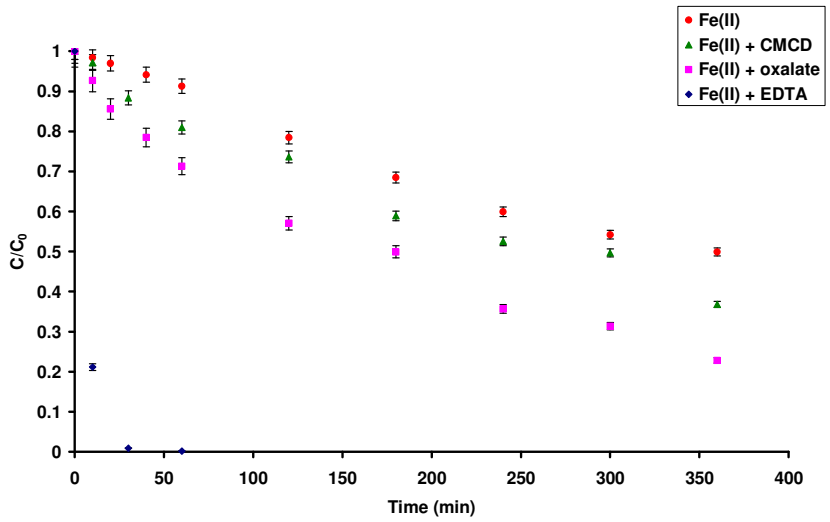

(b)

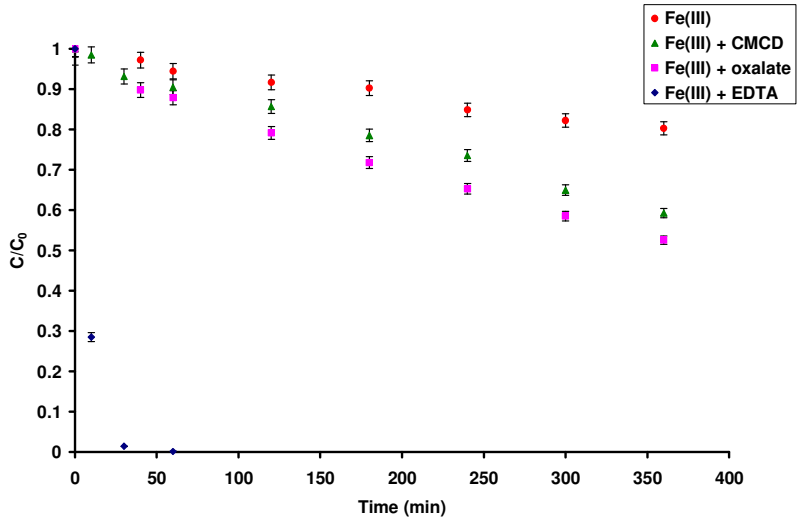

Figure 4.27. Effect of using dissolved FeII and FeIII. [PCP] = 50 mg L^{-1}, Fe^{III} ($Fe_2(SO_4)_3$) =Fe^{II} ($FeSO_4$) = 0.5mM , $Fe^{II}(Fe^{III})/H_2O_2$/CA = 1/100/1, pH7, 20°C. Dissolved Fe^{II} (a), dissolved Fe^{III} (b).

In Fenton-like homogeneous reaction, the dominant reaction is first a chain of reactions in the iron-catalysed Haber-Weiss cycle [Walling, 1975; Walling and Goosen, 1973]:

$Fe^{III} + H_2O_2 \rightarrow Fe^{II} + HO_2^{\bullet} / O_2^{\bullet-} + H^+$ 0.01 $M^{-1}s^{-1}$ (4.30)

$Fe^{II} + H_2O_2 \rightarrow Fe^{III} + HO^- + HO^{\cdot}$ 76 $M^{-1}s^{-1}$ (4.31)

Previous investigations suggest that the reduction of ≡Fe(III) to ≡Fe(II) (eq 4.30) is the rate limiting step in the overall reaction because the reaction of ≡Fe(II) with H_2O_2 is much faster than that of ≡Fe(III) [Kwan and Voelker, 2003; Matta et al., 2008b]. The superoxide/hydroperoxy radicals ($HO_2^{\bullet}$ / $O_2^{\bullet-}$) plays an important role in the redox cycle of iron in aqueous phase [Bielski et al., 1985]. Because the pKa of $HO_2^{\bullet}/O_2^{\bullet-}$ is 4.8, generation of hydroperoxide anion $HO_2^{\bullet}$ may be neglected at neutral pH.

$Fe^{III} + O_2^{\bullet-} \rightarrow Fe^{II} + O_2$ 1.4×10^5 $M^{-1}s^{-1}$ (4.32)

$Fe^{III} + HO_2^{\bullet} \rightarrow Fe^{II} + H^+ + O_2$ 3.6×10^5 $M^{-1}s^{-1}$ (4.33)

Generally, CA can bind iron ion, facilitating the initiation of Fenton-like reactions in the iron-catalysed Haber-Weiss cycle:

$Fe^{II} + CA \rightarrow Fe^{III}\text{-}CA$ (4.34)

$Fe^{III}\text{-}CA + H_2O_2 \rightarrow Fe^{II}\text{-}CA + H^+ + HO_2^{\bullet}$ (4.35)

$Fe^{III}\text{-}CA + HO_2^{\bullet} \rightarrow Fe^{II}\text{-}CA + H^+ + O_2$ (4.36)

$Fe^{III}\text{-}CA + O_2^{\bullet-} \rightarrow Fe^{II}\text{-}CA + O_2$ (4.37)

$Fe^{II}\text{-}CA + H_2O_2 \rightarrow Fe^{III}\text{-}CA + {}^{\bullet}OH + HO^-$ (4.38)

Table 4.4 showed that the enhancement factor of the oxidation efficiency with EDTA is much higher than with other CA. EDTA considerably enhances the generation of

hydroxyl radicals by the Fenton reaction. EDTA can strongly combine with Fe^{II} or Fe^{III} to form stable metal-chelate complex in the solution ($\log K(Fe^{II})$ = 12-14; $\log K(Fe^{III})$ = 20-24) [Blesa et al., 1984]. This is in agreement with previous results where the rate constant of the Fenton reaction for Fe-EDTA complex is much greater than without EDTA [Kwon et al., 2009]. Addition of EDTA generally depress the Fe^{III}/Fe^{II} redox potential, e.g. for Fe-EDTA it is 0.12V compared with 0.77 V for hexaaqua Fe, thereby making the Fenton reaction more thermodynamically favorable [Buxton et al., 1988; 2, Kwon et al., 2009].

Table 4.4. Degradation kinetic constant of PCP under different condition in the system. [PCP] = 50 mg L^{-1}, Fe^{III} ($Fe_2(SO_4)_3$) =Fe^{II} ($FeSO_4$) = 0.5mM, $Fe^{II}(Fe^{III})$/H2O2/chelating agent = 1/100/1, pH7, 20°C.

	Fe^{2+} k (min^{-1})	Fe^{3+} k (min^{-1})
EDTA	0.157	0.140
Oxalate	0.0041	0.0018
CMCD	0.0027	0.0014
Without chelating agent	0.002	0.0006

In addition, Fe(III)-EDTA complex can be reduced to Fe(II)-EDTA by The superoxide/hydroperoxy radicals ($HO_2^{\bullet}$ / $O_2^{\bullet -}$) [Bielski et al., 1985]. Subsequently, Fe(II)-EDTA reacts with the H_2O_2 and the Fenton-like reaction produces further hydroxyl radicals[Buxton et al., 1988].

Fe^{III}-EDTA + $O_2^{\bullet-}$ → Fe^{II}-EDTA + O_2 $2 \times 10^6\ M^{-1}\ s^{-1}$ (4.39)

Fe^{II}-EDTA + H_2O_2 → Fe^{III}-EDTA + $^{\bullet}OH$ + HO^- $2 \times 10^4\ M^{-1}\ s^{-1}$ (4.40)

The reduction reaction rate of Fe(III) to produce Fe(II) in the presence of EDTA (eq. 4.39) is much faster than that in the absence of EDTA. As the generation of Fe(II) from Fe(III) is the rate limiting step, the presence of EDTA can therefore considerably improve the overall rate of Fenton-oxidation reaction.

The binding constant of oxalate or CMCD with iron ion were found to be relatively lower than that of EDTA (logK (oxalate-Fe) = 7.5; logK (CMCD-Fe)= 2.1) at neutral pH [Hanna et al., 2005; Erdemoglu and Sarıkaya, 2006]. In addition, cyclodextrin can bind both iron and pollutant, which allowing the formation of the ternary complex and the generation of hydroxyls radicals in close proximity to pollutant. The formation of such complexes has been already demonstrated in homogeneous catalysis and has turned out to be related to the enhancement of the degradation of hydrophobic organic pollutants under Fenton's chemistry [Matta et al., 2008a; Hanna et al., 2005].
The oxalate-based Fenton system seems to be more efficiency than that of CMCD, probably due to its less scavenger effect of $^{\bullet}OH$ (hydroxyl radical reaction rate with cyclodextrin is about 1000-times greater than with oxalate) [Hanna et al., 2005; Deeble et al., 1989; Getoff et al., 1971; Hag and Yao, 1992].

In heterogeneous system, the presence of EDTA contributes to the enhancement of oxidation rate through the iron oxide dissolution and Fenton chelate-based reaction in solution. In contrast to the homogeneous system where the EDTA showed the highest oxidation rate, the enhancement of oxidation rate using EDTA is lower than oxalate in the presence of magnetite (Table 4.4). This behavior can not be explained by the scavenging effect of hydroxyl radical by EDTA or oxalate, which must occur in both heterogeneous and homogeneous systems. This inversed trend may be probably due to

the interactions of EDTA or oxalate with magnetite surface, occupying a fixed number of Fe-sites and then affect the decomposition of H_2O_2 or the oxidation of PCP. The surface interactions of species with the heterogeneous catalyst will be investigated in the following part.

4.3.4 Surface reactions in magnetite-chelate based reaction

In order to point out the reason of why the EDTA is less active in heterogeneous system compared to oxalate, three experiments are conducted: 1- The sorption of CA on the surface of magnetite was studied to determine the adsorption ability of CA (Figure 4.28a). 2- The sorption of PCP in the presence of different concentration of CA to highlight the competition between PCP and CA toward solid surface (Figure 4.28b). 3- Effect of CA sorption on the decomposition of H_2O_2 (Figure 4.29).

(a)

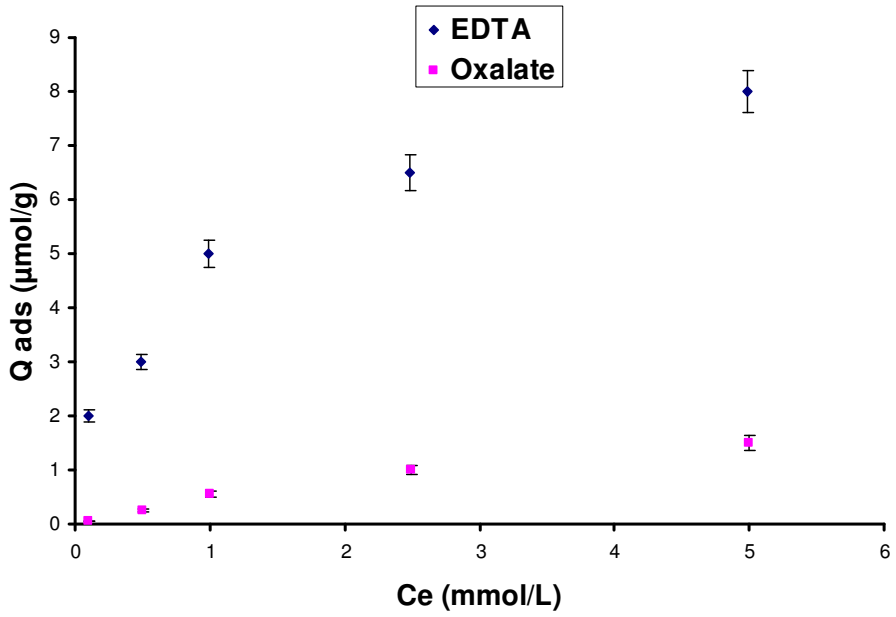

(b)

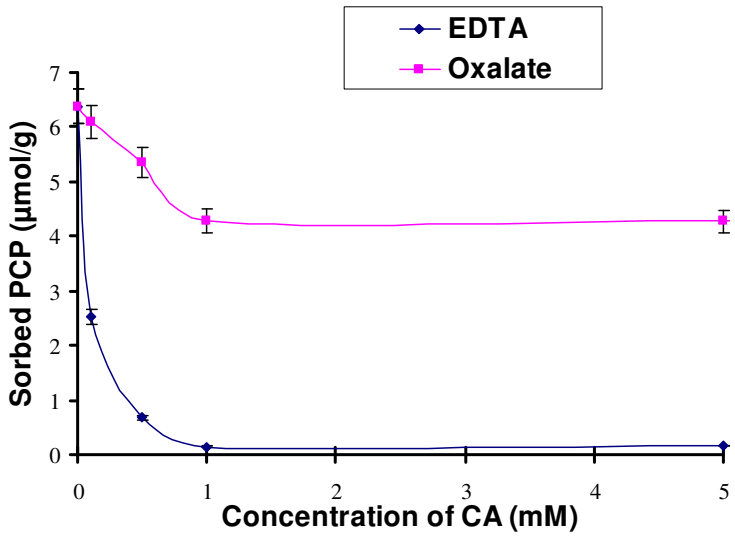

Figure 4.28. (a) Sorption of EDTA and oxalate on the magnetite. (b) Effect of CA on the adsorption of PCP onto the surface of magnetite. [PCP] = 50 mg L^{-1}, [Magnetite] = 2g L^{-1}, [CA] = 0.1mM ~ 50mM, V= 100ml, 20°C, pH7.

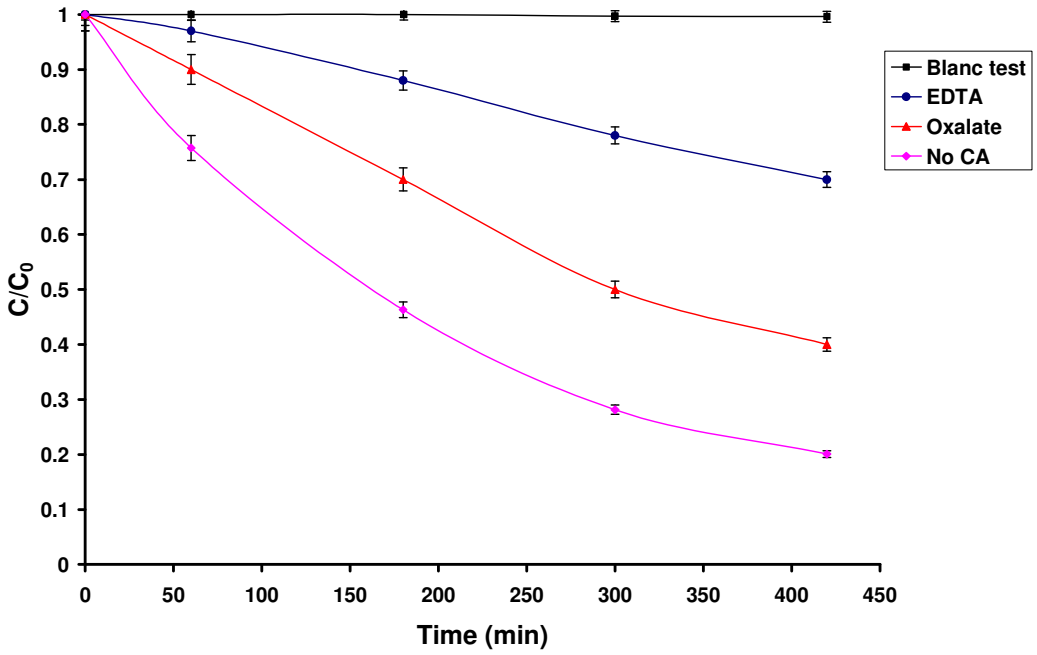

Figure 4.29. H_2O_2 decomposition versus time after EDTA or oxalate sorption. [H_2O_2] = 1 mM, [Magnetite] = 8 g L^{-1}, 20°C, and pH7.

EDTA has four carboxyl groups that may adsorb to four central Fe atoms [Stumm, 1997; Hag and Yao, 1992]. The mechanism is considered a ligand exchange in which the

ligand ($EDTA^{4-}$) adsorbs on specific sites (≡Fe-OH) on the surface. The affinity of EDTA for an oxide surface is heavily dependent on pH [Ballesteros et al., 1998]. It has been proposed that at pH values < 7, EDTA forms multinuclear surface complexes with goethite, and at pH values > 7 it will form mononuclear complexes [Stumm, 1997; Nowack and Sigg, 1997]. In contrast, [Blesa et al., 1984] examined the adsorption of EDTA on magnetite and found that the number of adsorption sites changes from 2 to 4 as pH increases.

The oxalate adsorption onto iron oxides was also widely studied and the formation of two different surface complexes on the oxide surface was evidenced [Stumm, 1992; Zhang et al., 1985]. The surface complexation mechanism is proposed in which the oxalate ligand binds to one or two iron surface sites. In all cases, the intrinsic surface complexartion constant was found to be much greater for EDTA ($\log K_{int}$ ~ 30) than for oxalate ($\log K_{int}$ ~ 7). [Stumm, 1992; Zhang et al., 1985; Ballesteros et al., 1998].

Figure 4.28a shows that the EDTA can sorb strongly to the magnetite surface at neutral pH. At about 1mM, sorption saturation plateau is reached corresponding to the total site density of solid. However, the sorption of oxalate is about 6-times lower than that of EDTA (Figure 4.28a). Figure 4.28b shows that PCP and chelating agent compete with each other to adsorb on the magnetite surface. Due to its strong complexing ability, the presence of EDTA (1mM) could entirely occupy the magnetite surface and displace the totality of previously PCP sorbed. However, the presence of oxalate (1mM) can reduce by only 32% of the PCP sorption on iron oxide surface.

In our previous work, we showed that the H_2O_2 competed with sorbate species for the fixation on magnetite active sites and displaced it from surface to aqueous phase [Xue et al., in press]. In addition, we reported that the sorbed PCP was removed form magnetite surface at the first stage of oxidation reaction. In order to point out a possible competition between oxidant and CA towards the magnetite sites, H_2O_2 decomposition experiments are conducted. Prior to this experiment, magnetite and CA solution were

stirred for 2h to reach equilibrium sorption with CA sorbed amount at sorption saturation plateau (Figure 4.28a). After that, the solid-sorbed CA was taken form sorption experiment and then reacted with H_2O_2.

The strong adsorption of CA on the surface of magnetite might reduce the surface sites available for specific interactions with H_2O_2, and lead to inactivation of iron mineral surfaces. Coherently, decrease in H_2O_2 decomposition rate value was observed with EDTA and oxalate (Figure 4.29). The H_2O_2 decomposition rate decreased from 0.004 min^{-1} to 0.0022 min^{-1} with oxalate and to 0.0008 min^{-1} with EDTA. This corroborates that the strong sorption of EDTA on the surface of magnetite can affect the H_2O_2 decomposition and therefore the whole degradation rate. FTIR spectrum of the solid recovered after oxidation reaction, showed the main spectral bands of EDTA, indicating that EDTA remain strongly sorbed even after the addition of H_2O_2. Therefore, the surface interactions of oxidant with iron surface sites, initiating the Fenton heterogeneous reactions, would be the rate-limiting step.

4.3.5 Conclusion

For the magnetite-system, the addition of oxalate improved PCP oxidation by a factor of about 6, while the EDTA improved by a factor of 4. All used CA contributed to the increase in iron oxide dissolution rate and so homogeneous Fenton's reaction was assumed to be in part responsible for the improvement of PCP degradation.

Despite its strong chelating ability to promote magnetite dissolution and its high efficiency in homogeneous reaction, EDTA is less reactive than oxalate in heterogeneous Fenton system. This observation could be explained by the inactivation of iron surface sites through the strong sorption of EDTA. Consequently, the actives surfaces sites of the heterogeneous catalyst become unavailable for the interactions with H_2O_2 to initiate Fenton-like surface reactions. This work demonstrated that the chelating agent-promoted dissolution of magnetite did not play the key role in

determining the efficiency of heterogeneous Fenton oxidation. The surface interactions of oxidant with the catalyst surface appear to be the rate-determining step in heterogeneous Fenton system, rather than the iron oxide dissolution rate. The CA-driven heterogeneous Fenton reaction seems to be controlled but the surface interactions with the active sites of catalyst.

It should be noted that EDTA is a toxic agent and there is increasing concern about the direct or indirect potential effects of the presence of EDTA in the environment. Moreover, it has been demonstrated here that EDTA can bind strongly to the naturally occurring iron minerals and make them inactive to promote Fenton-like reactions, when the heterogeneous Fenton system is considered for the treatment process. Carboxy-methyl-cyclodextrin (CMCD), an environmentally friendly agent and a non toxic metal chelatant. CMCD offer also the advantages, low reactivity with solid, relative insensitivity to pH and ionic strength effects, and high biodegradability. Oxalate, non toxic chelating agent, naturally occurring organic acid and offer also the advantages of high reactivity in heterogeneous Fenton system at low and high concentrations, and of low hydroxyl radical scavenging effect. Finally, oxalate can be a promising agent for the investigation in Fenton heterogeneous reaction at near neutral pH environment.

CHAPTER 5 GENERAL CONCLUSIONS

Base on the chapter 4, we have some general conclusion about this work:

(1) All the experiments were carried out at natural pH, results showed that using the heterogeneous Fenton-like system can remove the model pollutant (PCP and RhB) efficiently but not the mineralization. The PCP mineralization determined by TOC was completed after 7days, while total dechlorination was achieved at 4d treatment time. The first reaction of PCP oxidation should be the dechlorination since 90% of chloride was formed at the first 30 hours corresponding to the total disappearance of parent compound.

(2) The degradation rate of PCP by Fenton-like oxidation firstly increased with the dosage of H_2O_2 or with the amount of magnetite, reached a maximum value and then decreased. The similar trends were also found when we used the RhB as the model pollutant to carry out the experiments. Each type of iron oxide (fixed exposed surface area) versus different concentration of H_2O_2 had an optimums value. The occurrence of these maximums values for the effective degradation of PCP could be explained by the scavenging reaction with H_2O_2 or iron oxide surface. Too much H_2O_2 and iron oxide in the solution will make a big competition between the oxidation of model polltnats.

(3) On surface area basis, RhB sorption and H_2O_2 decomposition rates on the surface of oxide were higher for M2 (high crystallinity and FeII/FeIII ratio) than for M1 (low crystallinity and FeII/FeIII ratio). M2 exhibits better oxidation efficiency for dye removal than M1 based on both mass and surface area basis. The decomposition of RhB on M2 is higher than M1 even though the sorption mechanism of RhB on the surface of both oxides revealed a similar trend.

(4) Only heterogeneous Fenton reaction happened for the degradation of RhB and PCP, because Fe leaching from the oxide surface is negligible at neutral pH. The apparent reaction rate for heterogeneous Fenton reaction is dominated by the rate of intrinsic chemical reactions on the oxide surface rather than the rate of mass transfer. All batch experiments indicate that Fenton-like oxidation of PCP and RhB are mainly controlled by surface mechanism reaction and the species compete with each other for adsorption on a fixed number of magnetite active sites.

(5) Raman analysis suggested that the sorbed PCP was removed form magnetite surface at the first stage of oxidation reaction. Due to the complex nature of chemical surface species, it is difficult to fully understand the multiple interactions that occur on the oxide surface. Spectroscopic characterization in situ of surface active sites and solute surfaces complexes during the oxidation reaction are required for this purpose.

(6) Due to the result of two different kinds of iron oxides, the site density and sorption ability of RhB on catalyst surface may also influence the oxidation performance in iron oxide/ H_2O_2 system.

(7) The iron oxides catalysts exhibited low iron leaching, good structural stability and no loss of performance in second reaction cycle in the iron oxides/ H_2O_2 system. The sorption on the surface of iron oxide with catalytic oxidation using hydrogen peroxide would be an effective oxidation process for the contaminants.

(8) In the iron oxides/H2O2/chelating agent system, all the chelating agents we used can efficiently improve the degradation of pollutant. Among the chelating agents we investigated, EDTA and oxalic acid were the best two. It is reasonable that because EDTA has a strong chelating ability to promote magnetite dissolution and then to improve the oxidation efficiency. However, EDTA is less reactive than oxalate in heterogeneous Fenton reaction though the total dissolved iron under using EDTA was higher than oxalic acid. This observation could be explained by the inactivation of iron

surface sites which become unavailable for the interactions with H2O2 to initiate Fenton-like reactions.

(9) This work demonstrated that the chelating agent-promoted dissolution of magnetite did not play the key role in determining the efficiency of heterogeneous Fenton oxidation. The surface interactions of oxidant with the catalyst surface appear to be the rate-determining step in heterogeneous Fenton system, rather than the iron oxide dissolution rate.

(10) Finally, Carboxy-methyl-cyclodextrin (CMCD) and oxalate are recommended to use in the heterogeneous Fenton system to treat the pollutant, because they are environmentally friendly agent and a non toxic metal chelatant compared with EDTA. And these two types of chelating agents also have high reactivity in the system.

REFERENCES

Abel E., Über die katalytische Zersetzung von Wasserstoffsuperoxyd durch Eisensalze, Österreichische Chemiker-Zeitung. 1948 (49) 79-80.

Abe K.I., Tanaka K., Fe^{3+} and UV-enhanced ozonation of chlorophenolic compounds in aqueous medium. Chemosphere. 1997 (35) 2837–2847.

Ahlborg U.G., Thunberg T.M., Chlorinated phenols: occurrence, toxicity, metabolism and environmental impact. CRC Critical Reviews in Toxicol. 1980 (7) 1–35.

Ai Z., Lu L., Li J., Zhang L., Qiu J., Wu M., $Fe@Fe_2O_3$ core-shell nanowires as iron reagent.1.Efficient degradation of rhodamine B by a novel sono-Fenton process. Journal of physical chemistry C. 2007 (111) 4087-4093.

Aksu Z., Yener J., A comparative Adsorption/Biosorption study of Mono-Chlorinated phenols onto various sorbents. Waste Manage. 2001 (21) 695-702.

Al-Hayek L., Dor´e M., Oxidation des ph´enols par le peroxide d'hydrogene en milieu aqueux en pr´esence de fer support´e sur alumine. Water Research. 1990 (24) 973–982.

Andreozzi R., D'Apuzzo A., Marotta R., Oxidation of aromatic substrates in water/goethite slurry by means of hydrogen peroxide. Water Research. 2002a, 36 (19) 4691–4698.

Andreozzi R., Caprio, V., Marotta, R., Oxidation of 3, 4-dihydroxybenzoic acid by means of hydrogen peroxide in aqueous goethite slurry. Water Research. 2002b, 36 (11) 2761–2768.

Armbruster U., Martin A., Wilhelm S., Mothes S., Heterogen katalysierte Nassoxidation schadstoffhaltiger Abwässer bei erhöhten Drücken und Temperaturen. Chemie Ingenieur Technik. 2002 (74) 1450-1454.

Arnold S.M., Hickey W.J., Harris R.F., Degradation of atrazine by Fenton's reagent: condition optimization and product quantification. Environmental Science and Technology 1995, 29 (8) 2083–2089.

Bader H., Sturzenegger V., Hoigné J., Photometric method for the determination of low concentrations of hydrogen peroxide by the peroxidase catalyzed oxidation

of N,N-diethyl-p-phenylenediamine (DPD). Water Research. 1988 (22) 1109-1115.

Ballesteros M.C., Rueda E. H., Blesa M.A., The influence of iron (II) and (III) on the kinetics of goethite dissolution by EDTA. Journal of Colloid and Interface Science. 1998 (201) 13-19.

Barb W.G., Baxendale J.H., George P., Hargrave K.R., Reactions of ferrous and ferric ions with hydrogen peroxide. Nature. 1949 (163) 692-694.

Barb W.G., Baxendale J.H., George P., Hargrave K.R., Reactions of ferrous and ferric ions with hydrogen peroxide. Part I.- The ferrous ion reaction. Transactions of the Faraday Society. 1951 (47) 462-500.

Barb W.G., Baxendale J.H., George P., Hargrave K.R., Reactions of ferrous and ferric ions with hydrogen peroxide. Part II.- The ferric ion reaction. Transactions of the Faraday Society. 1951b (47) 591-616.

Barrault J., Abdellaoui M., Bouchoule C., Majeste A., Tatibouet J.M., Louloudi A., Papayannakeos N., Gangas N.H., Catalytic wet peroxide oxidation over mixed (Al–Fe) pillared clays. Applied Catalysis B: Environmental. 2000 (27) 225-230.

Barreiro J.C., Capelato M.D., Martin-Neto L., Hansen H.C.B., Oxidative decomposition of atrazine by a Fenton-like reaction in a H2O2/ferrihydrite system. Water Research. 2007 (41) 55-62.

Benitez F.J., Acero J.L., Real F.J., Rubio F.J., Leal A.L, The role of hydroxyl radicals for the decompositionof p-hydroxy phenylacetic acid in aqueous solutions. Water Research. 2001a (35) 1338-1343.

Benitez F.J., Acero J.L., Real F.J., Garcia J., Kinetics of photodegradation and ozonation of pentachlorophenol. Chemosphere. 2003 (51) 651–662.

Bielski B.H.J., Reevaluation of the spectral and kinetic properties of HO_2 and O_2^- free radicals. Photochemistry and Photobiology. 1978 (28) 645-649.

Bielski B.H.J., Cabelli D.E., Arudi R.L., Ross A.B., Reactivity of HO_2/O_2- Radicals in Aqueous Solution. Journal of Physical and Chemical Reference Data. 1985 (14) 1041-1100.

Bielski B.H.J., Cabelli D.E., Highlights of current research involving superoxide and

perhydroxyl radicals in aqueous solution. International Journal of Radiation Biology. 1991 (59) 291-319.

Bigda R.J., Consider Fenton's chemistry for wastewater treatment. Chemical Engineering Progress. 1995, 91 (12) 62-66.

Bishop D.F., Stern G., Fleischman M., Marshall L.S., Hydrogen peroxide catalytic oxidation of refractory organics in municipal waste waters. Industrial & Engineering Chemistry Process Design and Development. 1968 (7) 110-117.

Blesa M.A., Borghi E.B., Maroto A.J.G., Regazzoni A.E., Adsorption of EDTA and iron-EDTA complexes on magnetite and the mechanism of dissolution of magnetite by EDTA. Journal of Colloid and Interface Science. 1984, 98 (2) 295-305.

Bray W.C., The interaction of ozone and hydrogen peroxide in aqueous solution. Journal of the American Chemical Society. 1938 (60) 82-87.

Brown M.A., De Vito S.C., Predicting azo dye toxicity. Critical Reviews in Environmental Science and Technology. 1993 (23) 249-324.

Buda F., Ensing B., Gribnau M.C.M., Baerends E.J., DFT Study of the active intermediate in the Fenton reaction. Chemistry A European Journal. 2001,7 (13) 2775–2783.

Buitrago C., Centi G., Lodolo A., Miertus S., Compendium of Waste Water Treatment and Water Purification Technologies. International Centre for Science and High Technology-United Nations Industrial Development Organization. Trieste, 2002, 164 pp.

Burbano A.A., Dionysiou D.D., Suidan M.T., Richardson T.L., Oxidation kinetics and effect of pH on the degradation of MTBE with Fenton reagent. Water Research 2005 (39) 107–118.

Burkitt M.J., Gilbert B.C., Model studies of the iron-catalysed Haber- Weiss cycle and the ascorbate-driven Fenton reaction. Free Radical Research Communications. 1990, 10(4-5) 65-280.

Buxton G.V., Greenstock C.L., Helman W.P., Ross A.B., Critical review of rate

constants for reactions of hydrated electrons, hydrogen atoms and hydroxyl radicals (•OH/•O^-) in aqueous solution, Journal of Physical and Chemical Reference Data. 1988 (17) 513-886.

Carriazo J.G., Guelou E., Barrault J., Tatibouet J.M., Moreno S., Catalytic wet peroxide oxidation of phenol over Al-Cu or Al-Fe modified clays. Applied Clay Science. 2003 (22) 303–308.

Centi G., Perathoner S., Torre T., Verduna M.G., Catalytic wet oxidation with H_2O_2 of carboxilic acids on homogeneous and heterogeneuos Fenton-type catalyst. Catalysis Today. 2000 (55) 61–69.

Centi G., Perathoner S., Sustainable water use and technologies. La Chimica e L'Industria (Milan), 83, 2001, 43.

Chakchouk M., Hamdi M., Foussard J.N., Debellefontaine H., Complete treatment of olive mill wastewaters by a wet air oxidation process coupled with a biological step. Environmental Technology. 1994 (15) 323-332.

Chakinala A.G., Bremner D.H., Gogate P.R., Kyu-Cheol N., Burgess A.E., Multivariate analysis of phenol mineralisation by combined hydrodynamic cavitation and heterogeneous advanced Fenton processing. Applied Catalysis B: Environmental. 2008, 78 (1-2) 11-18.

Chamarro E., Marco A., Esplugas S., Use of Fenton reagent to improve organic chemical biodegradability. Water Research. 2001, 35 (4) 1047−1051.

Chen D.W., Ray A.K., Photodegradation kinetics of 4-nitrophenol in TiO_2 suspension. Water Research. 1998 (32) 3223-3234.

Chen R., Pignatello J.J., Role of quinone intermediates as electron shuttles in Fenton and photoassisted Fenton oxidations of aromatic compounds, Environmental Science and Technology. 1997 (31) 2399-2406.

Chen Q.Q., Wu P.X., Li Y.Y., Zhu N.W., Dang Z., Heterogeneous photo-Fenton photodegradation of reactive brilliant orange X-GN over iron-pillared montmorillonite under visible irradiation. Journal of Hazardous Materials. In Press. 2009.

Chiou C.T., Porter P.E., Schmedding D.W., Partition equilibrium of nonionic organic compounds between soil organic matter and water. Environmental Science and Technology. 1983 (17) 227-231.

Chiron S., Fernandez A.A., Rodriguez A., Calvo E.G., Pesticide chemical oxidation: State-of-the-art. Water Reserch. 2000, 34 (2) 366–377.

Chung K.T., Stevens S.E.J., Cerniglia C.E., The reduction of azo dyes by the intestinal microflora. Critical Reviews in Microbiology. 1992 (18) 175–197.

Costa R.C.C., Moura F.C.C., Ardisson J.D., Fabris J.D., Lago R.M.. Highly active heterogeneous Fenton-like systems based on Fe0/Fe3O4 composites prepared by controlled reduction of iron oxides. Applied Catalysis B: Environmental, 2008, 83 (1-2) 131-139.

Crosby D.G., Beynon K.I., Greve P.A., Korte F., Still G.G., Vonk J.W., Environmental chemistry of pentachlorophenol. Pure and Applied Chemistry. 1981 (53) 1051-1080.

Da costa G.M., De Grave E., De Bakker P.M.A., Vandenberghe R.E., Influence of nonstoichiometry and the presence of maghemite on the Mossbauer spectrum of magnetite. Clays & Clay Minerals. 1995 (43) 656-668.

Daneshvar N., Rabbani M., Modirshahla N., Behnajady M.A., Kinetic modeling of photocatalytic degradation of Acid Red 27 in UV/TiO_2 process, Journal of Photochemistry and Photobiology. A, 2004 (168) 39-45.

Dantas T.L.P., Mendonça V.P., José H.J., Rodrigues A.E., Moreira R.F.P.M.. Treatment of textile wastewater by heterogeneous Fenton process using a new composite Fe_2O_3/carbon. Chemical Engineering Journal, 2006, 118 (1-2) 77-82.

Daou T.J., Begin-Colin S., Greneche J.M., Thomas F., Derory A., Bernhardt P., Legare P., Pourroy G., Phosphate adsorption properties of magnetite-based nanoparticles, Chemistry of Materials. 2007 (19) 4494-4505.

Deeble D.J., Parsons B.J., Phillips G.O., Medical Biochemical and Chemical Aspects of Free Radicals, O. Hayaishi E., Niki M. K., Yoshikawa T., (eds.), Elsevier, Amsterdam, The Netherlands, Vol. 1, pp505-10, 1989.

De Heredia J.B., Torregrosa J., Dominguez J.R., Peres J.A., Kinetic model for phenolic

compound oxidation Fenton's reagent. Chemosphere. 2001 (45) 85-90.

De Laat J., Gallard H., Catalytic decomposition of hydrogen peroxide by Fe(III) in homogeneous aqueous solutions: mechanism and kinetic modeling. Environmental Science and Technology. 1999, 33 (16) 2726–2732.

De León M.A., Castiglioni J., Bussi J., Sergio M., Catalytic activity of an iron-pillared montmorillonitic clay mineral in heterogeneous photo-Fenton process. Catalysis Today. 2008 (133-135) 600-605.

Deng J.H., Jiang J., Zhang Y., Lin X., Du C., Xiong Y., FeVO4 as a highly active heterogeneous Fenton-like catalyst towards the degradation of Orange II. Applied Catalysis B: Environmental. 2008, 84 (3-4) 468-473.

Doocey D.J., Sharratt P.N., Zeolite-Mediated advanced oxidation of model chlorinated phenolic aqueous waste: Part 1: aqueous phase fenton catalysis. Process Safety and Environmental protection. 2004 (82) 352–358.

Duan Z.H., Zhu L., Zhu L., Yao K., Zhu X., Individual and joint toxic effects of pentachlorophenol and bisphenol A on the development of zebrafish (Danio rerio) embryo. Ecotoxicology and Environmental Safety. 2008 (71) 774–780.

Duarte F., Maldonado-Ho´dar F.J., Pe´rez-Cadenas A.F., Madeira L.M., Fenton-like degradation of azo-dye Orange II catalyzed by transition metals on carbon aerogels. Applied Catalysis B: Environmental. 2009 (85) 139–147.

Dutta K., Mukhopadhyay S., Bhattacharjee S., Chaudhuri B., Chemical oxidation of methylene blue using a Fenton-like reaction. Journal of Hazardous Materials B. 2001 (84)57–71.

Dzombak D.A., Morel F.M.M., Surface Complexation Modeling: Hydrous Ferric Oxide. Wiley-Interscience, New York. 1990.

EC Decision 2455/2001/EC of the European Parliament and of the Council of November 20, 2001 establishing the list of priority substances in the field of water policy and amending Directive 2000/60/EC (L 331 of 15-12-2001).

Englehardt J.D., Meeroff D.E., Echegoyen L., Deng Y., Raymo F.M., Shibata T., Oxidation of aqueous EDTA and associated organics and coprecipitation of inorganics by ambient iron-mediated aeration. Environmental Science and

Technology. 2007 (41) 270–276.

EPA, July 2002. http://www.scorecard.org.

EPA, USA, Report 440/5-80-034, PB 81-117459, 1980.

EPA, USA, EPA/600/R-92/182 US EPA, Washington DC, 1992a.

EPA, National Recommended Water Quality Criteria, Federal Register 57-60848, 1992b.

Erdemoglu M., Musa Sarıkaya., Effects of heavy metals and oxalate on the zeta potential of magnetite. Journal of Colloid and Interface Science. 2006 (300) 795–804

Esplugas S., Giménez J., Contreras S., Pascual E., Rodríguez M., Comparison of different advanced oxidation processes for phenol degradation. Water Research., 2002 (36) 1034−1042.

Fajerwerg K., Debellefontaine H., Wet oxidation of phenol by hydrogen peroxide using heterogeneous catalysis Fe-ZSM-5: a promising catalyst. Applied Catalysis B: Environmental. 1996 (10) L229–L235.

Faust B.C., Hoffmann M.R., Photoinduced reductive dissolution of R-Fe2O3 by bisulfite. Environmental Science and Technology. 1984 (20) 943-948.

Feng J.Y., Hu X., Yue P.L., Effect of initial solution pH on the degradation of Orange II using clay-based Fe nanocomposites as heterogeneous photo-Fenton catalyst. Water Research. 2006a, 40 (4) 641-646.

Feng J.Y., Hu X., Yue P.L., Mineralization of indigo carmine at neutral pH using a nanocomposite as a heterogeneous photo-fenton catalyst. Studies in Surface Science and Catalysis. 2006b (159) 389-392.

Feng J.Y., Hu X., Yue P.L., Zhu H.Y., Lu G.Q., Discoloration and mineralization of Reactive Red HE-3B by heterogeneous photo-Fenton reaction. Water Research. 2003, 37 (15) 3776-3784.

Fenton H.J.H., Oxidation of tartaric acid in the presence of ion. Journal of the Chemical Society. 1894 (65) 899-910.

Ferraz W., Oliveira L.C.A., Dallago R., Da Conceica˜o L., Effect of organic acid to enhance the oxidative power of the fenton-like system Computational and

empirical evidences. Catalysis Communications. 2007 (8) 131–134.

Flores Y., Flores R., Gallegos A.A., Heterogeneous catalysis in the Fenton-type system reactive black 5/H_2O_2. Journal of Molecular Catalysis A: Chemical 2008 (281) 184–191.

Folke J., Birklund J., Danish coastal levels of 2,3,4,6-tetrachlorophenol, pentachlorophenol, and total organohalogens in blue mussels (Mytrulus edulis). Chemosphere. 1986 (15) 895–900.

Fukushima M., Tatsumi K., Degradation pathways of pentachlorophenol by photo-Fenton systems in the presence of iron(III), humic acid and hydrogen peroxide. Environmental Science and Technology. 2001 (35) 1771-1778.

Gallard H., De Laat J., Kinetic modelling of Fe(BI)/H_20_2 oxidation reactions in dilute aqueous solution using atrazine as a model organic compound. Water Research. 2000 (34) 3107-3116.

Gemeay A.H., Mansour I.A., El-Sharkawy R.G., Zaki A.B., Kinetics and mechanism of the heterogeneous catalyzed oxidative degradation of indigo carmine. Journal of Molecular Catalysis A: Chemical. 2003 (193) 109-120.

George P., Some experiments on the reactions of potassium superoxide in aqueous solutions. The Discussions of the Faraday Society. 1947 (2) 196-205.

Getoff N., Schwoerer F., Markovic V.M., Sehested K., Nielsen S.O., Pulse radiolysis of oxalic acid and oxalates. Journal of Physical Chemistry. 1971 (75) 749-755.

Glaze W.H., Kang J.W., Chapin D.H., The chemistry of water treatment processes involving ozone, hydrogen peroxide and ultraviolet radiation. Ozone Science and Engineering. 1987 (9) 335-352.

Glaze W.H., An overview of advanced oxidation processes: current status and kinetic models. Chemical Oxidation. 1994 (2) 44–57.

Grimwood M., Mascarenhas R., Proposed environmental quality standards for 2-, 3- and 4-chlorophenol and 2,4-dichlorophenol in water. Environment Agency Technical Report P46/i688, WRc Report No. EA4215, 1997.

Guimarães I.R., Oliveira L.C.A., Queiroz P.F., Ramalho T.C., Pereira M., Fabris J.D., Ardisson J.D., Modified goethites as catalyst for oxidation of quinoline: Evidence

of heterogeneous Fenton process. Applied Catalysis A: General. 2008, 347 (1) 89-93.

Gupta S.S., Stadler M., Noser C.A., Ghosh A., Steinhoff B., Lenoir D., Horwitz C.P., Schramm K.W., Collins T.J., Rapid total destruction of chlorophenols by activated hydrogen peroxide. Science. 2002 (296) 326-328.

Haber F., Willstätter R., Unpaarigheit und Radikalkettenim Reaktion-Mechanismus organischer und enzymatischer Vorgänge. Chemische Berichte. 1931 (64) 2844-2856.

Haber F., Weiss J., Über die Katalyse des Hydroperoxydes. Naturwiss. 1932 (51) 948-950.

Haber F., Weiss J., The catalytic decomposition of hydrogen peroxide by ferrous salts. Proceedings of the Royal Society of London Series A . 1934 (147) 332-351.

Hag W.R., Yao C.C.D., Rate constants for reaction of hydroxyl radicals with several drinking water contaminants. Environ. Sci. Technol. 1992 (39) 1811-1818.

Hanna K., Kone T., Medjahdi G., Synthesis of the mixed oxides of iron and quartz and their catalytic activities for the Fenton-like oxidation. Catalysis Communications. 2008, 9 (5) 955-959.

Hanna K., De Brauer Ch., Germain P., Chovelon J.M., Ferronato C., Degradation of pentachlorophenol in cyclodextrin extraction effluent using photocatalytic process. Science of the Total Environment. 2004 (332) 51-60.

Hanna K., Chiron S., Oturan M., Coupling enhanced water solubilization with cyclodextrin to indirect electrochemical treatment for pentachlorophenol contaminated soil remediation. Water Research. 2005 (39) 2763-2773.

Hanna K., Sorption of two aromatic acids onto iron oxides: Experimental study and modeling. Journal of Colloid and Interface Science. 2007 (309) 419-428.

Hanna K., Carteret C., Sorption of 1-hydroxy-2-naphthoic acid to goethite, lepidocrocite and ferrihydrite: Batch experiments and infrared study. Chemosphere. 2007 (70) 178-186.

Hayward K., Drinking water contaminant hit-list for US EPA. Water 21.

September–October: 4 1998.

He Z., Song S., Zhou H., Ying H., Chen J., C.I. relative Black 5 decolorization by combined sonolysis and ozonation. Ultrasonics Sonochemistry. 2007 (14) 298–304.

Helz G.R., Zepp R.G., Crosby D.G., Aquatic and Surface Photochemistry. Lewis Publishers Boca Raton. CRC Press, 1994.

Herney Ramirez J., Costa C.A., Madeira L.M., Mata G., Vicente M.A., Rojas-Cervantes M.L., López-Peinado A.J., Martín-Aranda R.M., Fenton-like oxidation of Orange II solutions using heterogeneous catalysts based on saponite clay. Applied Catalysis B: Environmental. 2007, 71(1-2) 44-56.

Henke G.A., Bioremediation, Ullmann's Encyclopedia of Industrial Chemistry, Electronic Release, Wiley-VCH Verlag GmbH, Weinheim, Germany, 2002.

Herrmann J.M., Heterogeneous photocatalysis: fundamentals and applications to the removal of various types of aqueous pollutants. Catalysis Today. 1999 (53) 115-129.

Hickey W.J., Arnold S.M., R.F. Harris, Degradation of atrazine by Fenton's reagent: condition optimization and product quantification. Environmental Science and Technology. 1995, 29 (8) 2083–2089.

Hirvonen A., Trapido M., Hentunen J., Tarhanen J., Formation of hydroxylated and dimeric intermediates during oxidation of chlorinated phenols in aqueous solutions. Chemosphere. 2000 (41) 1211–1218.

Howard P.H., Handbook of Environmental Fate and Exposure Data for Organic Chemical, vol. I, Large Production and Priority Pollutants. Lewis Publishers, Chelsea, MI, USA. 1989.

Hsueh C.L., Huang Y.H., Wang C.C., Chen C.Y., Degradation of azo dyes using low iron concentration of Fenton and Fenton-like system. Chemosphere. 2005 (58) 1409–1414.

Huang C.P., Dong C., Tang Z., Advanced chemical oxidation: its present role and potential future in hazardous waste treatment. Waste Management. 1993 (13) 361–377.

Huang H.H., Lu M.C., Chen J.N., Catalytic decomposition of hydrogen peroxide and 2-cholorphoen with iron oxides. Water Research. 2001 (35) 2291-2299.

Huling S.G., Arnorld R.G., Sierka R.A., Jones P.K., Fine D.D., Contaminant adsorption and oxidation via Fenton reaction. Journal of Environment Engineering. 2000 (126) 595-600.

IARC Monographs on the Evaluation of Carcinogenic Risks to Humans Overall Evaluations of Carcinogenicity: An Updating of IARC Monographs Volumes 1-42. Supplement 7. 1987.

Ince N.H., Stefan M.I., Bolton J. R., UV/H_2O_2 degradation and toxicity reduction of textile azo dyes: Remazol Black-B, a case study. Journal of Advanced Oxidation Technologies. 1997 (2) 442–448.

Isabel Pariente M., Martínez F., Melero J.A., Botas J.Á., Velegraki T., Xekoukoulotakis N.P., Mantzavinos D., Heterogeneous photo-Fenton oxidation of benzoic acid in water: Effect of operating conditions, reaction by-products and coupling with biological treatment. Applied Catalysis B: Environmental. 2008, 85 (1-2) 24-32.

Ishtchenko V.V., Huddersman K.D., Vitkovskaya R.F., Part 1. Production of a modified PAN fibrous catalyst and its optimisation towards the decomposition of hydrogen peroxide. Applied Catalysis A: General. 2003 (242) 123–137.

Jaina R., Mathura M., Sikarwara S., Mittal A., Removal of the hazardous dye rhodamine B through photocatalytic and adsorption treatments. Journal of Environmental Management. 2007 (85) 956–964.

Jayson G.G., Parsons B.J., Swallow A.J., Oxidation of ferrous ions by perhydroxyl radicals. Journal of the Chemical Society, Faraday Transactions. 1973 (69) 236-242.

Johnson T.L., Fish W., Gorby Y.A., Tratnyek P.G., Degradation of carbon tetrachloride by iron metal: Complexation effects on the oxide surface. Journal of Contaminant Hydrology. 1998, 29 (4) 379-398.

Jones A.P., Watts R.J., Dry phase dioxide-mediated photocatalysis: basis for in situ surface destruction of hazardous chemicals. Journal of Environment Engineering.

1997, 123 (10) 974–981.

Kang Y.W., Hwang K.Y., Effects of reaction conditions on the oxidation efficiency in the Fenton process. Water Research. 2000, 34 (10), 2786–2790.

Kayashima T., Katayama T., Oxalic acid is available as a natural antioxidant in some systems. Biochimica et Biophysica Acta - General Subjects. 2002 (1573) 1-3.

Keating E.J., Brown R.A., Greenberg E.S., Phenolic problems solved with hydrogen peroxide oxidation, Industrial Water Engineering. 1978 (2) 22-27.

Keith L.H., Telliard W.A., Priority pollutants: a prospective view. Environmental Science and Technology. 1979, 13 (4) 416–424.

Khare V., Mullet M., Hanna K., Blumers M., Abdelmoula M., Klingelhöfer G., Comparative studies of ferric green rust and ferrihydrite coated sand: Role of synthesis routes. Solid State Sciences. 2008 (10) 1342-1351.

Kim J.K., Martinez F., Metcalfe I.S., The beneficial role of use of ultrasound in heterogeneous Fenton-like system over supported copper catalysts for degradation of p-chlorophenol. Catalysis Today. 2007, 124 (3-4) 224-231.

Kim S.C., Kim D.S., Oh S.S., Lee D.K., Yang Y.K., 76 Catalytic wet oxidation of dyehouse effluents with Cu/Al_2O_3 and Cu−Al pillared clay. Studies in Surface Science and Catalysis. 2003 (145) 355-361.

Klingelhöfer G., Morris R.V., Bernhardt B., Shröder C., Rodionov D.S. , P. De Souza A, Yen A., Gellert R., Evlanov E.N, Zubkov B., Foh J., Bonnes U., E Kankeleit., Gutlich P., Ming W., Renz F., Wdowiak T., Squyres S. W., Arvidson R.E., Jarosite and Hematite at Meridiani Planum from Opportunity's Mössbauer Spectrometer. Science. 2004, 306 (5702) 1740-1745.

Kochany J., Lipczynska-Kochany E., Application of the EPR spin trapping technique for the investigations of the reactions of carbonate, bicarbonate, and phosphate anions with hydroxyl radicals generated by the photolysis of H_2O_2. Chemosphere. 1992 (25) 1769–1782.

Kong S.H., Watts R.J., Choi J.H., Treatment of petroleum-contaminated soil using iron mineral catalyzed hydrogen peroxide. Chemosphere. 1998 (37) 1473-1482.

Koppenol W.H., The centennial of the Fenton reaction. Free Radical Biology &

Medicine. 1993 (15) 645-651.

Koppenol W.H., Butler J., Van Leeuwen J.W,. The Haber-Weiss cycle. Photochemistry and Photobiology. 1978 (28), 655-660.

Kremer M.L., Stein G., The catalytic decomposition of hydrogen peroxide by ferric perchlorate. Transactions of the Faraday Society. 1959 (55) 959-973.

Kremer M.L., Mechanism of the Fenton reaction. Evidence for a new intermediate. Physical Chemistry Chemical Physics. 1999 (1) 3595-3605.

Kremer M.L., Complex visas 'Free Radical' mechanism for the catalytic decomposition of H_2O_2 by Fe^{3+}. International Journal of Chemical Kinetics. 1985 (17) 1299-1314.

Kung K.H.S., McBride M.B., Bonding of chlorophenols on iron and Aliminum oxides. Environmental Science and Technology. 1991, 25 (703) 702-709.

Kuo W., Decolorizing dye wastewater with Fenton's reagent. Water Research. 1992 (26) 881–886.

Kušić H., Koprivanac N., Selanec I., Fe-exchanged zeolite as the effective heterogeneous Fenton-type catalyst for the organic pollutant minimization: UV irradiation assistance. Chemosphere. 2006, 65 (1) 65-73.

Kuznetsova E.V., Savinov E.N., Vostrikova L.A., Parmon V.N., Heterogeneous catalysis in the Fenton-type system FeZSM-5/H2O2. Applied Catalysis B: Environmental. 2004, 51 (3) 165-170.

Kwan W.P., Volker, B.M., Rates of hydroxyl radical generation and organic compound oxidation in mineral-catalyzed Fenton-like systems. Environmental Science and Technology. 2003 (37) 1150-1158.

Kwan W.P., Voelker B.M., Influence of electrostatics on the oxidation rates of organic compounds in heterogeneous Fenton systems. Environmental Science and Technology. 2004, 38 (12) 3425–3431.

Kwan W.P., Voelker B.M., Decomposition of hydrogen peroxide and organic compounds in the presence of dissolved iron and ferrihydrite. Environmental Science and Technology. 2002 (36) 1467-1476.

Kwan W.P., PhD Thesis, Massachutsets Institute of Technology. 2003.

Kwon B.G, Lee D.S., Kang N., Yoon J., Characteristics of p-chlorophenol oxidation by Fenton's reagent. Water Research. 1999 (33) 2110-2118.

Kwon B.G., Kim E., Lee J.H., Pentachlorophenol decomposition by electron beam process enhanced in the presence of Fe(III)-EDTA. Chemosphere. 2009 (74) 1335–1339.

Lagarec K., Rancourt D.G., Extended Voigt-based analytic lineshape method for determining N-dimensional correlated hyperfine parameter distributions in Mössbauer spectroscopy. Nuclear Instruments and Methods in Physics Research Section B : Beam Interactions with Materials and Atoms . 1997 (129) 266-280.

Lati J., Meyerstein D. J., Journal of the Chemical Society, Dalton Transactions. 1978 1105-1118.

Legrini O., Oliveros E., Braun A.M., Photochemical processes for water treatment. Chemical Reviews. 1993 (93) 671-698.

Lei L., Hu X., Chu H.P., Chen G., Yue P.L., Catalytic wet air oxidation of dyeing and printing wastewater. Water Science and Technology. 1997 (35) 311-319.

Letaief S., Casal B., Aranda P., Martı´n-Luengo M.A., Ruiz-Hitzky E., Fe-containing pillared clays as catalysts for phenol hydroxylation. Applied Clay Science. 2003 (22) 263–277.

Li F.B., Li X.Z., Liu C.S., Liu T.X.. Effect of alumina on photocatalytic activity of iron oxides for bisphenol A degradation. Journal of Hazardous Materials. 2007, 149 (1) 199-207.

Li F.B., Wang X., Li Y., Liu C., Zeng F., Zhang L., Hao M., Ruan H., Enhancement of the reductive transformation of pentachlorophenol by polycarboxylic acids at the iron oxide–water interface. Journal of Colloid and Interface Science. 2008 (321) 332–341.

Li L.X., Abe Y., Kanagawa K., Shoji T., Mashino T., Mochizuki M., Tanaka M., Miyata N., Iron-chelating agents never suppress Fenton reaction but participate in quenching spin-trapped radicals. Analytica Chimica Acta. 2007, 599(2) 315-319.

Li K.Z., Wang H., WEI Y., Liu M., Catalytic performance of cerium iron complex oxides for partial oxidation of methane to synthesis gas. Journal of Rare Earths.

2008, 26 (5) 705-710.

Li Y.C., Bachas L.G., Bhattacharyya D., Kinetics studies of trichlorophenol destruction by chelate-based Fenton reaction. Environmental Engineering Science. 2005, 22(6) 756-771.

Lin J.G., Ma Y.S., Oxidation of 2-Chlorophenol in water by ultrasound/Fenton method. Journal of the Environmental Engineering Division. (American Society of Civil Engineers) 2000 (76) 130-137.

Lin S.H., Lo C.C., Fenton process for treatment of desizing wastewater. Water Research. 1997, 31 (8) 2050–2056.

Lin S.H., Peng C.F., Treatment of textile wastewater by Fenton's reagent. Journal of Environmental Science and Health. 1995 (30) 89-98.

Lin S.H., Lin C.M., Leu H.G, Operating characterisitics and kinetic studies of surfactant wastewater treatment by Fenton oxidation. Water Research. 1999 (33) 1735-1741.

Lin S.H., Ho S.J., Treatment of high-strength industrial wastewater by wet air oxidation—a case study. Waste Manage. 1997 (17) 71-78.

Lin S.S., Gurol, M.D., Catalytic decomposition of hydrogen peroxide on iron oxide: kinetics, mechanism, and implications. Environmental Science and Technology. 1998, 32 (10) 1417-1423.

Liou R.M., Chen S.H., Hung M.Y., Hsu C.S., Catalytic oxidation of pentachlorophenol in contaminated soil suspensions by Fe^{3+}-resin/H_2O_2. Chemosphere. 2004 (55) 1271–1280.

Lipczynska-Kochany E., Sprah G., Harms S., Influence of some groundwater and surface waters constituents on the degradation of 4-chlorophenol by the Fenton reaction. Chemosphere. 1995 (30) 9-20.

Lipczynska-Kochany E., Kochany J., Effect of humic substances on the Fenton treatment of wastewater at acidic and neutral pH. Chemosphere. 2008 (73) 745-750.

Liu T., You H., Chen Q.W., Heterogeneous photo-Fenton degradation of polyacrylamide in aqueous solution over Fe(III)–SiO2 catalyst. Journal of

Hazardous Materials. 2009, 162 (2-3) 860-865.

Logan S.R., Redox reactions of organic radicals with ferrocene/ferricenium species in aqueous solution. Part 1. Radicals derived from carboxylic acids. Journal of the Chemical Society-Perkin Transactions 2. 1989 (7) 751-754.

Lu M.C., Chen J.N., Huang H.H., Role of goethite dissolution in the oxidation of 2-chlorophenol with hydrogen peroxide. Chemosphere. 2002 (46) 131–136.

Lu M.C., Oxidation of chlorophenols with hydrogen peroxide in the presence of goethite. Chemosphere. 1999, 40 (2) 125–130.

Lucas M.S., Peres J.A., Decolorization of the azo dye Reactive Black 5 by Fenton and photo-Fenton oxidation. Dyes and Pigments. 2006 (71) 236–244.

Lücking F., Köser H., Jank M., Ritter A., Iron powder, graphite and activated carbon as catalysts for the oxidation of 4-chlorophenol with hydrogen peroxide in aqueous solution. Water Research. 1998, 32 (9) 2607–2614.

Luck F., Wet Air Oxidation: Past, Present and Future. Catalysis Today. 1999 (53) 81-91.

Luo T., Ai Z., Zhang L., Fe@Fe2O3 core-shell nanowires as iron reagent. 4. Sono-Fenton degradation of pentachlorophenol and the mechanism analysis. Journal of Physics and Chemistry. 2008 (112) 8675–8681.

Marmier N.N., Delisée A., Fromage F., Surface complexation modeling of Yb(III), Ni(II), and Cs(I) sorption on magnetite. Journal of Colloid and Interface Science. 1999 (211) 54-60.

Martínez F., Calleja G., Melero J.A., Molina R., Iron species incorporated over different silica supports for the heterogeneous photo-Fenton oxidation of phenol. Applied Catalysis B: Environmental. 2007, 70 (1-4) 452-460.

Martell A.E., Smith R.M., Critical stability constants A, Plenum Press, New York, 1, 204-211 1974.

Matta R., Hanna K., Chiron S., Fenton-like oxidation of 2, 4, 6-trinitrotoluene using different iron mineral. Science of the Total Environment. 2007 (385) 242-251.

Matta R., Hanna K., Chiron S., Oxidation of phenol by green rust and hydrogen peroxide at neutral pH. Separation and Purification Technology. 2008a (61)

442-446.

Matta R., Hanna K., Kone T., Chiron S., Oxidation of 2,4,6-trinitrotoluene in the presence of different iron-bearing minerals at neutral pH. Chemical Engineering Journal. 2008b (144) 453-458.

McAllister K.A., Lee H., Trevors J.T., Microbial degradation of pentachlorophenol. Biodegradation. 1996 (7) 1-40.

McGregor D.B., Brown, A.G., Howgate, S., McBride, D., Riach, C., Caspary, W.J., Responses of the l5178y mouse lymphoma cell forward mutation assay. 5.27 coded chemicals. Environmental and Molecular Mutagenesis. 1991 (17) 196–219.

Mecozzi R., Palma L.D., Pilone D., Cerboni L., Use of EAF dust as heterogeneous catalyst in Fenton oxidation of PCP contaminated wastewaters. Journal of Hazardous Materials B. 2006 (137) 886–892.

Medalia A.I., Kolthoff I.M., Redox recipes. I. Reaction between ferrous iron and peroxides. General considerations. Journal of Polymer Science. 1949 (4) 377-398.

Mijangos F., Varona F., Villota N., Changes in solution color during phenol oxidation by Fenton reagent. Environmental Science and Technology. 2006, 40 (17) 5538–5543.

Miller W.P., Zelazny L.W., Martens D.C., Dissolution of synthetic crystalline and noncrystalline iron oxides by organic acids. Geoderma. 1986 (37) 1-13.

Miller C.M., Valentine R.L., Mechanistic studies of surface catalyzed H_2O_2 decomposition and contaminant degradation in the presence of sand. Water Research. 1999 (33) 2805-2816.

Mills G., Hoffman M., Photocatalytic degradation of pentachlorophenol on TiO_2 particles: identification of intermediates and mechanism of reaction. Environmental Science and Technology. 1993 (27) 1681-1689.

Mirsalis J.C., Tyson C.K., Steinmetz K.L., Loh E.K., Hamilton C.M., Baleke J.P., Spalding J.W., Measurement of unscheduled DNA synthesis and s-phase synthesis in rodent hepatocytes following in vivo treatment: testing of 24 compounds. Environmental and Molecular Mutagenesis. 1989 (14) 155-164.

Mittal A.K., Venkobachar C., Uptake of cationic dyes by sulfonated coal: sorption

mechanism. Industrial & Engineering Chemistry Research. 1996 (35) 1472-1474.

Mueller J.G., Middaugh D.P., Lantz S.E., Chapman P.J., Biodegradation of creosote and pentachlorophenol in contaminated groundwater: chemical and biological assessment. Applied and Environmental Microbiology. 1991 (57) 1277-1285.

Murad E., Johnston J.H., Mössbauer Spectroscopy Applied to Inorganic Chemistry, Vol. 2, ed., G.J. Long, Plenum, New York, 1987.

Muthuvel I., Swaminathan M., Photoassisted Fenton mineralisation of Acid Violet 7 by heterogeneous Fe(III)–Al2O3 catalyst. Catalysis Communications, 2007, 8 (7) 981-986.

Naka D., Kim D., Starthmann T.J., Abiotic Reduction of Nitroaromatic Compounds by Aqueous Iron(II)−Catechol Complexes. Environmental Science Technology. 2006 (40) 3006-3012.

Nakomoto K., Infrared and Raman spectra of inorganic and coordination compounds, 4th ed., J. Wiley Sons, New York, 1986.

Neff D., Bellot-Gurlet L., Dillmann P., Reger S., Legrand L., Raman imaging of ancient rust scales on archaeological iron artefacts for long-term atmospheric corrosion mechanisms study. Journal of Raman Spectroscopy. 2006 (37) 1228-1237.

Nesheiwat F.K., Swanson A.G., Clean contaminated sites using Fenton's reagent. Chemical Engineering Progress. 2000, 96 (4) 61-66.

Neyens E., Baeyens J., A review of classic Fenton’s peroxidation as an advanced oxidation technique. Journal of Hazardous Materials. 2002 (B98) 33–50.

Noradoun C.E., Cheng I.F., EDTA degradation induced by oxygen activation in a zero valent iron/air/water system. Environmental Science Technology. 2005 (39) 7158–7163.

Nowack B., Kari F., Hilger S., Sigg L., Determination of Dissolved and Adsorbed EDTA Species in Water and Sediments by HPLC. Analytical Chemistry. 1996 (68) 561-566.

Nowack B., Sigg L., Dissolution of Fe(III) (hyr)oxides by metal-EDTA complexes. Geochimica et Cosmochimica Acta. 1997 (61) 951-963.

Oliveira L.C.A., Gonçalves M., Guerreiro M.C., Ramalho T.C., Fabris J.D., Pereira M.C., Sapag K., A new catalyst material based on niobia/iron oxide composite on the oxidation of organic contaminants in water via heterogeneous Fenton mechanisms Applied Catalysis A: General. 2007, 316 (1) 117-124.

Oliveira R., Almeida M.F., Santos L., Madeira L.M., Experimental design of 2,4-dichlorophenol oxidation by Fenton's reaction. Industrial and Engineering Chemistry Research. 2006, 45 (4) 1266–1276.

Ollis D.F., Serpone N., Pelizzetti E., In Photocatalysis Fundamentals and Applications; Serpone, N., Pelizzetti, E., Eds. Wiley, New York, 1989.

Ormad M.P., Ovelleiro J.L., Kiwi J., Photocatalytic degradation of concentrated solutions of 2,4-dichlorophenol using low energy light - Identification of intermediates. Applied Catalysis B. 2001 (32) 157-166.

Othmer D.F., Kirk R.E., Encyclopedia of Chemical Technology. Wiley Interscience, New York, 5 (325) 1979.

Paasivirta J., Sarkka J., Leskijarvi T., Roos A., Transportation and enrichment of chlorinated phenolic compounds in different aquatic food chains. Chemosphere. 1980 (9) 441–456.

Parks G.A., Bruyn P.L.J., The zero point charge of oxides. Physical Chemistry. 1962 (66) 967-973.

Parkhomchuk (Kuznetsova) E.V., Vanina M.P., Preis S., The activation of heterogeneous Fenton-type catalyst Fe-MFI. Catalysis Communiaction. 2008 (9) 381–385.

Pera-Titus M., García-Molina V., Baños M.A., Giménez J., Esplugas S., Degradation of chlorophenols by means of advanced oxidation processes: a general review. Applied Catalysis B: Environmental. 2003 (47) 219-256.

Perathoner S., Centi G., Wet hydrogen peroxide catalytic oxidation (WHPCO) of organic waste in agro-food and industrial streams. Topics in Catalysis. 2005, 33 (1-4) 207-224.

Perez M., Torrades F., Jose A., Domenech X., Peral J., Removal of organic contaminants in paper pulp treatment effluents under Fenton and photo-Fenton

conditions. Applied Catalysis B. 2002, 36 (1) 63–74.

Petigara B.R., Blough N.V., Mignerey A.C., Mechanisms of hydrogen peroxide decomposition in soils. Environmental Science Technology. 2002 (36) 639-645.

Pignatello J., Oliveros E., MacKay A., Advanced oxidation processes for organic contaminant destruction based on the Fenton reaction and related chemistry. Critical Reviews in Environmental Science and Technology. 2006 (36) 1–84.

Pignatello J.J., Dark and photoassisted iron(3+)-catalyzed degradation of chlorophenoxy herbicides by hydrogen peroxide. Environmental Science Technology. 1992 (26) 944-951.

Pintar A., Bercic G., Besson M., Gallezot P., Catalytic wet-air oxidation of industrial effluents: total mineralization of organics and lumped kinetic modeling. Applied Catalysis B: Environmental. 2004 (47) 143-152.

Pintar A., Besson M., Gallezot P., Catalytic wet air oxidation of Kraft bleach plant effluents in a trickle-bed reactor over a Ru/TiO2 catalyst. Applied Catalysis B: Environmental. 2001 (31) 275-290.

Pintar A., Besson M., Gallezot P., Gibert J., Martin D., Toxicity to Daphnia magna and Vibrio fischeri of Kraft bleach plant effluents treated by catalytic wet-air oxidation. Water Research. 2004 (38) 289-300.

Potter F.J., Roth J.A., Oxidation of chlorinated phenols using Fenton reagent. Hazardous Waste and Hazardous Materials. 1993, 10 (2) 151−170.

Prousek J., Advanced oxidation processes for water treatment. Chemical processes. Chemicke Listy. 1996 (90) 229–237.

Prengle H.W., Ozone/UV oxidation of chlorinated compounds in water, Proc. Internat. Ozone Inst. Forum on Ozone Disinfection, International Ozone Institute, Chicago, 286-295, 1976.

Rahhal S., Richter H.W., Reduction of hydrogen peroxide by the Ferrous iron chelate of diethylenetriamine-N, N, N', N'', N'''-pentaacetate. Journal of American Chemical Society. 1988, 110 (10), 3126–3133.

Ramirez J.H., Lampinen M., Vicente M.A., Costa C.A., Madeira L.M., Experimental Design to Optimize the Oxidation of Orange II Dye Solution Using a Clay-based

Fenton-like Catalyst. Industrial & Engineering Chemistry Reseach. 2008 (47) 284–294.

Ramirez J.H., Costa C.A., Madeira L.M., Mata G., Vicente M.A., Rojas-Cervantes M.L., Lo´ pez-Peinado A.J., Martı´n-Aranda R.M.. Fenton-like oxidation of Orange II solutions using heterogeneous catalysts based on saponite clay. Applied Catalysis B: Environmental. 2007 a (71) 44–56.

Ramirez J.H., Maldonado-Hódar F.J., Pérez-Cadenas A.F., Moreno-Castilla C., Costa C.A., Madeira L.M.. Azo-dye Orange II degradation by heterogeneous Fenton-like reaction using carbon-Fe catalysts. Applied Catalysis B: Environmental. 2007b, 75 (3-4) 312-323.

Rajeshwar K., Osugi M.E., Chanmanee W., Chenthamarakshan C.R., Zanoni M.V.B., Kajitvichyanukul P., Krishnan-Ayer R., Heterogeneous photocatalytic treatment of organic dyes in air and aqueous media. Journal of Photochemistry and Photobiology C: Photochemistry Reviews. 2008 (9) 171–192.

Rajeshwar K., Ibanez J., Environmental Electrochemistry, Academic Press, San Diego, 1997.

Richardson S.D., Wilson, C.S., Rusch, K.A., Use of rhodamine water tracer in the marshland upwelling system. Ground Water. 2004, 42 (5) 678–688.

Rivas F.J., Beltran F.J., Frades J., Buzeda P., Oxidation of p-hydroxybenzoic acid by Fenton's reagent. Water Research. 2001 (35) 387-393.

Rios-Enriquez M., Shahin N., Durán-de-Bazúa C., Lang J., Oliveros E., Bossmann S.H., Braun A.M., Optimization of the heterogeneous Fenton-oxidation of the model pollutant 2,4-xylidine using the optimal experimental design methodology. Solar Energy. 2004, 77 (5) 491-501.

Rochat J., Demenge, P., Rerat, J.C., Toxicologic study of a fluorescent tracer: rhodamine b. Toxicological European Research. 1978 (1) 23–26.

Rodriguesa C.S.D., Madeirab L.M., Boaventura R.A.R., Optimization of the azo dye Procion Red H-EXL degradation by Fenton’s reagent using experimental design. Journal of Hazardous Materials. In Press, Corrected Proof, Available online 10 September 2008.

Sabhi S., Kiwi J., Degradation of 2,4-dichlorophenol by immobilized iron catalysts. Water Research. 2001 (35) 1994-2002.

Santos A., Yustos P., Quintanilla A., Rodríguez S., García-Ochoa F., Route of the catalytic oxidation of phenol in aqueous phase. Applied Catalysis B: Environmental. 2002 (39) 97−113.

Sawyer D.T., Valentine T.S., How super is superoxide. Accounts Chemical Research. 1981 (14) 393-400.

Schellenberg K., Leunberger C., Schwarzenbach R.P., Sorption of chlorinated phenols by natural sediments and aquifer materials. Environmental Science Technology. 1984 (18) 652-657.

Schwertmann U., Cornell R.M., Iron Oxides in the Laboratory: Preparation and Characterization. Wiley-VCH, New York, 2000.

Sedlak D.L., Andren A.W., Oxidation of chlorobenzene with Fenton reagent. Environmental Science and Technology. 1991 (125) 777−782.

Seignez C., Pulgarin C., Peringer P., Degradation of industrial organic pollutants. Electrochemical and biological treatment and combined treatment. Swiss Chemical Society. 1992, 14(1) 25-30.

Seol Y.K., Javandel I., Citrate acid-modified Fenton's reaction for the oxidation of chlorinated ethylenes in soil solution systems. Chemosphere. 2008, 72 (4) 537-542.

Seung H.H., Veriansyah B., Kim J.D., Lee J.C., Pentachlorophenol oxidation rates in supercritical water. Journal of Environmental Science and Health Part A. 2007 (42) 2105-2109.

Sevimli M.F., Kinacl C., Decolorization of textile wastewater by ozonation and Fenton's process. Water Science Technology. 2002, 45 (12) 279–286.

Sheldon R.A., Kochi J.K., Metal-catalyzed Oxidation of Organic Compounds. Academic Press, New York. 1980.

Sheng H.L., Cho C.L., Fenton process for treatment of desizing wastewater. Water Research. 1997 (31) 2050–2056.

Sherwood T.K., Pigford R.L., Wilke C., Mass Transfer; McGraw-Hill, New York,

1975.

Shi F., Tse M.K., Pohl M.M., Radnik J., Brückner A., Zhang S., Beller M., Nano-iron oxide-catalyzed selective oxidations of alcohols and olefins with hydrogen peroxide. Journal of Molecular Catalysis A: Chemical. 2008, 292 (1-2) 28-35.

Shiavello M., Photocatalysis and environment : trends and applications, NATO ASI Series C, Kluwer Academic publischers, London, 1987.

Shimada T., Yamazaki H., Mimura M., Inui Y., Guengerich F.P., Interindividual variations in human liver cytochrome P-450 enzymes involved in the oxidation of drugs, carcinogens, toxic chemicals: studies with liver microsomes of 30 Japanese, 30 Caucasians. Journal of Pharmacology and Experimental Therapy. 1994 (270) 414–423.

Shin S., Yoon H., Jang J., Polymer-encapsulated iron oxide nanoparticles as highly efficient Fenton catalysts. Catalysis Communications. 2008, 10 (2) 178-182.

Shulpin G.B., Bochkova M.M., Nizova G.V., Kozlova N.B., Aerobic photodegradation of phenols in aqueous solutions promoted by metal compounds. Applied Catalysis B: Environmental. 1997 (12) 1–19.

Sigg L., Stumm W., The interactions of anions and weak acids with the hydrous goethite surface. Colloids Surfaces. 1981 (2) 101-117.

Song W.J., Cheng M., Ma J., Ma W., Chen C., Zhao J., Decomposition of Hydrogen Peroxide Driven by Photochemical Cycling of Iron Species in Clay. Environmental Science Technology. 2006, 40 (15) 4782-4787.

Sonnen D.M., Reiner R.S., Atalla R.H., Weinstock I.A., Degradation of pulpmill effluent by oxygen and polyoxometalate, a multipurpose delignification and wet air oxidation catalyst. Industrial and Engineering Chemistry Research. 1997 (36) 4134-4142.

Spadaro J.T., Isabelle L., Renganathan V., Hydroxyl radical mediated degradation of azo dyes: evidence for benzene generation. Environmental Science Technology. 1994 (28) 1389-1393.

Strathmann T.J., Stone A.T., Reduction of Oxamyl and Related Pesticides by FeII: Influence of Organic Ligands and Natural Organic Matter. Environmental Science

Technology. 2002 (36) 5172-5183.

Stumm W., Chemistry of the Solid-Water Interface, John Wiley & Sons, Inc., New York, pp 428 (1992).

Stumm W., Morgan J., Journal of Aquatic Chemistry, 3rd ed., Wiley-Interscience, New York, 1996.

Stumm, W.. Reactivity at the mineral-water interface: dissolution and inhibition. Colloids and Surfaces A: Physiochemical and Engineering Aspects. 1997 (120) 143-166.

Sturzenegger B.V., Hoigne J., Photometric method for the determination of low concentration of hydrogen peroxide by the peroxidase catalyzed oxidation of N,N-Diethyl p-Phenylenedlamine (DPD). Water Research. 1988 (22) 1109-1115.

Sun Y.F., Pignatello J.J., Chemical treatment of pesticide wastes. Evaluation of Fe(III) chelate for catalytic hydrogen peroxide oxidation of 2,4-D at circumneutral pH, Journal of Agricultural Food Chemistry. 1992 (40) 322–327.

Sun Y.F., Pignatello J.J., Photochemical reactions involved in the total mineralization of 2,4-D by $Fe^{3+}/H_2O_2/UV$. Environmental Science and Technology. 1993 (27) 304-310.

Tabet D., Saidi M., Houari M., Pichat P., Khalaf H., Fe-pillared clay as a Fenton-type heterogeneous catalyst for cinnamic acid degradation Journal of Environmental Management. 2006, 80 (4) 342-346.

Tamura H., Goto K., Yotsuyanagi T., Nagayama M., Spectroscopic determination of iron with 1,10- phenantroline in the presence of large amounts of iron, Talanta. 1974 (21) 314-318.

Tang W.Z., Tassos S., Oxidation kinetics and mechanisms of trihalomethanes by Fenton's reagent. Water Research. 1997, 31 (5) 1117–1125.

Tang W.Z., Chen R.Z., Decolorization kinetics and mechanisms of commercial dyes by H_2O_2/iron powder system. Chemosphere. 1996 (32) 947-958.

Tachiev G., Roth J.A., Bowers A.R., Kinetics of Hydrogen Peroxide Decomposition with Complexed and "Free" Iron Catalysts. International Journal of Chemical Kinetics. 2000 (32) 24–35.

Teel A.L., Watts R.J., Degradation of carbon tetrachloride by modified Fenton's reagent. Journal of Hazardous Materials B. 2002 (94) 179–189.

Tekbaş M., Cengiz Yatmaz H., Bektaş N., Heterogeneous photo-Fenton oxidation of reactive azo dye solutions using iron exchanged zeolite as a catalyst. Microporous and Mesoporous Materials. 2008, 115 (3) 594-602.

Thomas H.Y., Traina S. J., Cr(VI) Reduction and Immobilization by Magnetite under Alkaline pH Conditions: The Role of Passivation. Environmental Science Technology. 2005 (39) 4499-4504.

Tokumura M., Nakajima R., Znad H.T., Kawase Y., Chemical absorption process for degradation of VOC gas using heterogeneous gas–liquid photocatalytic oxidation: Toluene degradation by photo-Fenton reaction. Chemosphere. 2008, 73 (5) 768-775.

Tyre B. W., Watts R. J., Miller G. C., Treatment of four biorefractory containinats in solis using catalyzed hydrogen peroxide.Journal of Environmental Quality. 1991 (20) 832-838.

Ullmann's Encyclopedia of Industrial Chemistry, 6th ed., Wiley, New York, 1998.

Valentine R.L., Wang H.C.A., Iron oxide surface catalyzed oxidation of quinoline by hydrogen peroxide. Journal of Environmental Engineering. 1998 (124) 31-38.

Valenzuela J., Bumann U., Ce´spedes R., Padilla L., Gonza´lez B., Degradation of chlorophenols by alcaligenes eutrophus JMP134(pJP4) in bleached Kraft Mill effluent. Applied and Environment Microbiology. 1997 (63) 227-232.

Venkatadri R., Peters R.W., Chemical oxidation technologies: ultraviolet light/hydrogen peroxide, Fenton's reagent and titanium dioxide-assisted photocatalysis. Hazardous Waste and Hazardous Material. 1993 (10) 107–149.

Veschueren H.K., Handbook of Environmental Data on Organic Chemicals, VNR, New York, 1983.

Voelker B.M., Sulzberger B., Iron redox cycling in surface waters: effects of humic substances and light. Environmental Science Technology. 1997 (31) 1004-1011.

Von Sonntag C., Schuchmann H.P., Peroxyl radicals in aqueous solutions, In Peroxyl Radicals, Z. B. Alfassi, ed., John Wiley and Sons, New York, 173-234, 1997.

Walling C., Fenton's reagent revisited. Accounts of Chemical *Research.* 1975 (8) 125-131.

Walling C., Cleary M., Oxygen evolution as a critical test of mechanism in the ferric-ion catalyzed decomposition of hydrogen peroxide. Internatinal Journal of Chemical Kinetics. 1977 (9) 595-601.

Walling C., Amarnath K., Oxidation of mandelic acid by Fenton's reagent. Journal of American Chemical Society. 1982 (104) 1085-1089.

Walling C., Goosen A., Mechanism of the ferric ion catalysed decomposition of hydrogen peroxide: effects of organic substrate. Journal of American Chemical Society. 1973, 95 (9) 2987–2991.

Walling C., Kato S., The oxidation of alcohols by Fenton's reagent: the effect of copper ion. Journal of American Chemical Society. 1971 (93) 4275–4281.

Waters W. A., The chemistry of free radicals. Oxford: Oxford. Univeristy Press; 1946.

Watts R.J., Udell M.D., Rauch P.A., Leung S.W., Treatment of PCP-contaminated soils using Fenton reagent. Hazardous Waste and Hazardous Material. 1990 (7) 335-345.

Watts R.J., Foget M.K., Kong S.H., Teel A.L., Hydrogen peroxide decomposition in model subsurface systems. Journal of Hazardous Material. 1999 (69) 229-243.

Watts R.J., Udell M.D., Kong S., Leung S.W., Fenton-like soil remediation catalysed by naturally occurring iron minerals, Environmental Engineering Science. 1999 (16) 93–103.

Wegman R.C.C., Van den Broek H.H., Chlorophenols in river sediment in The Netherlands, Water Res. 17 (1983) 227.

WHO, Chlorophenols other than pentachlorophenol, Environmental Health Criteria 93, World Health Organisation, 1989.

Wieland H., Franke W., Uber den Mechanismus der Oxydationsvorgange. XII. Die Aktivierung des Hydroperoxyds durch Eisen. Justus Liebigs Annalen der Chemie. 1927 (457) 1-70..

Will I.B., Moraes J.E., Teixeira A.C., Photo-Fenton degradation of wastewater containing organic compounds in solar reactors. Separation and Purification

Technology. 2004, 34 (1-3) 51-57.

Willberg D.M., Lang P.S., Höchemer R.H., Kratel A., Hoffmann M.R., Degradation of 4-chlorophenol, 3,4-dichloroaniline, and 2,4,6-trinitrotoluene in an electrohydraulic discharge reactor. Environmental Science Technology. 1996 (30) 2526–2534.

Wink D.A., Nims R.W., Desrosiers M. F., Ford P.C., Keefer L.K., A Kinetic investigation of intermediates formed during the Fenton reagent mediated degradation of N-nitrosodimethyl amine: evidence for an oxidative pathway not involving hydroxyl radical. Chemical Research in Toxicology. 1991 (4) 510-512.

Wu J.J., Muruganandham M., Yang J.S., Lin S.S., Oxidation of DMSO on goethite catalyst in the presence of H_2O_2 at neutral pH. Catalysis Communications 2006 (7) 901–906.

Xuan S.H., Hao L.Y., Jiang W.Q., Gong X.L., Hu Y., Chen Z.Y., Preparation of water-soluble magnetite nanocrystals through hydrothermal approach. Journal of Magnetism and Magnetic Material. 2007 (308) 210-213.

Xue X., Hanna K., Abdelmoula M., Deng N., Adsorption and oxidation of PCP on the surface of magnetite: Kinetic experiments and spectroscopic investigations. Applied Catalysis B: Environmental. In Press, Corrected Proof, Available online 15 January 2009.

Yang S.J., He H., Wu D., Chen D., Liang X., Qin Z., Fan M., Zhu J., Yuan P., Decolorization of methylene blue by heterogeneous Fenton reaction using Fe3−xTixO4 ($0 \leq x \leq 0.78$) at neutral pH values. Applied Catalysis B: Environmental, In Press, Corrected Proof, Available online 29 January 2009.

Yang S.J., Hongping He, Daqing Wu, Dong Chen, Xiaoliang Liang, Zonghua Qin, Mingde Fan, Jianxi Zhu, Peng Yuan. Decolorization of methylene blue by heterogeneous Fenton reaction using $Fe_{3-x}Ti_xO_4$ ($0 \leq x \leq 0.78$) at neutral pH values Applied Catalysis B: Environmental, In Press, Corrected Proof, Available online 29 January 2009.

Zelmanov G., Semiat R., Phenol oxidation kinetics in water solution using iron(3)-oxide-based nano-catalysts. Water Research. 2008, 42(14) 3848-3856.

Zepp R.G., Faust B.C., Hoigne J., Hydroxyl radical formation in aqueous reactions (pH 3-8) of iron(II) with hydrogen peroxide: the photo-Fenton reaction. Environmental Science Technology. 1992 (26) 313-319

Zhang C.J., Richard C., Catlow A., The mechanism of propene oxidation to acrolein on iron antimony oxide. Journal of Catalysis. 2008, 259 (1) 17-25.

Zhang Y., Kallay N., Matijevic E., Interaction of metal hydrous oxides with chelating agents. 7. Hematite-oxalic acid and -citric acid systems. Langmuir. 1985, 1 (2) 201-206.

Zhang Y., Dou X., Liu J., Yang M., Zhang L., Kamagata Y., Decolorization of reactive brilliant red X-3B by heterogeneous photo-Fenton reaction using an Fe–Ce bimetal catalyst. Catalysis Today. 2007, 126 (3-4) 387-393.

Zhou T., Xiaohua Lu, Jia Wang, Fook-Sin Wong, Yaozhong Li. Rapid decolorization and mineralization of simulated textile wastewater in a heterogeneous Fenton like system with/without external energy. Journal of Hazardous Materials, In Press, Corrected Proof, Available online 2 October 2008.

Zhou T., Li Y., Wong F.S., Lu Xi., Enhanced degradation of 2,4-dichlorophenol by ultrasound in a new Fenton like system (Fe/EDTA) at ambient circumstance. Ultrasonics Sonochemistry. 2008, 15(5) 782-790.

Zhu W., Bin Y., Li Z., Jiang Z., Yin T., Application of catalytic wet air oxidation for the treatment of H-acid manufacturing process wastewater. Water Research. 2002 (36) 1947-1954.

Zollinger H., Color Chemistry, VCH,Weinheim, New York, Basel, Cambridge, 1991.

APPENDIX

LIST OF FIGURES

LIST OF TABLES